Supplementary information

Features of the mechanochemical synthesis of methylmethoxysilanes from silicon and dimethyl carbonate in the presence of promoters.

I.N. Kryzhanovskiy[1], M.N. Temnikov[1*], A.K. Ratnikov[1], I.V. Frank[1,2], M.V. Shishkanov[1,2], A.A. Anisimov[1,2], A.V. Naumkin[1], S.M. Chistovalov[1], and A.M. Muzafarov[1,3].

[1]*A. N. Nesmeyanov Institute of Organoelement Compounds, Russian Academy of Sciences, 119334, Moscow, Russia*

[2]*Moscow Institute of Physics and Technology (National Research University), 117303, Dolgoprudny, Moscow Region, Russia*

[3]*Enikolopov Institute of Synthetic Polymeric Materials, Russian Academy of Sciences, 117393, Moscow, Russia*

Corresponding author email: temnikov88@gmail.com

Contents

1. Common information and methods

1.1. Materials

Technical grade silicon KR-1 (1000–2000 μm, purity > 98%, impurities Fe < 0.7%, Al < 0.7, and Ca < 0.6%) was used as the source of silicon. Commercial CuCl were used as the copper catalysts. Dimethyl carbonate (DMC) was purchased from abcr. DMC was stored over molecular sieves (4 Å). The water content in DMC was less than 150 ppm. Commercial Zn powder was used as additive. Commercial Sn powder was used as additive. Commercial $SnCl_2$ was used as additive. The reactors were made of stainless steel (12c18n10t, major impurities: Ni 9– 11%, Cr 17–19%, and Ti 0.4–1%). The grinding bodies were made of stainless steel 12c18n10t (this steel composition is similar to AISI 321, major impurities: Ni 9–11%, Cr 17–19%, and Ti 0.4–1%), zirconium oxide ZrO_2 (doped with yttrium oxide Y_2O_3 - 5,2%), brass L-59 (composition: Fe <0.3%, P < 0.01%, Cu 57 – 60%, As <0.01%, Pb <0.5%, Zn 39.1 – 43%, Sb <0.01%, Bi <0.003%, Sn <0.2%), tungsten carbide WC-3 (contains Co 3,5–5,3%,). The tin coating on brass and steel milling bodies was obtained by electrochemical deposition in a drum electrolyzer. The coating thickness was about 70 μm.

1.2. Methods and analysis

1.2.1. NMR

^{1}H, and ^{29}Si NMR spectra were recorded on a Bruker Avance™ 500 and Bruker Avance™ 600 spectrometers (Germany) (at 500.13 and 600.22, 99.36 MHz for 1H and 29Si, respectively). The ^{1}H chemical shifts were measured relative to TMS using residual signal of solvent $CDCl_3$ (7.26 ppm). The ^{29}Si NMR spectra were measured in $CDCl_3$ containing $Cr(acac)_3$ (30 mmol/L). The ^{29}Si chemical shifts were measured relative to TMS used as the external standard.

1.2.2. Gas chromatography analysis (GC)

Gas chromatography (GC) analysis was performed on a Chromatec Crystal 5000 chromatograph (Russia) at 50–250 °C, 20° min^{-1}; catharometer detector, columns (2 mm × 2 m) with 5% SE-30 stationary phase deposited onto Chromaton-N-AW-HMDS, helium as a carrier gas (20 mL min^{-1}). Data were recorded and processed using the Chromatec Analytic program package (Chromatec, Russia).

1.2.3. Powder X-ray diffraction (PXRD)

XRD patterns were performed on a Proto AXRD θ-2θ diffractometer with a copper anode, a nickel Kβ filter (Kα=1.541874 Å) and a Dectris Mythen 1K 1D detector in the Bragg-Brentano geometry in the angular range of 20°–100° with a step of 0.02° along the angle 2θ.

Qualitative phase analysis was performed using Crystallography Open Database and the ICDD PDF-2.

1.2.4. Scanning electron microscopy (SEM)

The surface morphology was studied by scanning electron microscopy using a JSM-6000 PLUS scanning electron microscope (JEOL, Japan). The studied samples were dispersed as powders on a conducting carbon adhesive tape. The elemental composition of each surface was determined using an EX-230**BU system with integrated energy dispersive analysis.

1.2.5. X-Ray photoelectron spectroscopy (XPS)

X-Ray photoelectron spectroscopy (XPS) was carried out on an Axis Ultra DLD spectrometer (Kratos) using monochromatic Al Kα radiation with an X-ray beam power of 150 W. Survey spectra and high-resolution spectra were recorded at pass energies of 160 and 40 eV, respectively. Survey spectra were recorded with a step of 1 eV, while high-resolution spectra were recorded with a step of 0.1 eV. The dimensions of the explored area were 300 × 700 μm^2. Samples were mounted on a holder using a double-sided adhesive tape and studied at room temperature at the residual pressure in the spectrometer chamber no higher than 10^{-8} Torr. The energy scale of the spectrometer was calibrated according to the standard procedure based on the following binding energies: 932.62, 368.21 and 83.96 eV for Cu $2p_{3/2}$, Ag $3d_{5/2}$, and Au $4f_{7/2}$, respectively. To eliminate the effect of sample charging, the spectra were recorded using a neutralizer. Surface charging was taken into account based on the Si $2p_{3/2}$ peak of the Si(0) state with a binding energy of 99.34 eV.[1] The background due to electron inelastic energy losses was subtracted by the Shirley method. Quantification was performed using atomic sensitivity factors included in the software of the spectrometer.

1.2.6. Gas chromatography-mass spectrometry analysis (GC-MS)

GC-MS measurements were performed using Shimadzu QP2020 gas chromatograph-mass spectrometer with the following parameters: column: Shimadzu SH-Rtx-5MS (30 m × 0.25 mm × 0.25 μm); oven temperature: 50 °C, hold for 3 min, ramp to 200 °C at 30 °C/min, hold for 11 min; injection

temperature: 250 °C; splitting ratio: split 1:10; MS ion source temperature: 200 °C; interface temperature: 250 °C; total run time: 20 min. Solvent cut-off time was 2 minutes for diethyl ether and 5 minutes for decane.

1.3. Experimental

1.3.1. Typical experiment with copper (I) chloride as a source of copper

Design and parameters of the HPMR that was used in the direct synthesis was described in our previous work [2]. Commercial grade KR-1 silicon (particle size 1.5 mm, 1 g, 35.7 mmol), DMC 6.4 g, 71 mmol, copper chloride(I) 0.2 g and milling bodies (14 pcs) were loaded into the autoclave. The reactors with attached micanite heaters were mounted in cradles. After that, heating (the temperature settings were 250°C) and the vibration drive were activated synchronously. The vibrational acceleration was 19 g. The silicon particles were ground up and stirred with copper source by vibration milling. The resulting particles reacted with DMC to give mixture of methylmethoxysilanes (tetramethyl orthosilicate (M0), methyltrimethoxysilanes (M1), dimethyldimethoxysilanes (M2) trimethylmethoxysilanes (M3)) and siloxanes. After the specified amount of time of simultaneous heating and vibration, the mixture was cooled to room temperature. Liquid reaction products were analyzed using GC. The contact mass was separated from the reaction products by centrifugation then washed three time with hexane, dried and studied using SEM-DX, XPS, and PXRD.

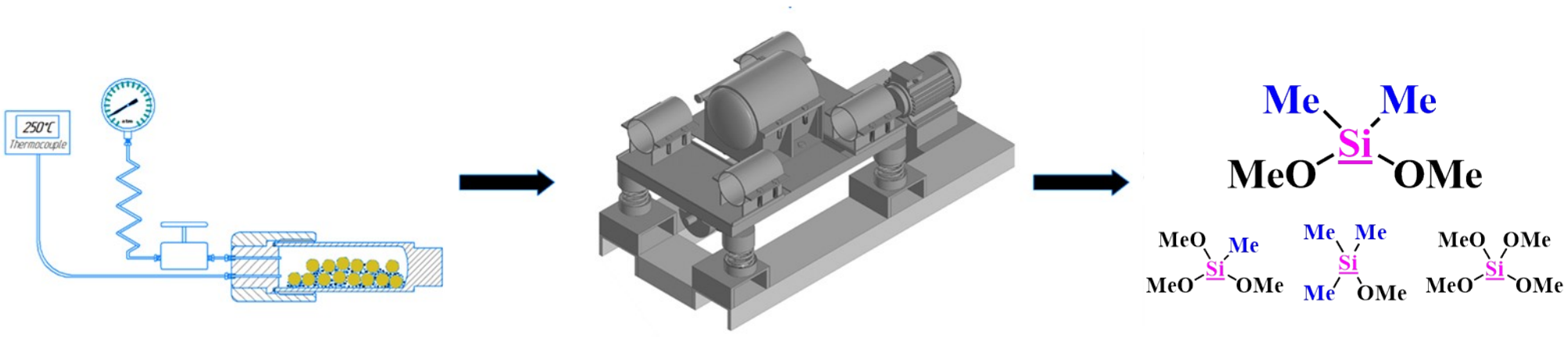

Figure S1. Experimental scheme.

1.3.2. Additional experimental data

Table S1. Influence of co-additive on parameters of Si/Cu + DMC reaction, synthesis conditions: grinding bodies made from ZrO_2, 14 pcs. (Total weight 38,38 g), 250 °C, 1 g Si, 0,2 g CuCl, DMC 2 eq., 5 mg $SnCl_2$.

№	Co-additive	Co-additive mass, mg	Si conversion, %	DMC conversion, %	Selectivity, %				
					M3	M2	M1	M0	Siloxanes
1	Standart experiment	-	30,1	30,8	4,4	70,2	9,6	2,4	13,3
2	$ZnCl_2$	5	36,6	36,2	9,7	57,5	17,1	3,9	11,7
3	$(F_5C_6)_3B$ 2 wt% in toluene	50 µl	23,5	31,0	4,6	65,8	10,8	6,7	12,1
4	$CoCl_2$	5	10,8	17,5	5,1	65,4	15,5	9,0	5,0
5	$MgCl_2$	5	0,0	14,2	0	0	0	0	0
6	CeO_2	5	0,0	100,0	0	0	0	0	0
7	2,2'-Dipyridyl	12,4 *	8,8	12,4	3,7	51,1	5,9	31,8	7,5
8	1,10-phenanthroline	14,3 *	9,3	15,1	2,6	52,3	33,4	4,3	7,5
9	TiO_2	5	22,0	30,9	4,4	68,1	10,5	3,4	13,7
10	V_2O_5	5	22,1	30,6	5,1	63,6	12,6	4,1	14,5
11	$CoSi_2$	5	24,6	31,2	4,2	68,4	10,1	2,8	14,4
12	Cs_2CO_3	5	21,3	19,3	2,7	72,1	1,4	10,5	13,3
13	$(AcO)_2AlOH$	5	17,9	38,3	4,5	60,6	12,6	3,2	19,2
14	Mg_2Si	5	12,2	44,8	4,9	50,6	16,7	8,9	18,8
15	Ni_2Si	5	20,7	37,2	3,4	65,1	12,1	3,2	16,1
16	$CrSi_2$	5	26,6	33,5	3,5	68,3	10,1	2,9	15,1
17	$HgOAc_2$	5	32,0	41,5	3,6	74,6	7,8	2,2	11,8
18	$MoSi_2$	5	25,7	31,7	5,0	67,0	9,8	2,7	15,5
19	Zn	5	68,5	65,7	11,2	47,6	12,4	2,7	26,2
20	K_2CO_3	5	13,3	16,0	1,1	66,9	14,7	4,5	12,8
21	AcOBiO	5	4,0	10,1	0,0	32,4	27,0	25,6	15,0
22	$AlCl_3$	5	17,9	45,1	4,2	62,7	11,6	2,9	18,6
23	$NiCl_2$	5	26,5	31,9	3,6	67,1	11,5	3,2	14,6

2. * – 3 equivalent to 5 mg $SnCl_2$

Table S2. Synthesis with brass balls.

Name	Catalyst mix, reaction time (hours)	Si conv. (%)	DMC conv. (%)	M3 select. (%)	M2 select. (%)	M1 select. (%)	M0 select. (%)
B	Without CuCl and additives, 6	4	61	0	0	11	74
B-Cu	Without additives, 2	15	22	6	43	19	15
B-Cu-Sn	$SnCl_2$ (5 mg), 2	55	60	13	45	18	3
B-Cu-Sn-long	$SnCl_2$ (5 mg), 2 + decompression + 3.2 г DMC, 2	74	67	11	40	19	10
B-Cu-Zn	Zn (5 mg), 2	15	21	6	47	17	7
B-Cu-Sn-Zn	$SnCl_2$ (5 mg), Zn (5 mg), 2	59	67	16	40	14	3

2.1. Calculations

The silicon conversion and selectivity of products were estimated as follows:

Concentration data obtained with GC give us mass relations between components of the reaction mixture. It allows us to determine the selectivities of components (S_i) by this equation:

$$S_i = \frac{W_i}{\sum W_i}$$

To determine Si conversion, we need to calculate the mass of the liquid products (m_{lp}):

$$m_{lp} = m_{DMC} + m_{Si} * C_{Si} - m_{gas}$$

m_{gas} – mass of gaseous products, mostly CO_2. m_{DMC} and m_{Si} are 6.4 g and 1 g respectively. C_{Si} is the Si conversion.

$$C_{Si} = \frac{n_{reacted\ Si}}{n_{loaded\ Si}} = \frac{\sum \frac{W_i * m_{mix}}{M_i}}{\frac{m_{Si}}{M_{Si}}}$$

m_{gas} – mass of gaseous products, mostly CO_2 determined by weighing the autoclave with reacted mixture before and after depressurization.

C_{DMC} is the DMC conversion. $m_{DMC}$is 6.4 g.

$$C_{DMC} = \frac{n_{reacted\ DMC}}{n_{loaded\ DMC}} = \frac{m_{loaded\ DMC} - m_{lp} * W_{DMC}}{m_{loaded\ DMC}}$$

W_{DMC} – obtained from GC data.

SEM-EDX elemental analyses

Table S3. SEM-EDX elemental analyses data table (% wt).

Sample	Area	Elements (% wt)										
		Si	Cu	C	O	Al	Cl	Fe	Cr	Zn	Zr	Sn
Sn-30	Reacted	8,73	71,48	4,65	4,39	1,22	0,60	1,16		7,27		0,52
	Non reacted	70,63	4,14	15,12	7,97	0,60	0,7	0,18		0,31		0,88
Sn-60	Reacted	42,27	17,43	17,56	15,55	0,35	0,78	2,82		2,56		0,68
	Non reacted	74,04	0,25	20,29	3,87	0,24	0,05			0,13		1,14
Sn-120	Reacted	27,70	9,85	17,08	40,05	0,35	1,11	3,04		0,30		0,52
	Non reacted	78,58	0,10	17,73	1,81	0,23	0,01	0,11		0,17		1,25
Sn-240	Reacted	16,16	25,28	19,25	9,86	0,44	2,45	15,42	4,73	1,42		1,55
	Non reacted	48,23	1,57	35,95	9,92	0,21	0,75	2,31		0,17		0,89
$SnCl_2$-30	Reacted	23,33	65,93	2,78	2,48	0,76	0,09	1,66		2,43		0,54
	Non reacted	77.87	1.38	14.75	3.99	0.41	0.04	0.19		0.03		1.34
$SnCl_2$-60	Reacted	22,23	60,65	7,07	4,93	0,49	0,60	1,12		2,45		0,26
	Non reacted	84,75	0,70	11,18	2,31	0,34	0,01	0,09		0,02		0,59
$SnCl_2$-120	Reacted	75,80	1,88	14,96	3,99	0,29	0,32	0,99		0,37		1,40
	Non reacted	71,65	1,11	20,65	3,65	0,40	0,18	1,06		0,15		1,16
$SnCl_2$-240	Reacted	42.86	6.36	18.57	14.50	0.37	1.96	8.91	2.61	1.09		1,12
	Non reacted	71.79	2.24	14.31	7.25	0.29	0.56	1.43	0.42	0.04		1.43

Table S4. SEM-EDX elemental analyses data table (% at)

Sample	Area	Elements (% at)										
		Si	Cu	C	O	Al	Cl	Fe	Cr	Zn	Zr	Sn
Sn-30	Reacted	13,54	49,02	16,85	11,95	1,96	0,74	0,91		4,84		0,19
	Non reacted	57,42	1,49	28,74	11,38	0,51	0,11	0,07		0,11		0,17
Sn-60	Reacted	34,65	6,32	33,66	22,38	0,29	0,51	1,16		0,90		0,13
	Non reacted	57,40	0,08	36,78	5,26	0.20	0,03			0,04		0,21
Sn-120	Reacted	19,06	3,00	27,48	48,38	0.25	0,60	1,05		0,09		0,08
	Non reacted	63,41	0,03	33,45	2,57	0,19	0,01	0,05		0,06		0,24
Sn-240	Reacted	15,39	10,64	42,87	16,49	0,44	1,85	7,39	2.44	0,58		0,35
	Non reacted	31,59	0,45	55,07	11,41	0,14	0,39	0,76		0,05		0,14
$SnCl_2$-30	Reacted	35,25	44,02	0,14	6,57	1,19	0,11	1,26		1,58		0,19
	Non reacted	64,43	0,51	28,54	5,79	0,35	0,02	0,08		0,01		0,26
$SnCl_2$-60	Reacted	28,77	34,70	21,40	11,21	0,67	0,62	0,73		1,36		0,08
	Non reacted	73,18	0,27	22,58	3,50	0,30	0,1	0,04		0,01		0,12
$SnCl_2$-120	Reacted	63,07	0,69	29,12	5,83	0,25	0,21	0,41		0,13		0,28
	Non reacted	55,86	0,38	37,65	5,00	0,32	0,11	0,42		0,05		0,21
$SnCl_2$-240	Reacted	34,59	2,27	35,05	20,54	0,31	1,25	3,62	1,14	0,38		0,21
	Non reacted	59,26	0,82	27,62	10,51	0,25	0,37	0,59	0,19	0,01		0,28

3. XPS elemental analyses

Table S5. Element concentrations determined by XPS from the survey spectra.

Sample	**Element, at%**								
	C	O	Si	Zn	Cu	Sn	Cr	Fe	Cl
Sn-30	24.8	35.9	34.8	1.1	0.6	0.2		0.4	2.2
Sn-60	37.2	31.4	28.0	0.9	0.4	0.1		0.5	1.6
Sn-120	52.5	27.7	13.5	1.2	0.5	0.2	0.6	1.7	
Sn-240	49.7	26.9	10.9	1.1	0.4	0.3	1.3	4.8	4.8
$SnCl_2$-30	25.3	39.9	30.3	0.6	0.9	0.1	0.2	0.9	1.7
$SnCl_2$-60	28.4	34.6	32.4	1.0	0.5	0.1	0.5	0.7	1.7
$SnCl_2$-120	45.3	28.7	17.8	1.3	0.4	0.2	1.1	2.5	2.8
$SnCl_2$-240	45.4	29.8	14.0	1.1	0.3	0.2	1.6	4.1	3.6

Table S6. Element concentrations determined by XPS from the high-resolution spectra.

Sample	**Element, at%**							
	C	O	Si	Zn	Cu	Sn	Cr	Fe
Sn-30	26.1	33.2	38.5	1.0	0.5	0.2		0.4
Sn-60	38.8	28.6	31.0	0.7	0.4	0.1		0.4
Sn-120	54.3	26.4	15.8	0.9	0.4	0.1	0.6	1.6
Sn-240	51.2	26.8	14.2	1.0	0.4	0.3	1.4	4.8
$SnCl_2$-30	27.1	36.8	33.5	0.6	0.8	0.1	0.4	0.8
$SnCl_2$-60	29.3	32.2	36.0	0.8	0.4	0.1	0.5	0.7
$SnCl_2$-120	46.8	27.5	20.8	1.1	0.3	0.2	1.2	2.2
$SnCl_2$-240	46.9	28.9	17.8	1.0	0.3	0.2	1.4	3.7

4. Spectra and other additional information

4.1. SEM-EDX – images and spectra

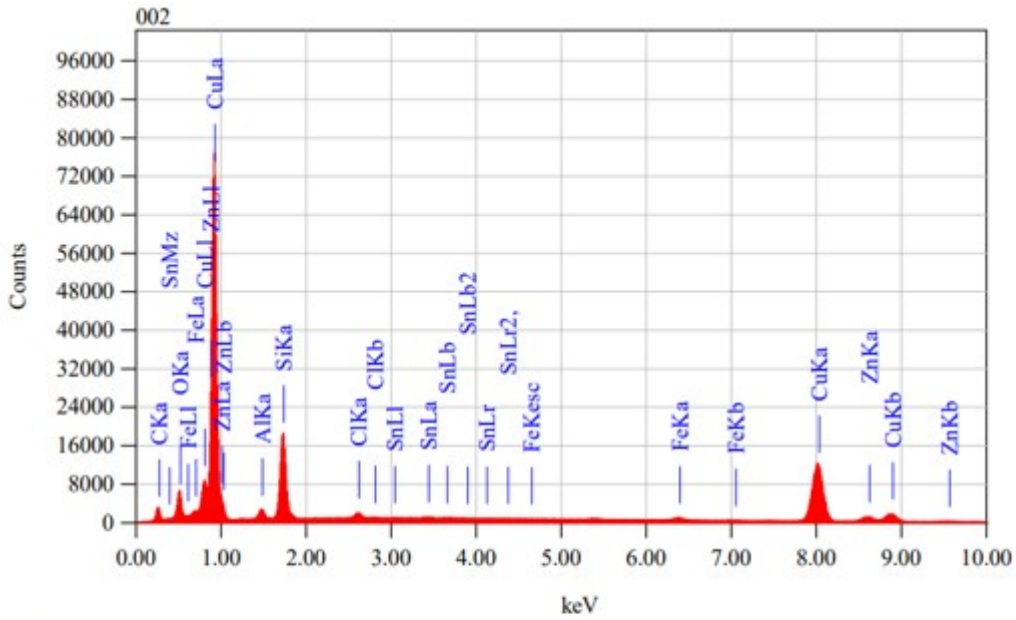


```
Acquisition Parameter
Instrument    : JCM-6000PLUS
Acc. Voltage  : 15.0 kV
Probe Current: 1.00000 nA
PHA mode      : Standard
Real Time     : 200.00 sec
Live Time     : 170.22 sec
Dead Time     : 14 %
Counting Rate: 10284 cps
Energy Range :  0 - 20 keV
```

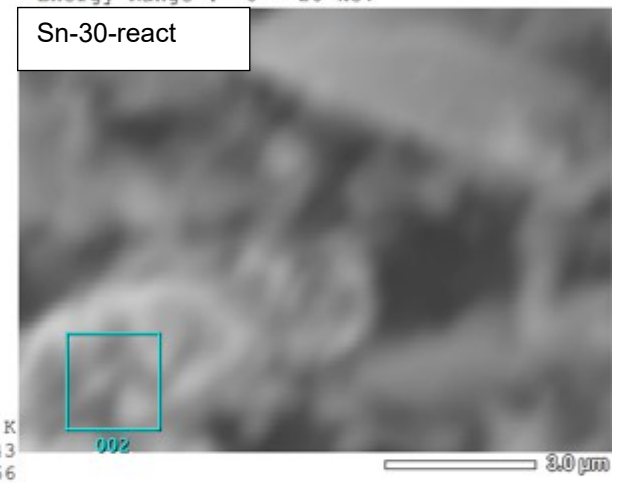


```
ZAF Method Standardless Quantitative Analysis
Fitting Coefficient : 0.2094
Element          (keV)   Mass%   Sigma   Atom%  Compound   Mass%  Cation          K
 C K             0.277    4.65    0.03   16.85                                  0.9643
 O K             0.525    4.39    0.03   11.95                                  3.6566
Al K             1.486    1.22    0.02    1.96                                  0.6094
Si K             1.739    8.73    0.04   13.54                                  5.7327
Cl K             2.621    0.60    0.01    0.74                                  0.6104
Fe K             6.398    1.16    0.02    0.91                                  1.4939
Cu K             8.040   71.48    0.26   49.02                                 78.5039
Zn K             8.630    7.27    0.11    4.84                                  7.9736
Sn L             3.442    0.52    0.02    0.19                                  0.4553
```

Figure S2. Sn-30-react area.

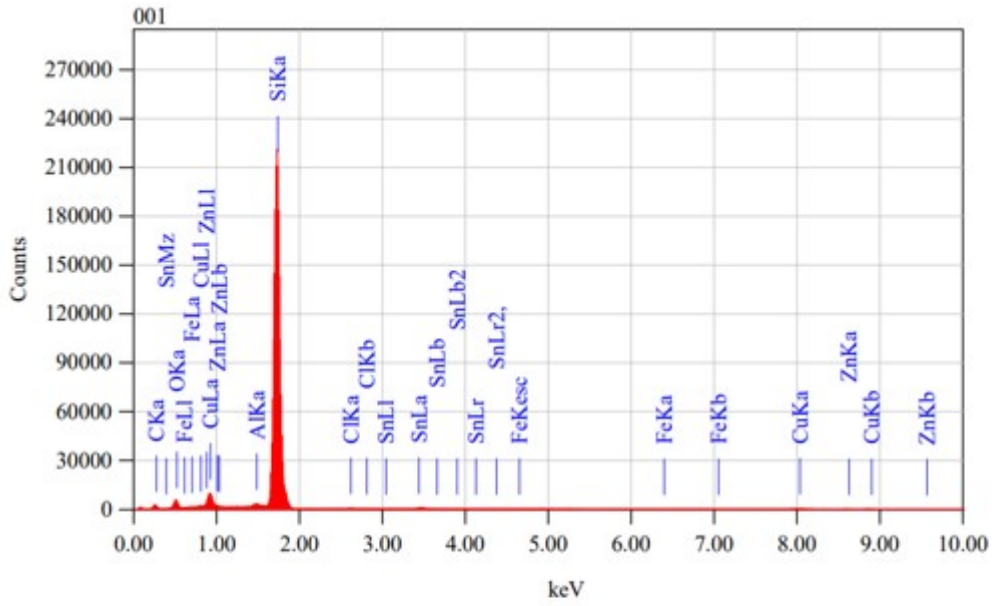


```
Acquisition Parameter
Instrument    : JCM-6000PLUS
Acc. Voltage  : 15.0 kV
Probe Current: 1.00000 nA
PHA mode      : Standard
Real Time     : 200.00 sec
Live Time     : 157.92 sec
Dead Time     : 20 %
Counting Rate: 15500 cps
Energy Range :  0 - 20 keV
```

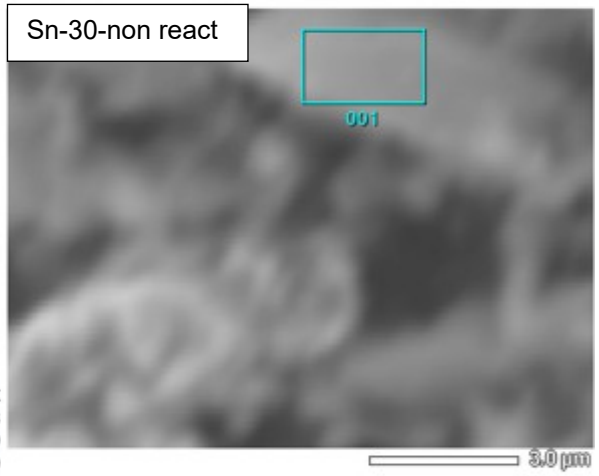

ZAF Method Standardless Quantitative Analysis
Fitting Coefficient : 0.2178

Element	(keV)	Mass%	Sigma	Atom%	Compound	Mass%	Cation	K
C K	0.277	15.12	0.09	28.74				1.1503
O K	0.525	7.97	0.06	11.38				4.2079
Al K	1.486	0.60	0.01	0.51				0.6969
Si K	1.739	70.63	0.09	57.42				87.8776
Cl K	2.621	0.17	0.01	0.11				0.1689
Fe K	6.398	0.18	0.02	0.07				0.2098
Cu K	8.040	4.14	0.08	1.49				4.5771
Zn K	8.630	0.31	0.04	0.11				0.3360
Sn L	3.442	0.88	0.03	0.17				0.7756
Total		100.00		100.00				

Figure S3. Sn-30-non react area.

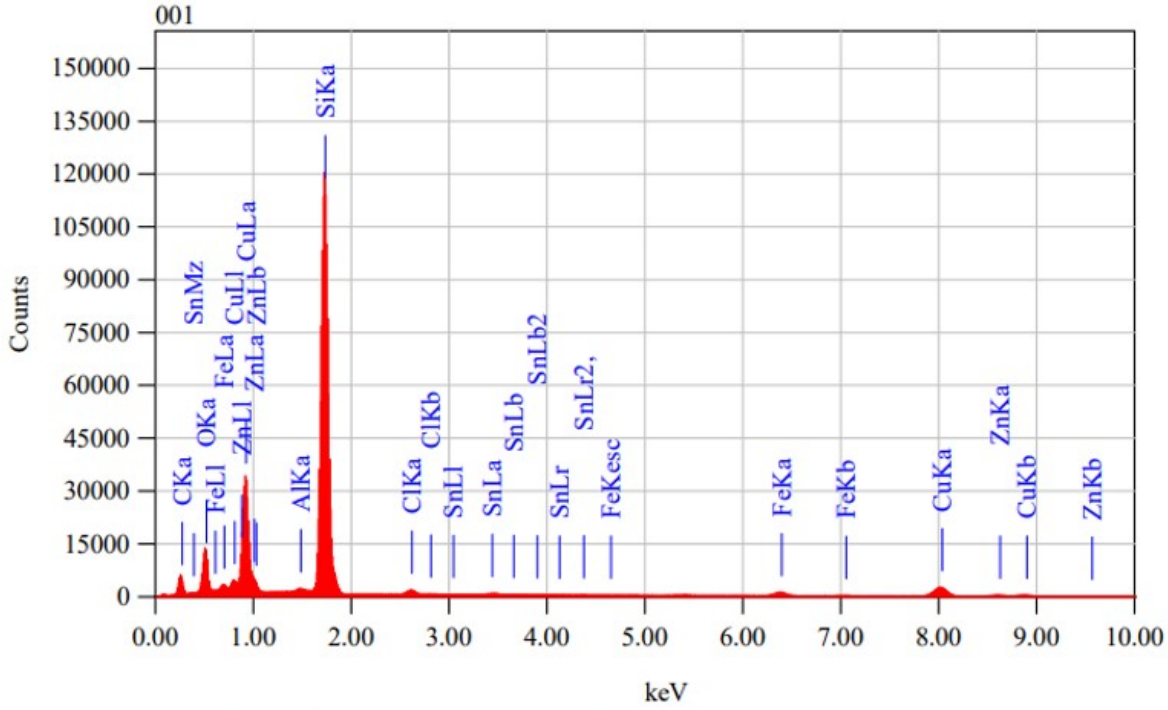


```
Acquisition Parameter
Instrument    : JCM-6000PLUS
Acc. Voltage  : 15.0 kV
Probe Current: 1.00000 nA
PHA mode      : Standard
Real Time     : 200.00 sec
Live Time     : 167.13 sec
Dead Time     : 16 %
Counting Rate: 12008 cps
Energy Range :  0 - 20 keV
```

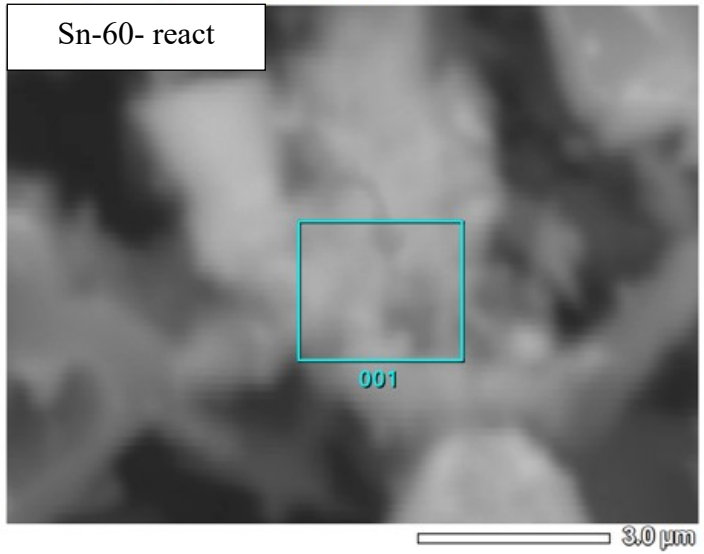

ZAF Method Standardless Quantitative Analysis
Fitting Coefficient : 0.1997

Element	(keV)	Mass%	Sigma	Atom%	Compound	Mass%	Cation	K
C K	0.277	17.56	0.07	33.66				2.5466
O K	0.525	15.55	0.07	22.38				11.5087
Al K	1.486	0.35	0.01	0.29				0.3621
Si K	1.739	42.27	0.07	34.65				52.5376
Cl K	2.621	0.78	0.01	0.51				1.0123
Fe K	6.398	2.82	0.04	1.16				4.1387
Cu K	8.040	17.43	0.14	6.32				23.6683
Zn K	8.630	2.56	0.07	0.90				3.4640
Sn L	3.442	0.68	0.02	0.13				0.7618
Total		100.00		100.00				

Figure S4. Sn-60 reacted area.

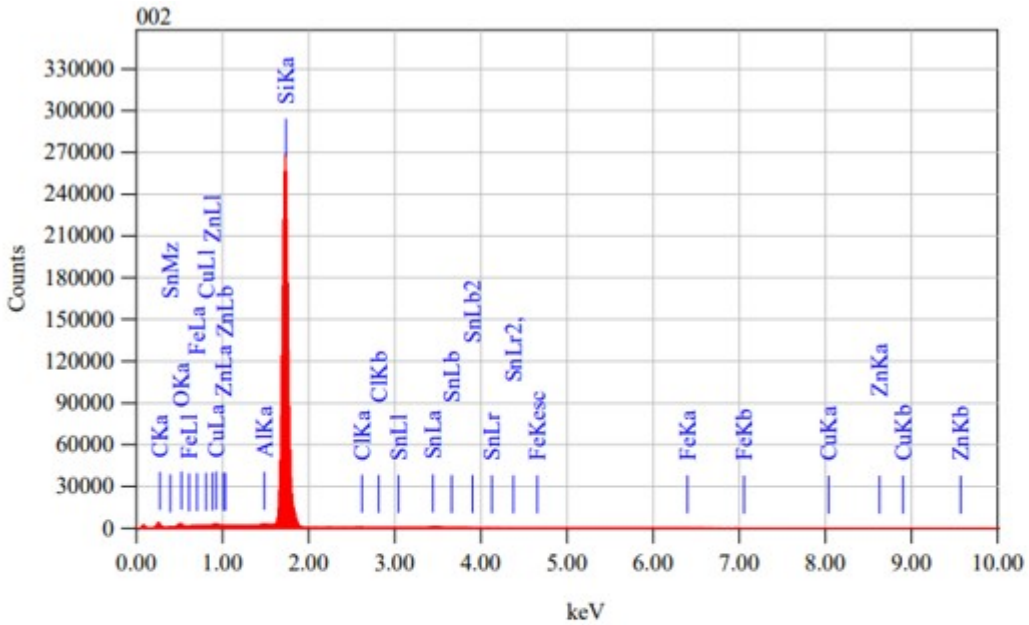


```
Acquisition Parameter
Instrument    : JCM-6000PLUS
Acc. Voltage  : 15.0 kV
Probe Current: 1.00000 nA
PHA mode      : Standard
Real Time     : 200.00 sec
Live Time     : 151.25 sec
Dead Time     : 24 %
Counting Rate: 19139 cps
Energy Range :  0 - 20 keV
```

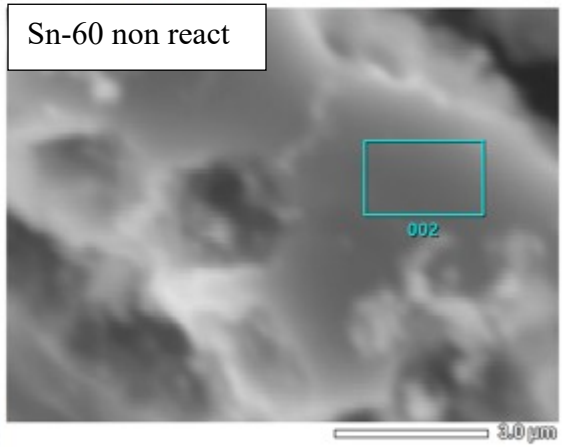

ZAF Method Standardless Quantitative Analysis
Fitting Coefficient : 0.2148

Element	(keV)	Mass%	Sigma	Atom%	Compound	Mass%	Cation	K
C K	0.277	20.29	0.10	36.78				1.4336
O K	0.525	3.87	0.04	5.26				1.7799
Al K	1.486	0.24	0.01	0.20				0.3015
Si K	1.739	74.04	0.08	57.40				95.0628
Cl K	2.621	0.05	0.01	0.03				0.0440
Fe K		ND		ND				
Cu K	8.040	0.25	0.03	0.08				0.2647
Zn K	8.630	0.13	0.03	0.04				0.1371
Sn L	3.442	1.14	0.03	0.21				0.9765
Total		100.00		100.00				

Figure S5. Sn-60 non reacted area.

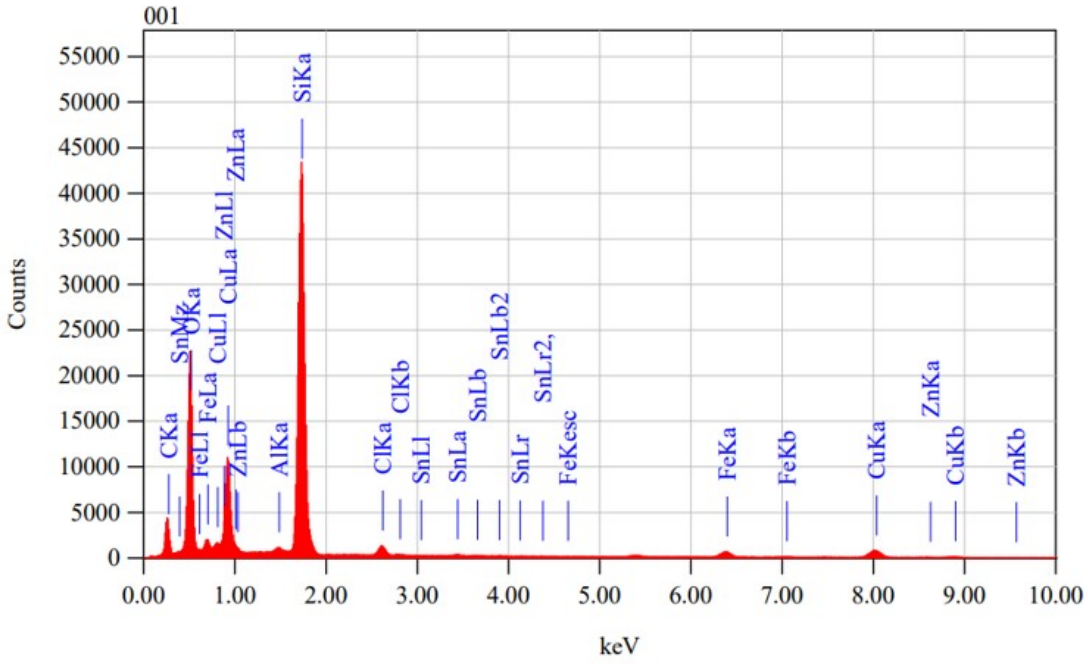

Acquisition Parameter
Instrument : JCM-6000PLUS
Acc. Voltage : 15.0 kV
Probe Current: 1.00000 nA
PHA mode : Standard
Real Time : 200.00 sec
Live Time : 186.30 sec
Dead Time : 6 %
Counting Rate: 4692 cps
Energy Range : 0 - 20 keV

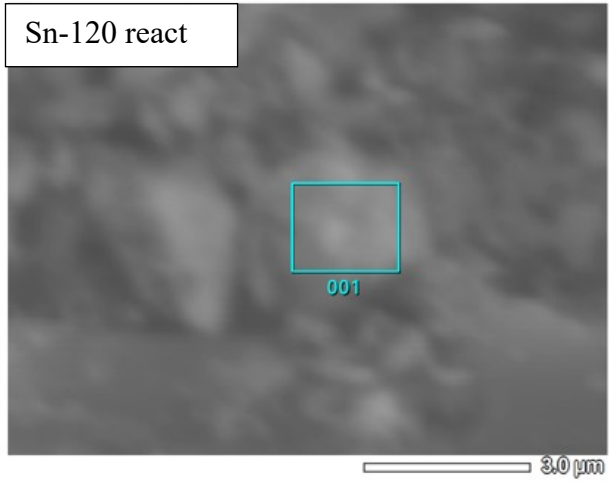

ZAF Method Standardless Quantitative Analysis
Fitting Coefficient : 0.2006

Element	(keV)	Mass%	Sigma	Atom%	Compound	Mass%	Cation	K
C K	0.277	17.08	0.08	27.48				3.6906
O K	0.525	40.05	0.14	48.38				37.6551
Al K	1.486	0.35	0.01	0.25				0.3933
Si K	1.739	27.70	0.08	19.06				37.0548
Cl K	2.621	1.11	0.02	0.60				1.6301
Fe K	6.398	3.04	0.05	1.05				4.6223
Cu K	8.040	9.85	0.14	3.00				13.8997
Zn K	8.630	0.30	0.05	0.09				0.4212
Sn L	3.442	0.52	0.03	0.08				0.6330
Total		100.00		100.00				

Figure S6. Sn-120 reacted area.

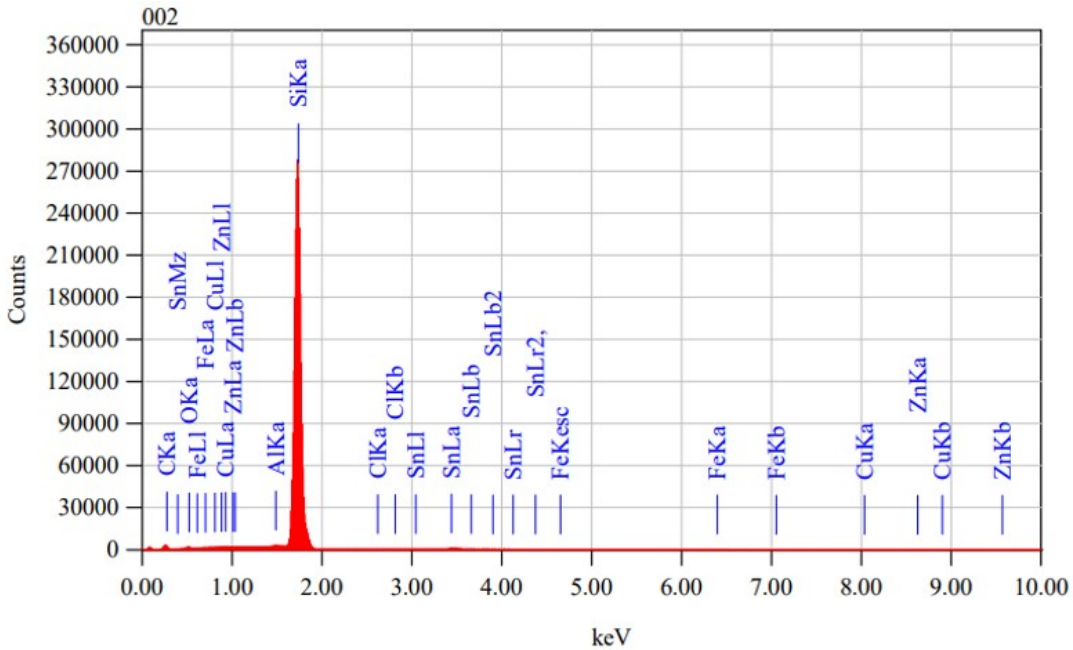

Acquisition Parameter
Instrument : JCM-6000PLUS
Acc. Voltage : 15.0 kV
Probe Current: 1.00000 nA
PHA mode : Standard
Real Time : 200.00 sec
Live Time : 150.88 sec
Dead Time : 24 %
Counting Rate: 19363 cps
Energy Range : 0 - 20 keV

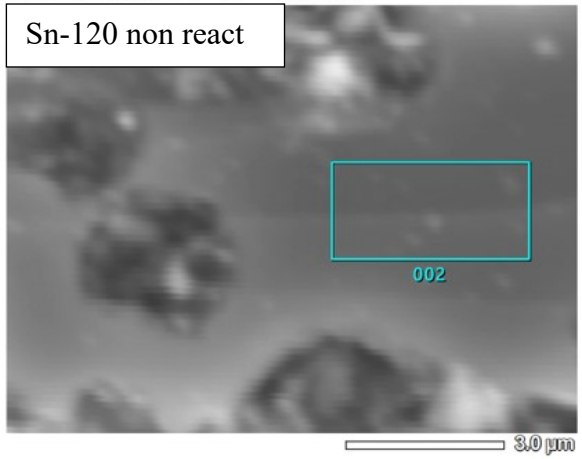

ZAF Method Standardless Quantitative Analysis
Fitting Coefficient : 0.2090

Element	(keV)	Mass%	Sigma	Atom%	Compound	Mass%	Cation	K
C K	0.277	17.73	0.10	33.45				1.1186
O K	0.525	1.81	0.03	2.57				0.7964
Al K	1.486	0.23	0.01	0.19				0.2735
Si K	1.739	78.58	0.09	63.41				96.4013
Cl K	2.621	0.01	0.01	0.01				0.0103
Fe K	6.398	0.11	0.01	0.05				0.1210
Cu K	8.040	0.10	0.03	0.03				0.0973
Zn K	8.630	0.17	0.03	0.06				0.1733
Sn L	3.442	1.25	0.03	0.24				1.0082
Total		100.00		100.00				

Figure S7. Sn-120 non reacted area.

CM-20 react

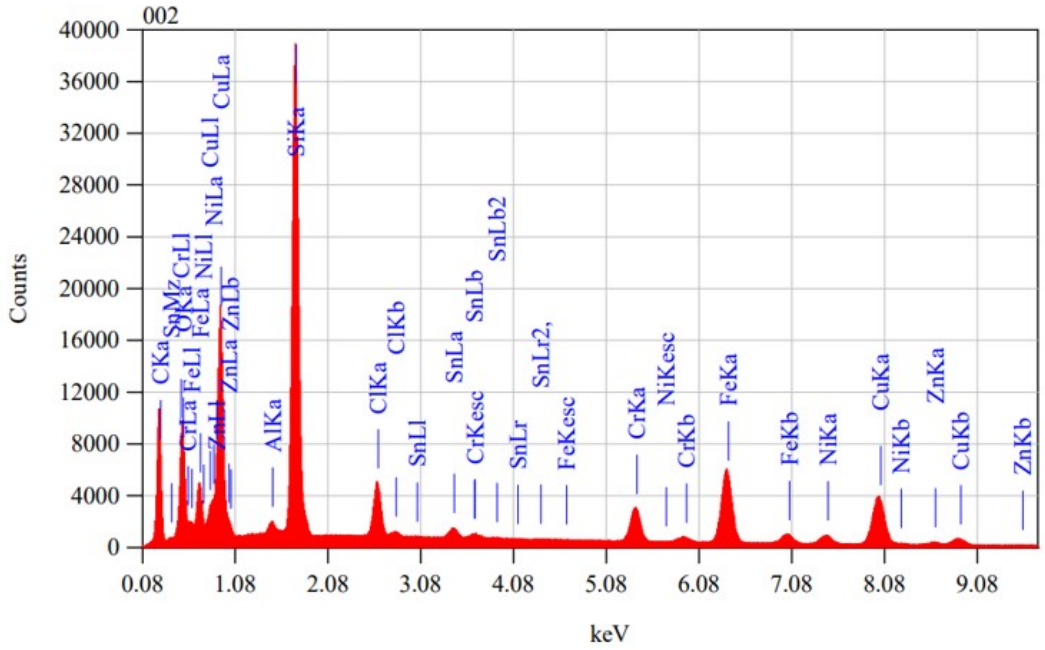


```
Acquisition Parameter
Instrument    : JCM-6000PLUS
Acc. Voltage  : 15.0 kV
Probe Current: 1.00000 nA
PHA mode      : Standard
Real Time     : 200.00 sec
Live Time     : 176.31 sec
Dead Time     : 11 %
Counting Rate: 7992 cps
Energy Range :  0 - 20 keV
```

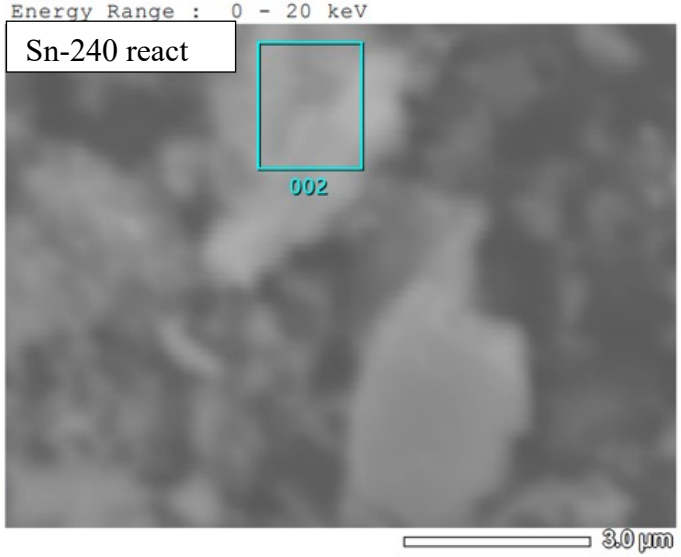

ZAF Method Standardless Quantitative Analysis
Fitting Coefficient : 0.2209

Element	(keV)	Mass%	Sigma	Atom%	Compound	Mass%	Cation	K
C K	0.277	19.25	0.06	42.87				4.2843
O K*	0.525	9.86	0.05	16.49				7.5817
Al K*	1.486	0.44	0.01	0.44				0.3417
Si K	1.739	16.16	0.05	15.39				15.8902
Cl K	2.621	2.45	0.02	1.85				3.2075
Cr K*	5.411	4.73	0.04	2.44				6.6565
Fe K	6.398	15.42	0.08	7.39				21.5335
Ni K	7.471	3.44	0.06	1.57				4.6286
Cu K	8.040	25.28	0.17	10.64				32.3773
Zn K	8.630	1.42	0.06	0.58				1.8161
Sn L*	3.442	1.55	0.03	0.35				1.6827
Total		100.00		100.00				

Figure S8. Sn-240 reacted area.

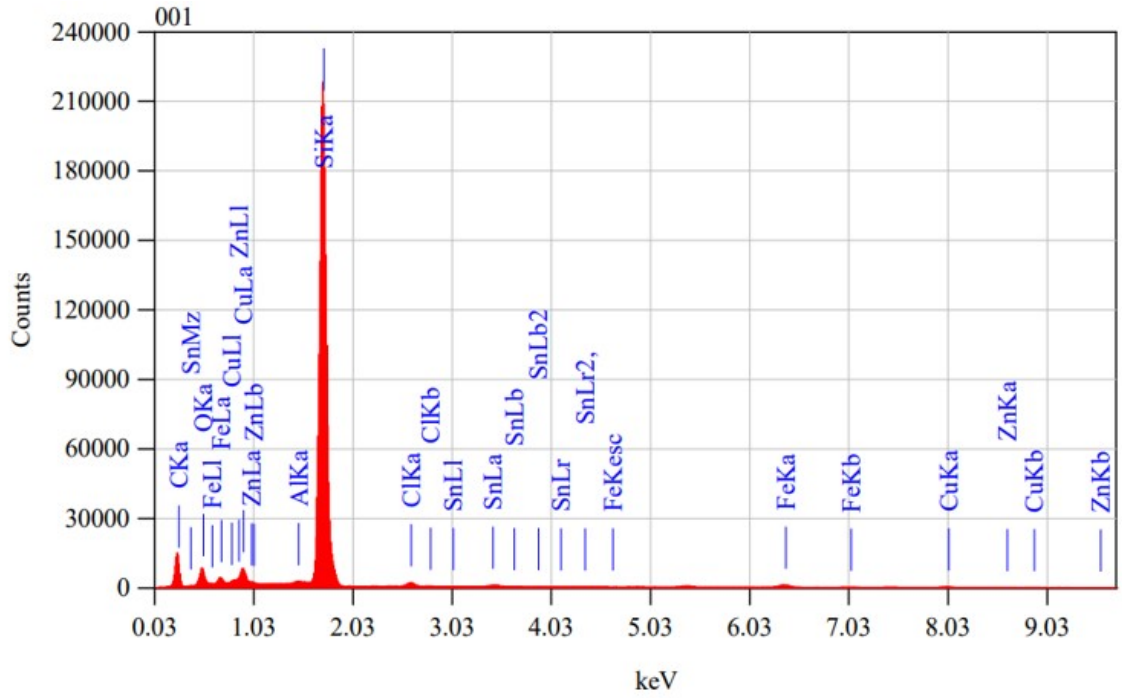


```
Acquisition Parameter
Instrument    : JCM-6000PLUS
Acc. Voltage  : 15.0 kV
Probe Current: 1.00000 nA
PHA mode      : Standard
Real Time     : 200.00 sec
Live Time     : 154.79 sec
Dead Time     : 20 %
Counting Rate: 15914 cps
Energy Range :  0 - 20 keV
```

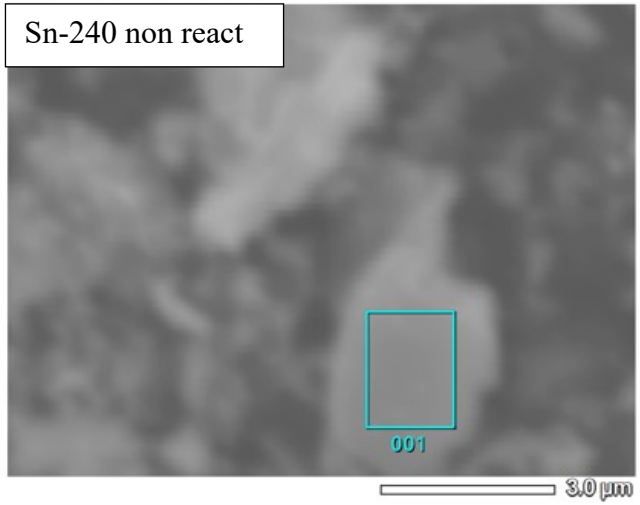

ZAF Method Standardless Quantitative Analysis
Fitting Coefficient : 0.2227

Element	(keV)	Mass%	Sigma	Atom%	Compound	Mass%	Cation	K
C K	0.277	35.95	0.09	55.07				5.3688
O K*	0.525	9.92	0.06	11.41				5.8333
Al K*	1.486	0.21	0.01	0.14				0.3137
Si K	1.739	48.23	0.06	31.59				80.1447
Cl K	2.621	0.75	0.01	0.39				1.0918
Fe K	6.398	2.31	0.03	0.76				3.5879
Cu K	8.040	1.57	0.04	0.45				2.3068
Zn K*	8.630	0.17	0.03	0.05				0.2462
Sn L*	3.442	0.89	0.02	0.14				1.1068
Total		100.00		100.00				

Figure S9. Sn-240 non reacted area.

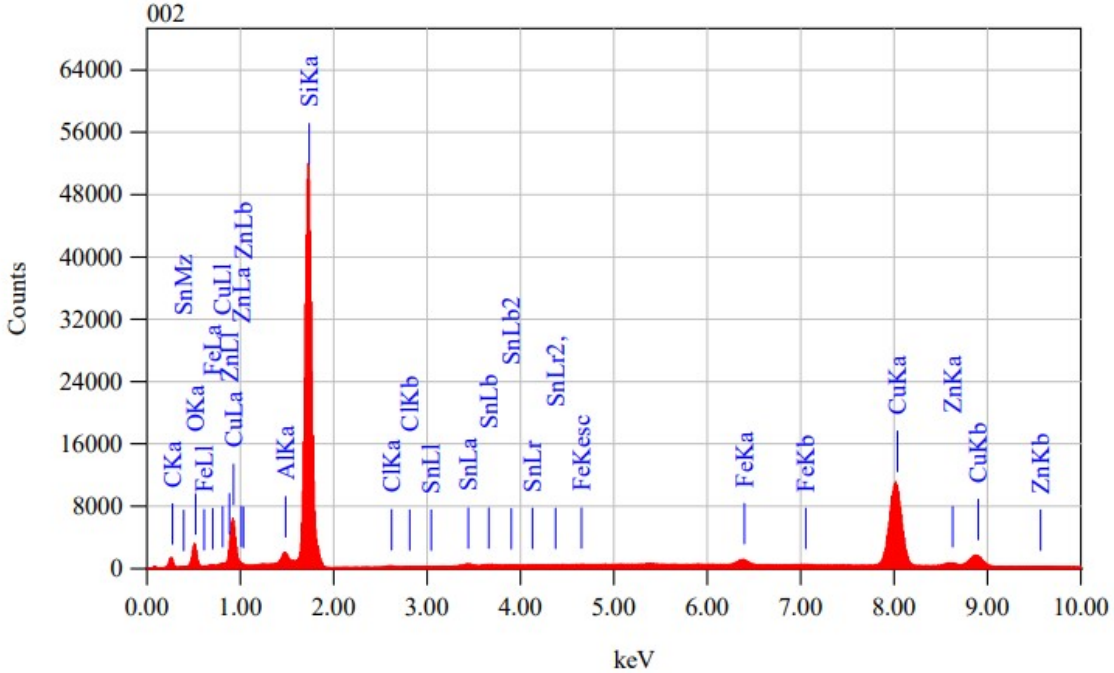


```
Acquisition Parameter
Instrument    : JCM-6000PLUS
Acc. Voltage  : 15.0 kV
Probe Current: 1.00000 nA
PHA mode      : Standard
Real Time     : 200.00 sec
Live Time     : 180.65 sec
Dead Time     : 9 %
Counting Rate: 6759 cps
Energy Range  :  0 - 20 keV
```

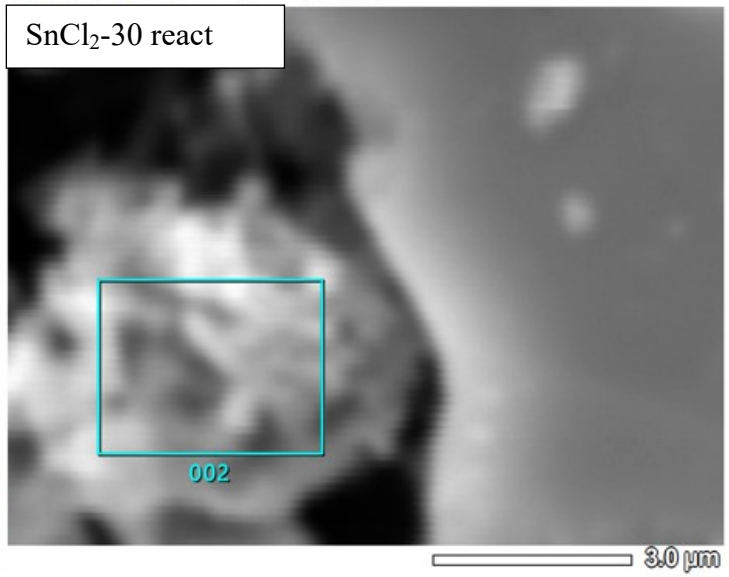

ZAF Method Standardless Quantitative Analysis
Fitting Coefficient : 0.1816

Element	(keV)	Mass%	Sigma	Atom%	Compound	Mass%	Cation	K
C K	0.277	2.78	0.02	9.83				0.4704
O K	0.525	2.48	0.02	6.57				2.0380
Al K	1.486	0.76	0.01	1.19				0.4317
Si K	1.739	23.33	0.06	35.25				17.1072
Cl K	2.621	0.09	0.00	0.11				0.0903
Fe K	6.398	1.66	0.03	1.26				2.1478
Cu K	8.040	65.93	0.25	44.02				74.4835
Zn K	8.630	2.43	0.08	1.58				2.7432
Sn L	3.442	0.54	0.02	0.19				0.4878
Total		100.00		100.00				

Figure S10. $SnCl_2$-30 reacted area.

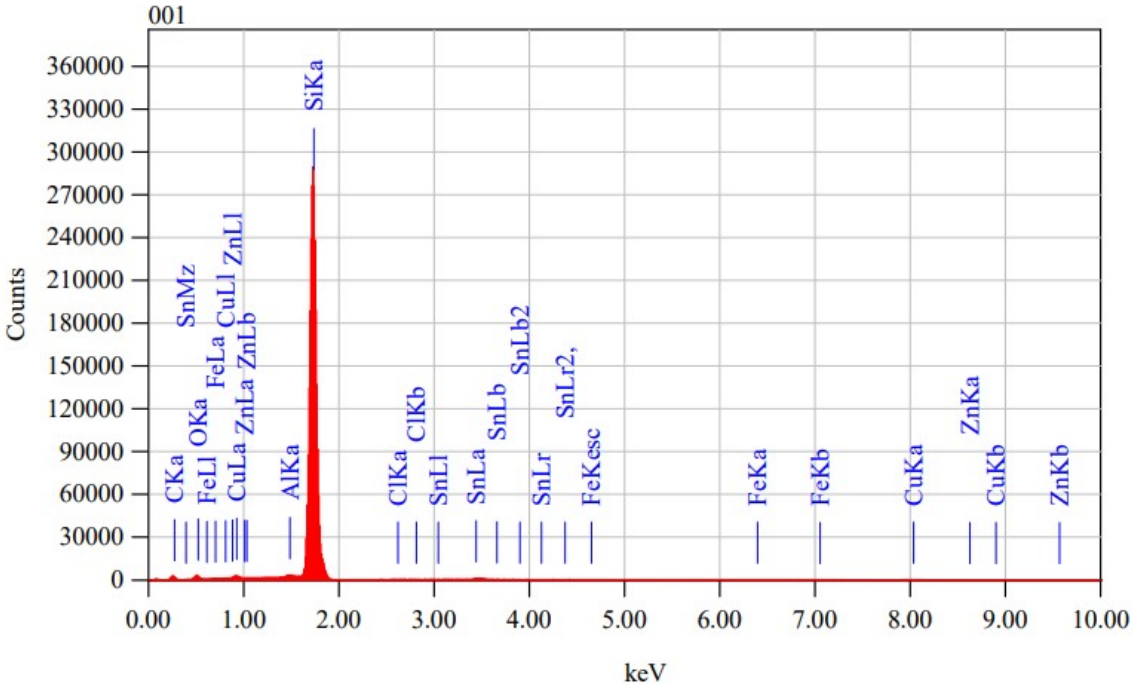


```
Acquisition Parameter
Instrument    : JCM-6000PLUS
Acc. Voltage  : 15.0 kV
Probe Current: 1.00000 nA
PHA mode      : Standard
Real Time     : 200.00 sec
Live Time     : 148.81 sec
Dead Time     : 24 %
Counting Rate: 19026 cps
Energy Range  :  0 - 20 keV
```

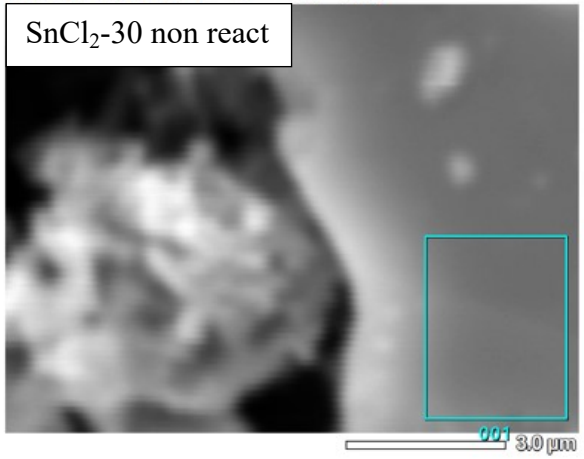

ZAF Method Standardless Quantitative Analysis
Fitting Coefficient : 0.2121

Element	(keV)	Mass%	Sigma	Atom%	Compound	Mass%	Cation	K
C K	0.277	14.75	0.09	28.54				0.9469
O K	0.525	3.99	0.04	5.79				1.8517
Al K	1.486	0.41	0.01	0.35				0.4699
Si K	1.739	77.87	0.08	64.43				93.9639
Cl K	2.621	0.04	0.01	0.02				0.0325
Fe K	6.398	0.19	0.02	0.08				0.2042
Cu K	8.040	1.38	0.05	0.51				1.4156
Zn K	8.630	0.03	0.03	0.01				0.0332
Sn L	3.442	1.34	0.03	0.26				1.0821
Total		100.00		100.00				

Figure S11. $SnCl_2$-30 non reacted area.

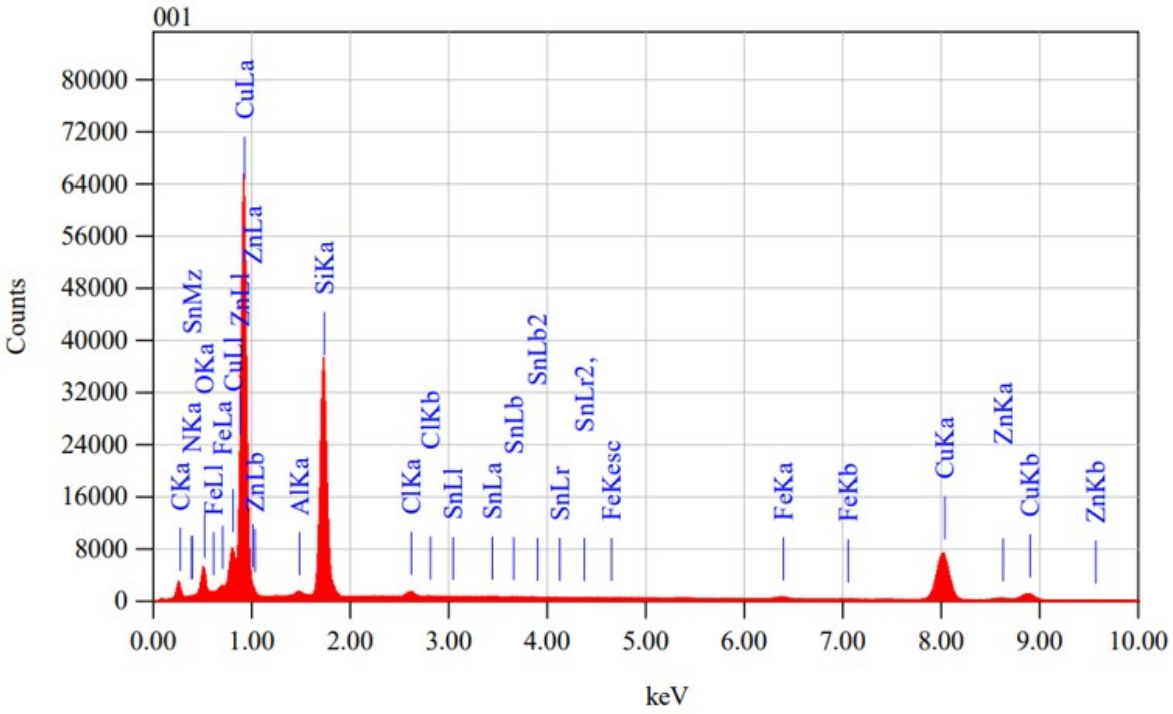


```
Acquisition Parameter
Instrument    : JCM-6000PLUS
Acc. Voltage  : 15.0 kV
Probe Current: 1.00000 nA
PHA mode      : Standard
Real Time     : 200.00 sec
Live Time     : 175.51 sec
Dead Time     : 11 %
Counting Rate: 8584 cps
Energy Range :  0 - 20 keV
```

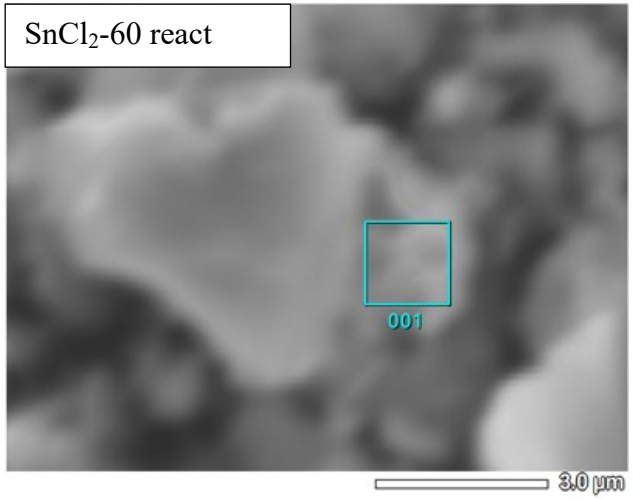

ZAF Method Standardless Quantitative Analysis
Fitting Coefficient : 0.2123

Element	(keV)	Mass%	Sigma	Atom%	Compound	Mass%	Cation	K
C K	0.277	7.07	0.04	21.40				1.2460
N K	0.392	0.18	0.02	0.47				0.1618
O K	0.525	4.93	0.04	11.21				3.9989
Al K	1.486	0.49	0.01	0.67				0.3020
Si K	1.739	22.23	0.07	28.77				17.4961
Cl K	2.621	0.60	0.01	0.62				0.6533
Fe K	6.398	1.12	0.03	0.73				1.5097
Cu K	8.040	60.65	0.28	34.70				71.4939
Zn K	8.630	2.45	0.09	1.36				2.8884
Sn L	3.442	0.26	0.03	0.08				0.2499
Total		100.00		100.00				

Figure S12. $SnCl_2$-60 reacted area.

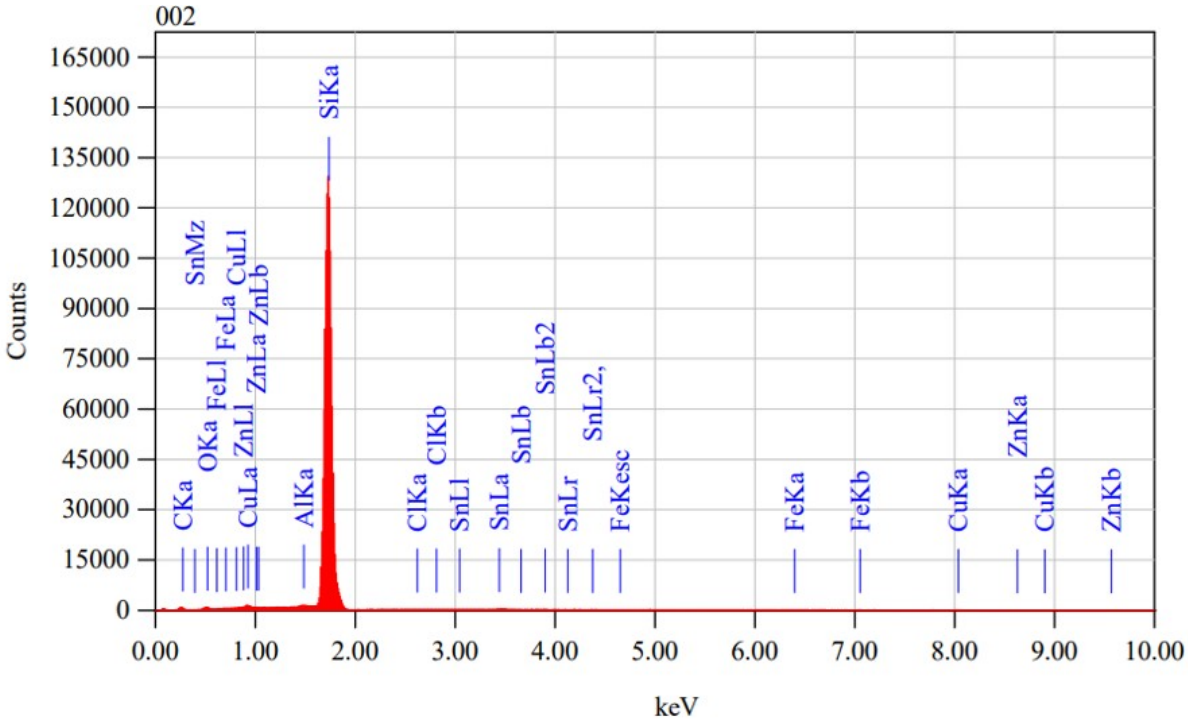


```
Acquisition Parameter
Instrument    : JCM-6000PLUS
Acc. Voltage  : 15.0 kV
Probe Current: 1.00000 nA
PHA mode      : Standard
Real Time     : 200.00 sec
Live Time     : 179.40 sec
Dead Time     : 9 %
Counting Rate: 7185 cps
Energy Range :  0 - 20 keV
```

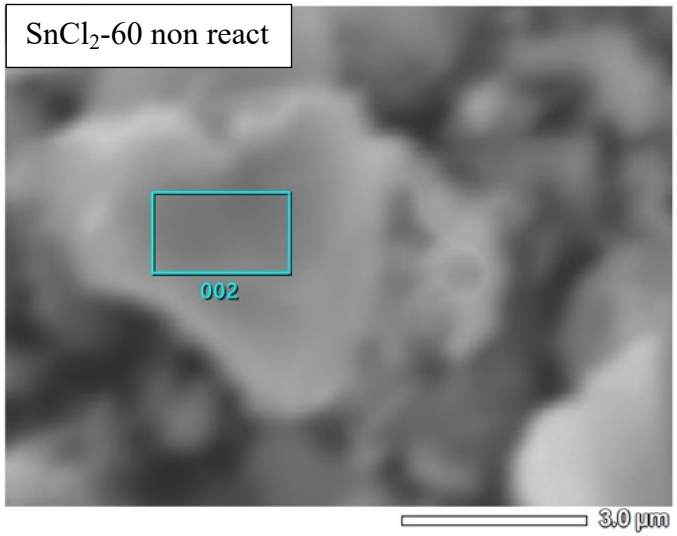

ZAF Method Standardless Quantitative Analysis
Fitting Coefficient : 0.2141

Element	(keV)	Mass%	Sigma	Atom%	Compound	Mass%	Cation	K
C K	0.277	11.18	0.12	22.58				0.6070
O K	0.525	2.31	0.05	3.50				1.0247
Al K	1.486	0.34	0.01	0.30				0.3766
Si K	1.739	84.75	0.14	73.18				96.7754
Cl K	2.621	0.01	0.01	0.01				0.0111
Fe K	6.398	0.09	0.02	0.04				0.0845
Cu K	8.040	0.70	0.06	0.27				0.6626
Zn K	8.630	0.02	0.05	0.01				0.0208
Sn L	3.442	0.59	0.04	0.12				0.4372
Total		100.00		100.00				

Figure S13. $SnCl_2$-60 non reacted area.

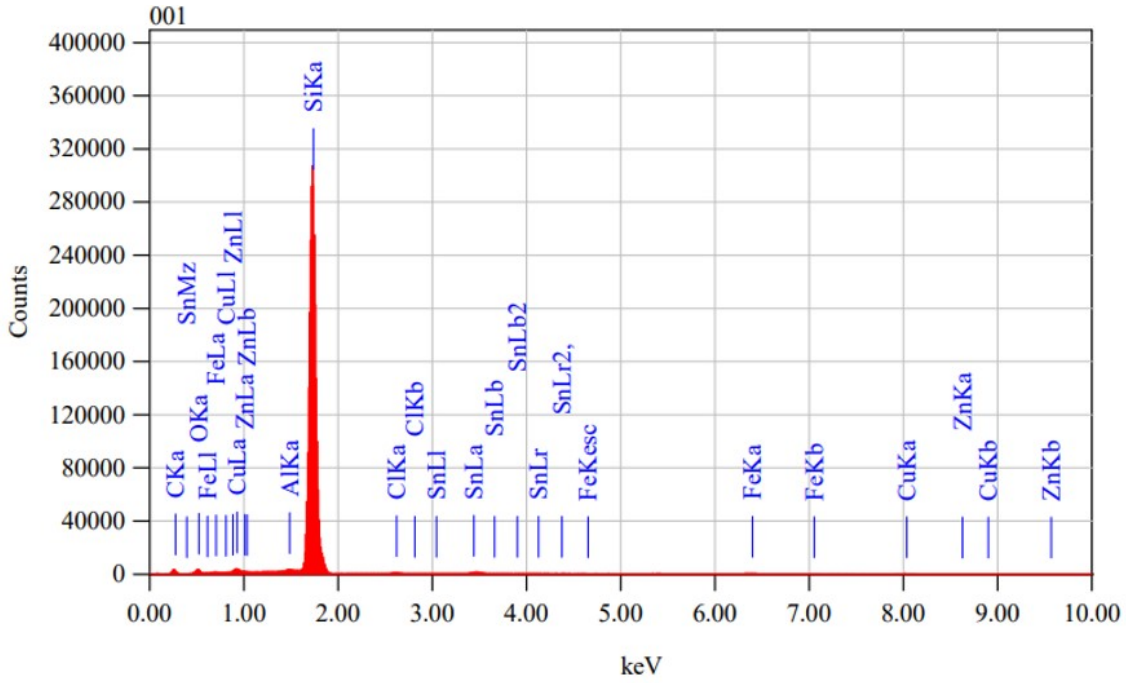


```
Acquisition Parameter
Instrument    : JCM-6000PLUS
Acc. Voltage  : 15.0 kV
Probe Current: 1.00000 nA
PHA mode      : Standard
Real Time     : 200.00 sec
Live Time     : 143.28 sec
Dead Time     : 28 %
Counting Rate: 22860 cps
Energy Range  :  0 - 20 keV
```

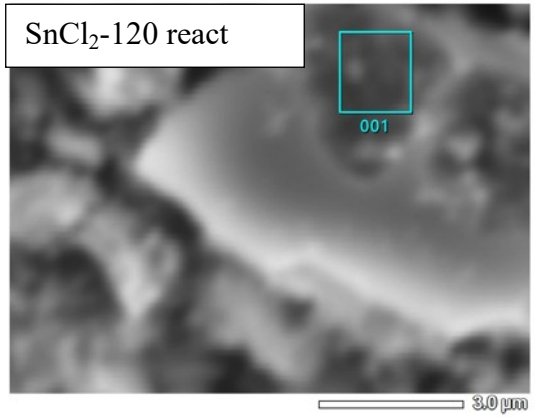

ZAF Method Standardless Quantitative Analysis
Fitting Coefficient : 0.1987

Element	(keV)	Mass%	Sigma	Atom%	Compound	Mass%	Cation	K
C K	0.277	14.96	0.08	29.12				1.0037
O K	0.525	3.99	0.04	5.83				1.8986
Al K	1.486	0.29	0.01	0.25				0.3288
Si K	1.739	75.80	0.08	63.07				91.8937
Cl K	2.621	0.32	0.01	0.21				0.2988
Fe K	6.398	0.99	0.02	0.41				1.0761
Cu K	8.040	1.88	0.05	0.69				1.9637
Zn K	8.630	0.37	0.04	0.13				0.3811
Sn L	3.442	1.40	0.03	0.28				1.1556
Total		100.00		100.00				

Figure S14. $SnCl_2$-120 reacted area.

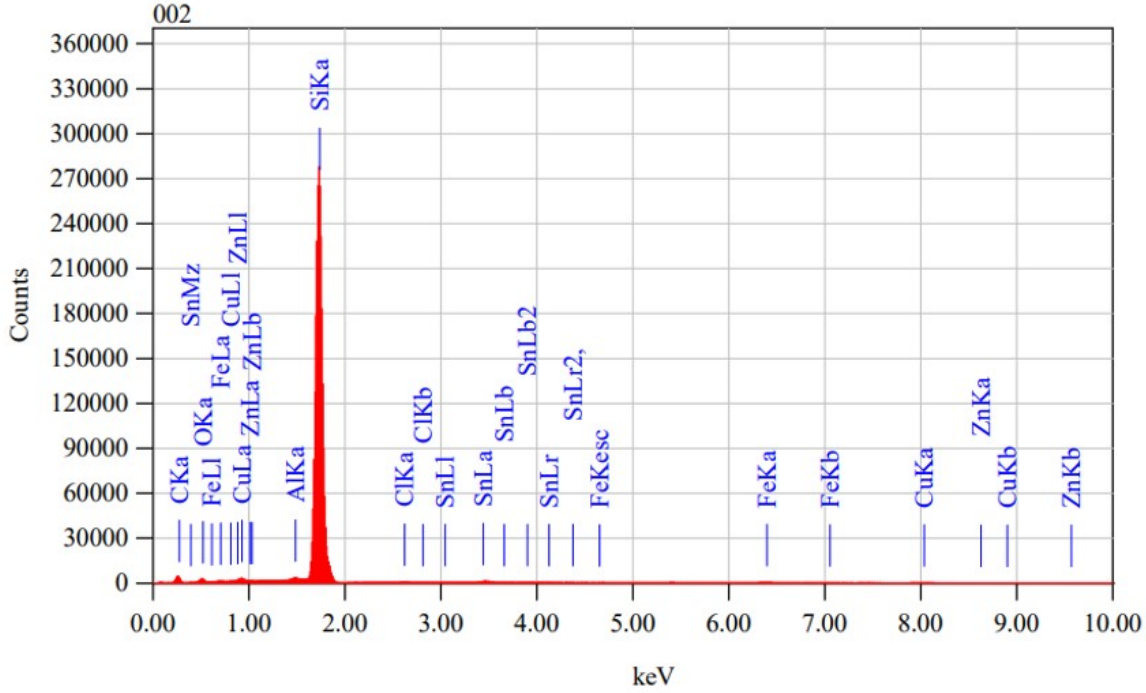


```
Acquisition Parameter
Instrument    : JCM-6000PLUS
Acc. Voltage  : 15.0 kV
Probe Current: 1.00000 nA
PHA mode      : Standard
Real Time     : 200.00 sec
Live Time     : 149.53 sec
Dead Time     : 23 %
Counting Rate: 18661 cps
Energy Range :  0 - 20 keV
```

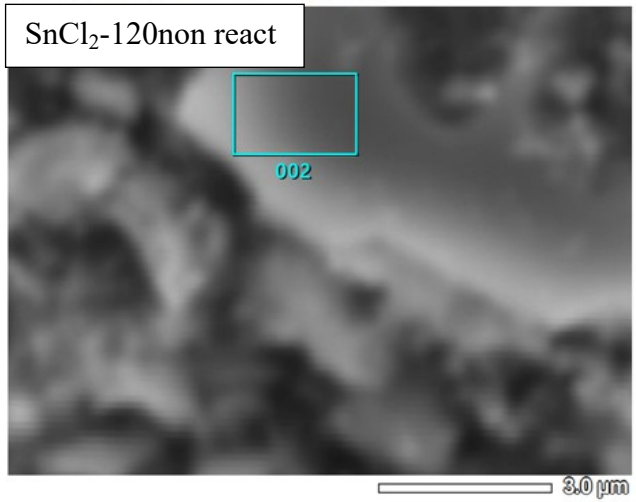

ZAF Method Standardless Quantitative Analysis
Fitting Coefficient : 0.2025

Element	(keV)	Mass%	Sigma	Atom%	Compound	Mass%	Cation	K
C K	0.277	20.65	0.10	37.65				1.5448
O K	0.525	3.65	0.04	5.00				1.7346
Al K	1.486	0.40	0.01	0.32				0.4857
Si K	1.739	71.65	0.08	55.86				92.4373
Cl K	2.621	0.18	0.01	0.11				0.1738
Fe K	6.398	1.06	0.02	0.42				1.2162
Cu K	8.040	1.11	0.04	0.38				1.2257
Zn K	8.630	0.15	0.03	0.05				0.1599
Sn L	3.442	1.16	0.03	0.21				1.0220
Total		100.00		100.00				

Figure S15. $SnCl_2$-120 non reacted area.

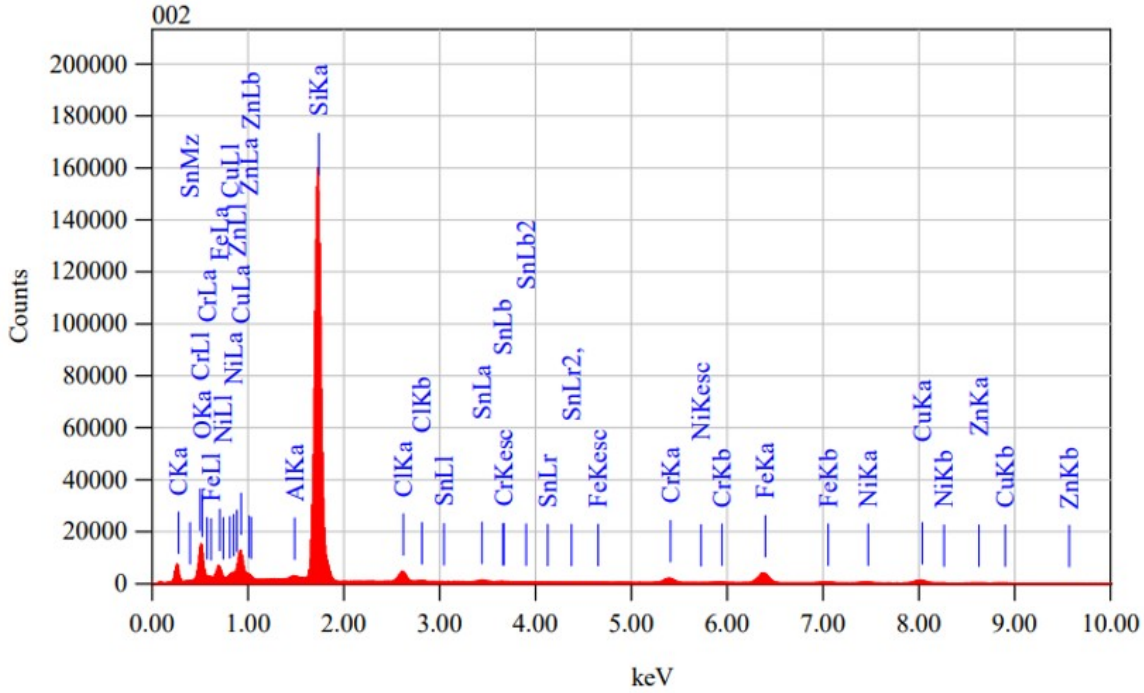


```
Acquisition Parameter
Instrument    : JCM-6000PLUS
Acc. Voltage  : 15.0 kV
Probe Current: 1.00000 nA
PHA mode      : Standard
Real Time     : 200.00 sec
Live Time     : 158.68 sec
Dead Time     : 20 %
Counting Rate: 15259 cps
Energy Range :  0 - 20 keV
```

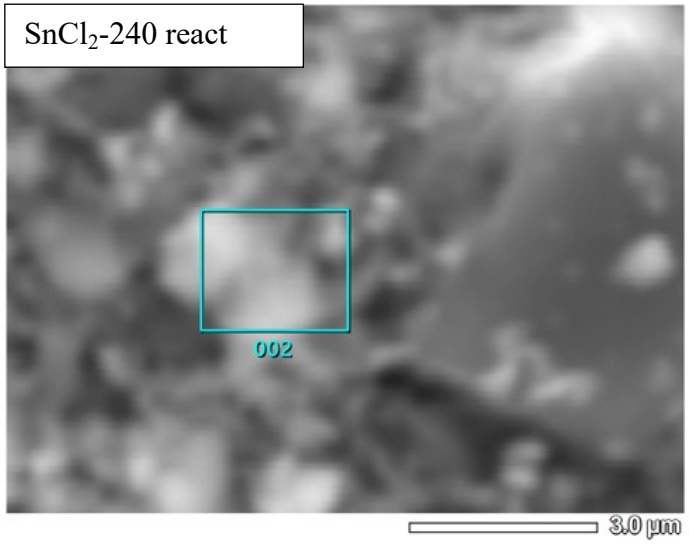

ZAF Method Standardless Quantitative Analysis
Fitting Coefficient : 0.2165

Element	(keV)	Mass%	Sigma	Atom%	Compound	Mass%	Cation	K
C K	0.277	18.57	0.07	35.05				2.5671
O K	0.525	14.50	0.06	20.54				10.1982
Al K	1.486	0.37	0.01	0.31				0.4062
Si K	1.739	42.86	0.06	34.59				54.8538
Cl K	2.621	1.96	0.02	1.25				2.5242
Cr K	5.411	2.61	0.03	1.14				3.6723
Fe K	6.398	8.91	0.06	3.62				12.4569
Ni K	7.471	1.65	0.04	0.64				2.2972
Cu K	8.040	6.36	0.08	2.27				8.3690
Zn K	8.630	1.09	0.05	0.38				1.4328
Sn L	3.442	1.12	0.02	0.21				1.2224
Total		100.00		100.00				

Figure S16. $SnCl_2$-240 reacted area.

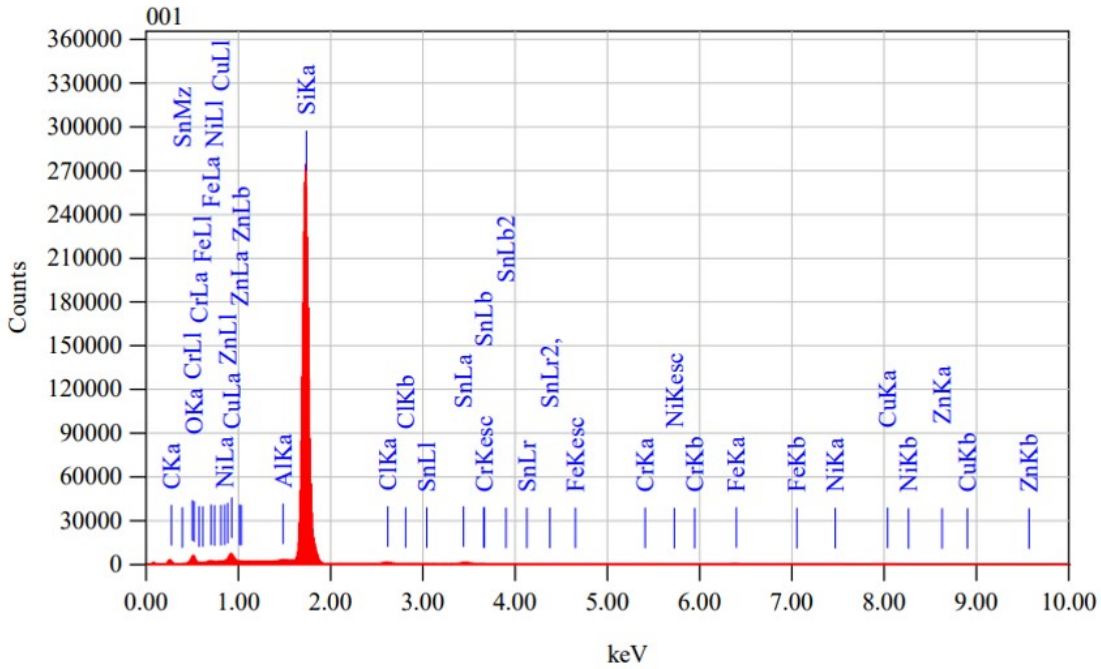


```
Acquisition Parameter
Instrument    : JCM-6000PLUS
Acc. Voltage  : 15.0 kV
Probe Current: 1.00000 nA
PHA mode      : Standard
Real Time     : 200.00 sec
Live Time     : 147.00 sec
Dead Time     : 25 %
Counting Rate: 20649 cps
Energy Range :  0 - 20 keV
```

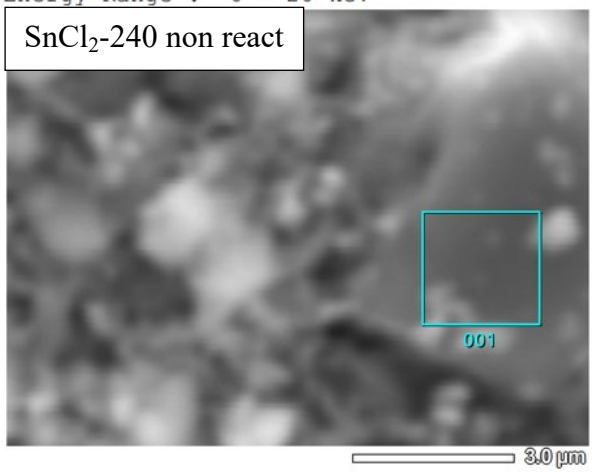

ZAF Method Standardless Quantitative Analysis
Fitting Coefficient : 0.2232

Element	(keV)	Mass%	Sigma	Atom%	Compound	Mass%	Cation	K
C K	0.277	14.31	0.08	27.62				1.0465
O K	0.525	7.25	0.05	10.51				3.6964
Al K	1.486	0.29	0.01	0.25				0.3384
Si K	1.739	71.79	0.08	59.26				88.3385
Cl K	2.621	0.56	0.01	0.37				0.5424
Cr K	5.411	0.42	0.02	0.19				0.4673
Fe K	6.398	1.43	0.03	0.59				1.6064
Ni K	7.471	0.24	0.02	0.09				0.2705
Cu K	8.040	2.24	0.05	0.82				2.4200
Zn K	8.630	0.04	0.03	0.01				0.0452
Sn L	3.442	1.43	0.03	0.28				1.2285
Total		100.00		100.00				

Figure S17. $SnCl_2$-240 non reacted area.

4.2. PXRD – data

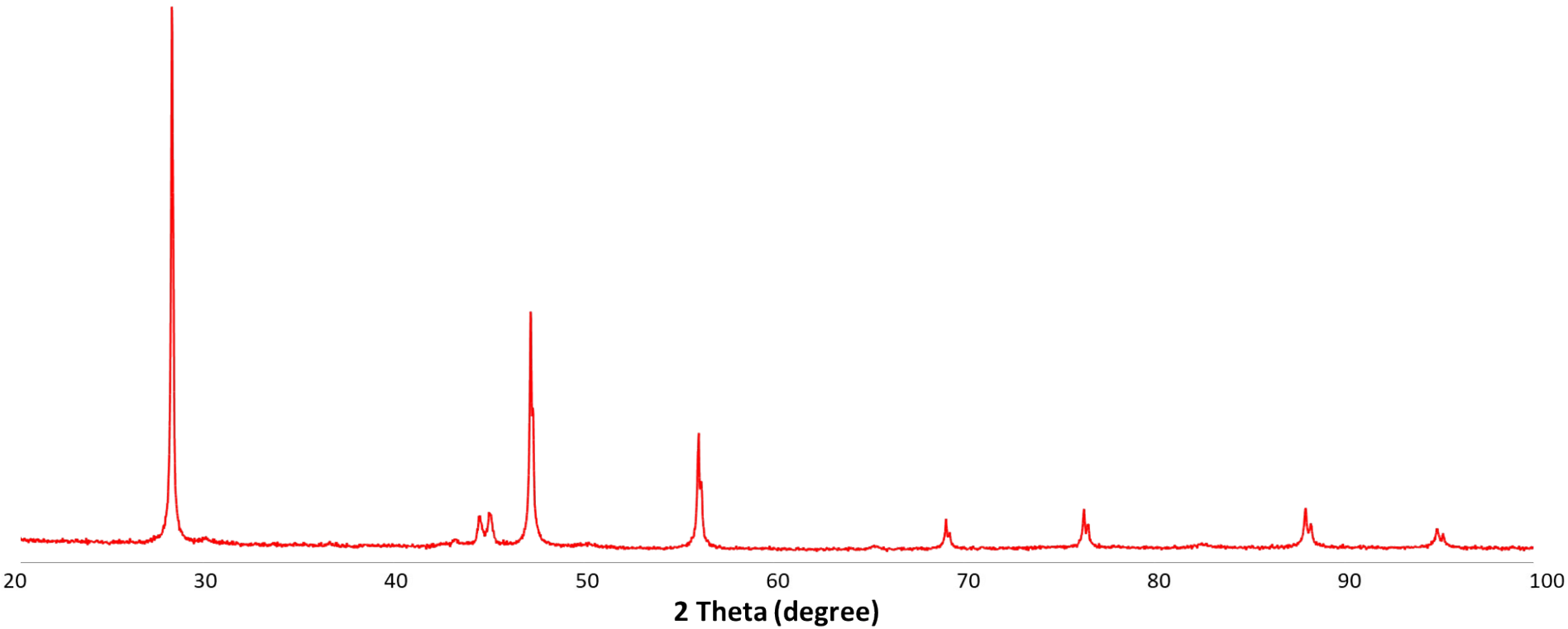

Figure S18. PXRD of contact mass Zr-Cu.

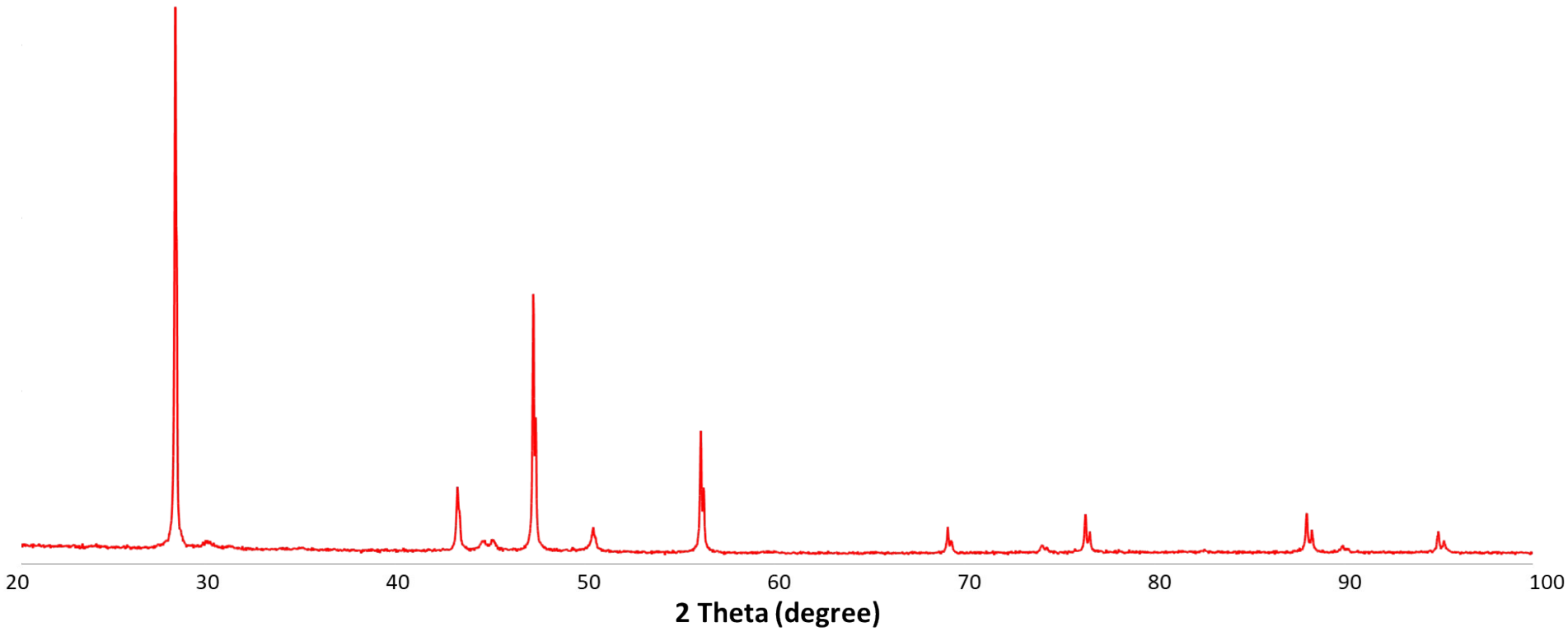

Figure S19. PXRD of contact mass Zr-Cu-Zn.

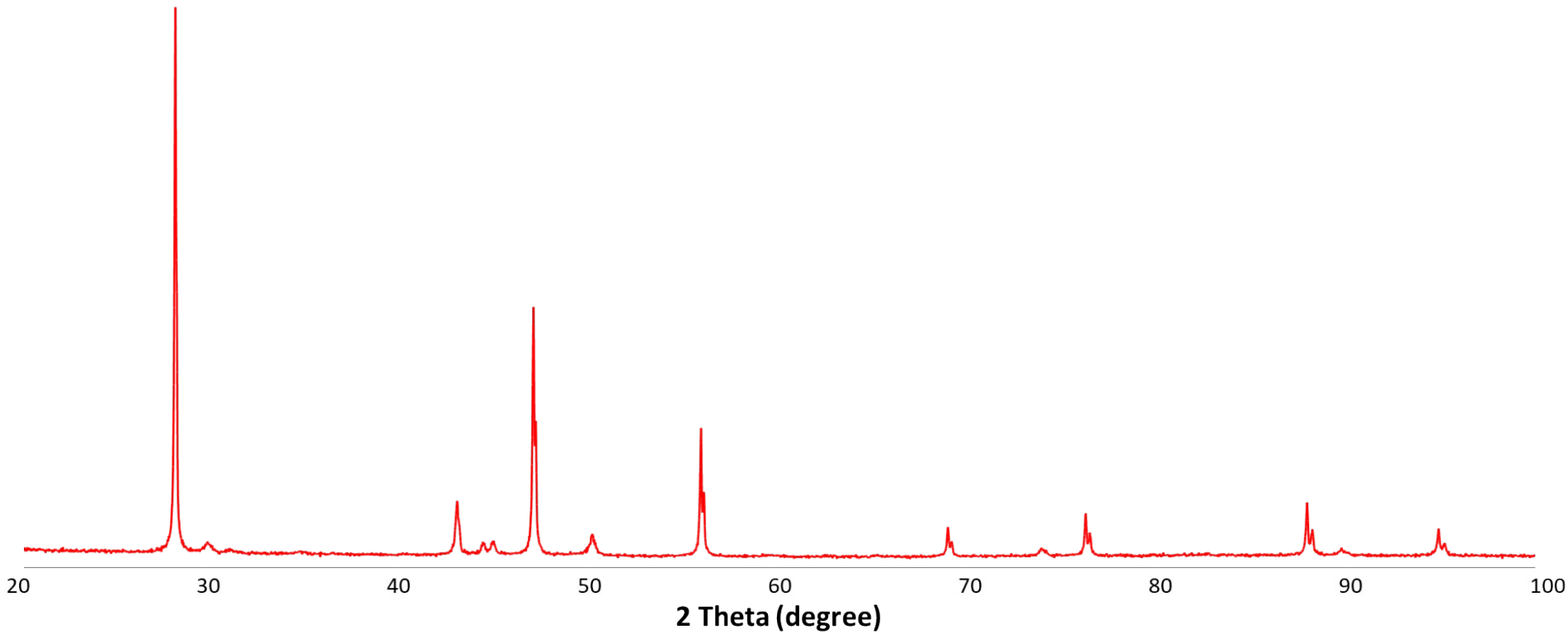

Figure S20. PXRD of contact mass Zr-Cu-Sn.

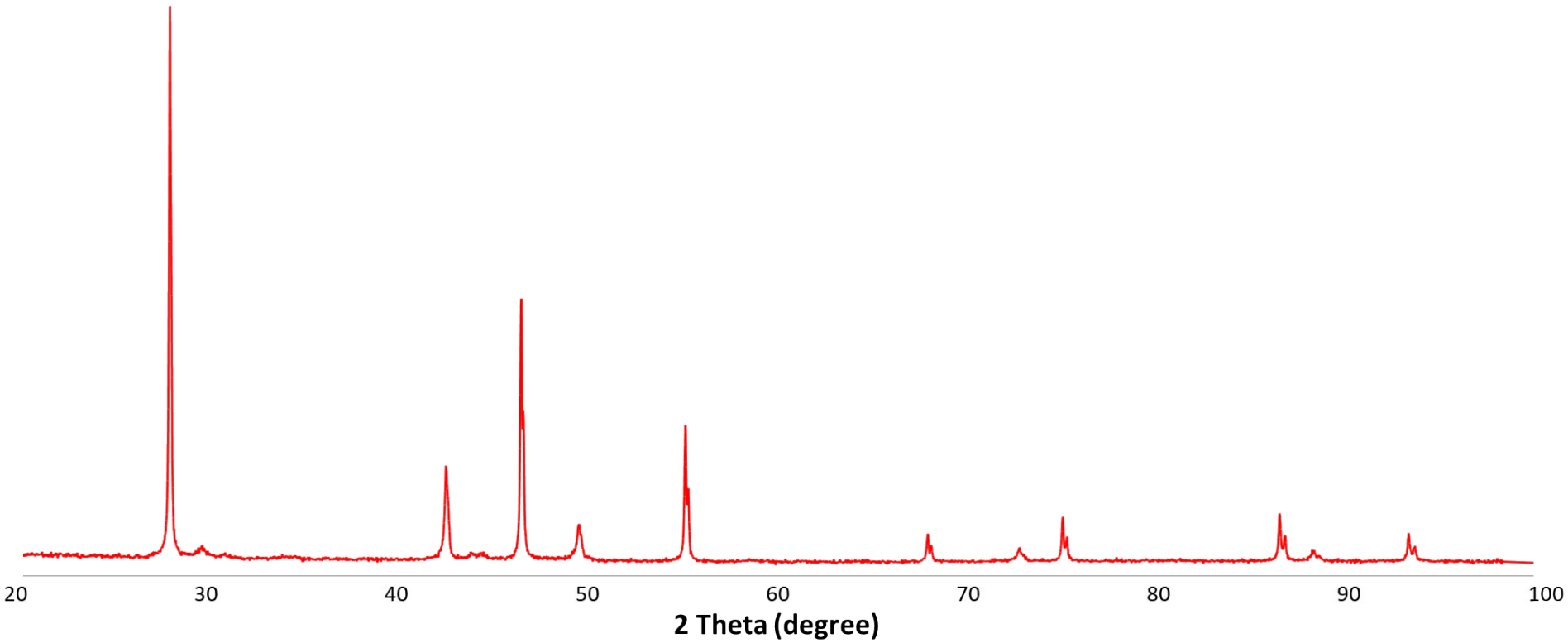

Figure S21. PXRD of contact mass Zr-Cu-Sn-Zn.

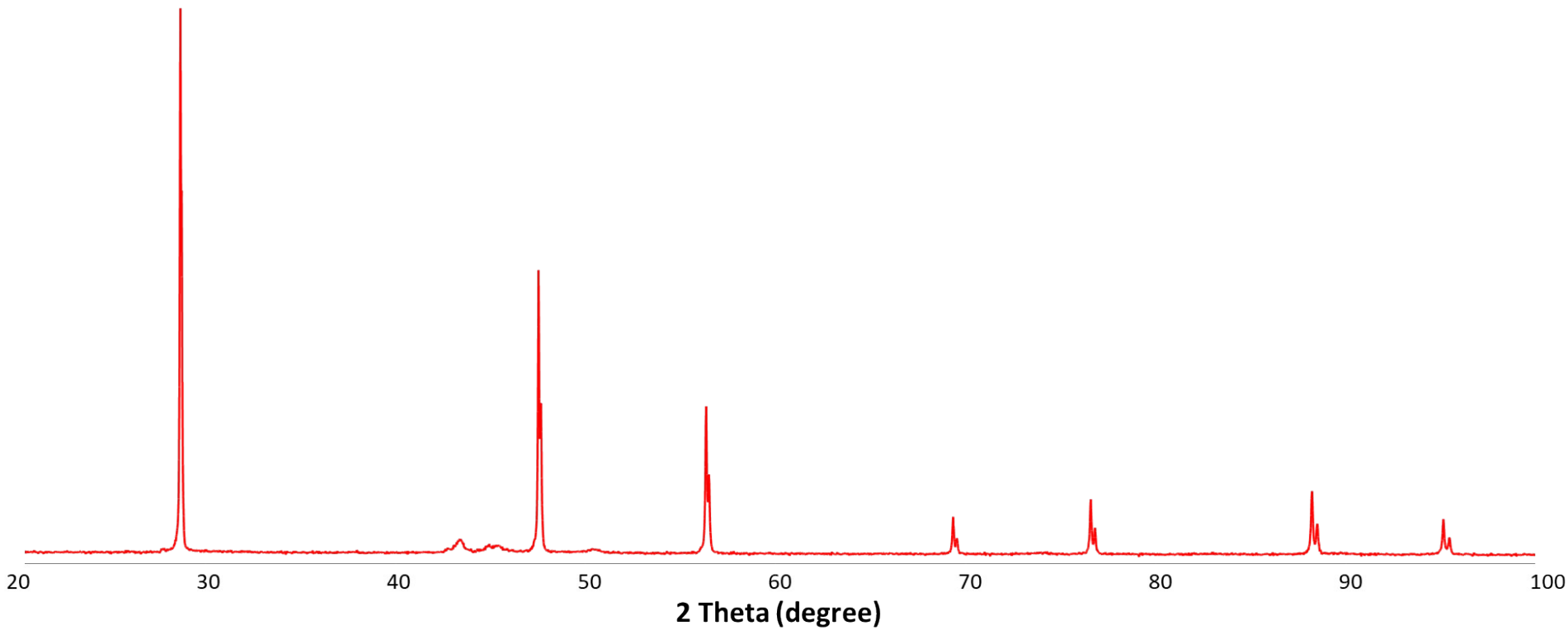

Figure S22. PXRD of contact mass Sn-30.

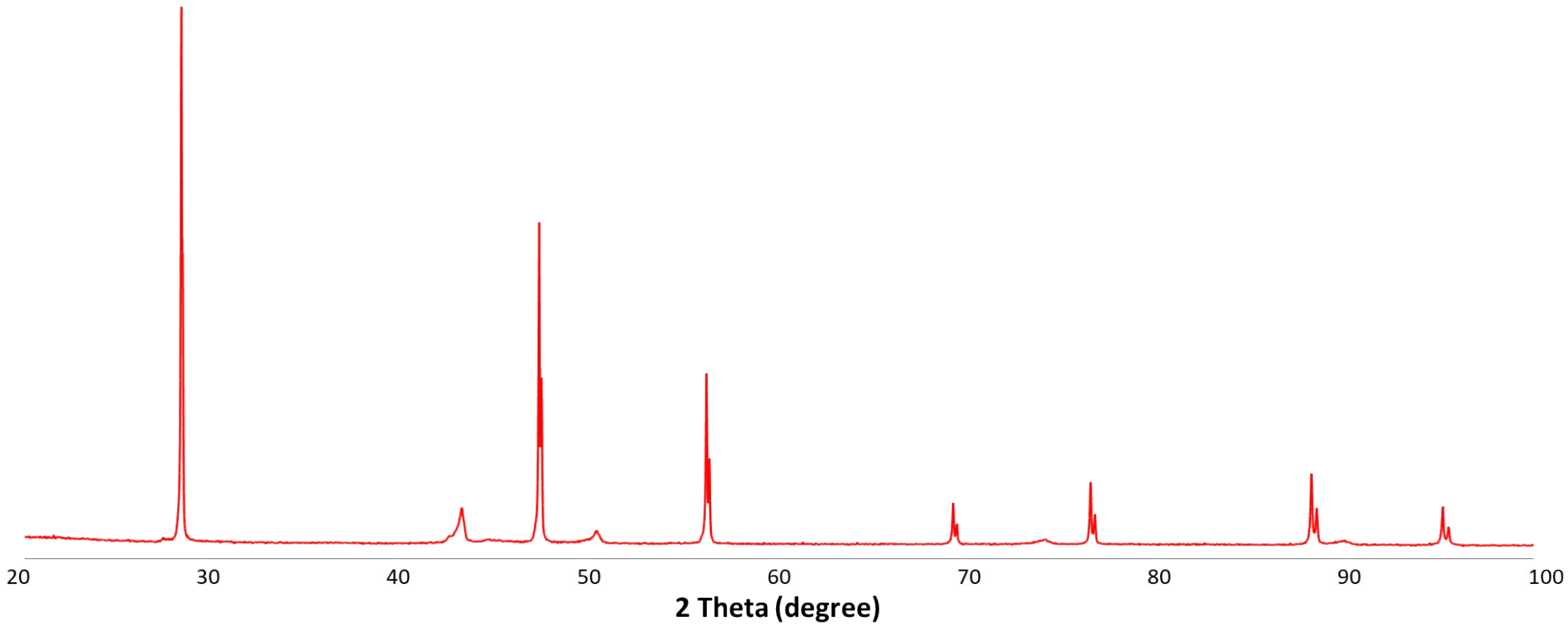

Figure S23. PXRD of contact mass Sn-60.

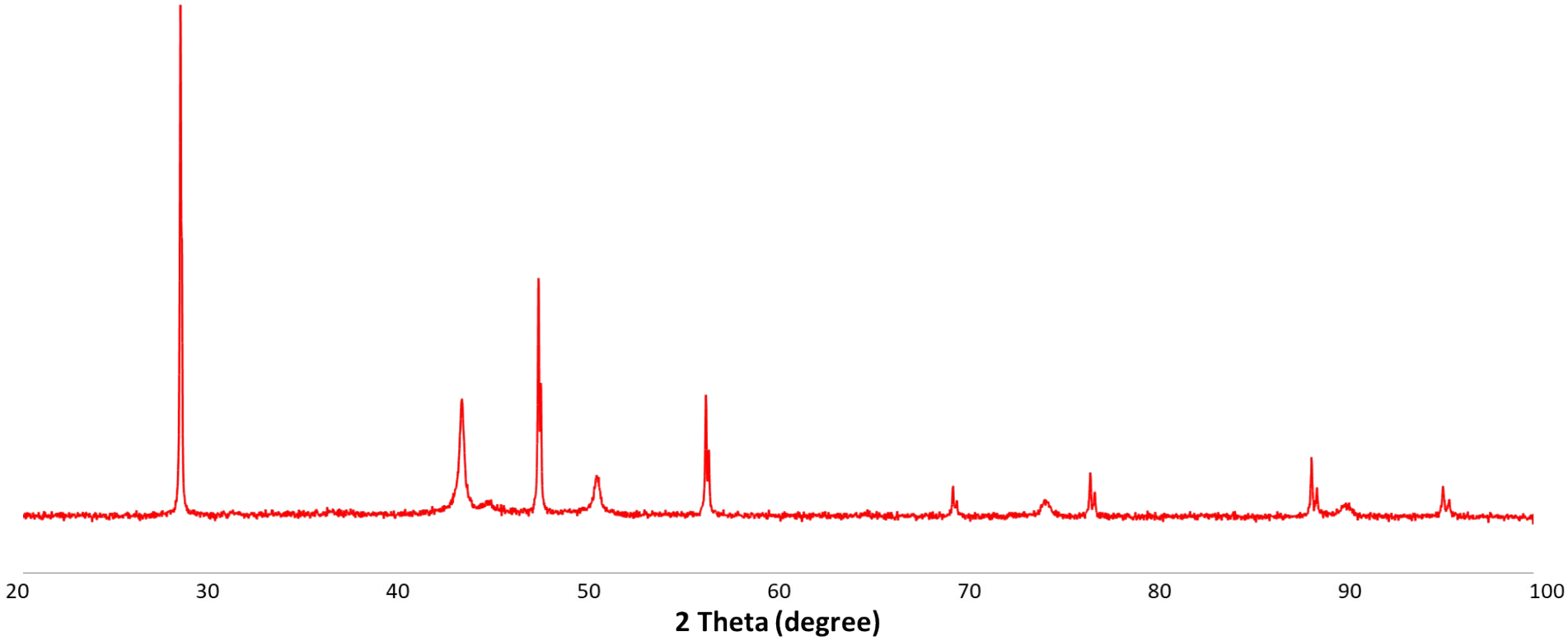

Figure S24. PXRD of contact mass Sn-120.

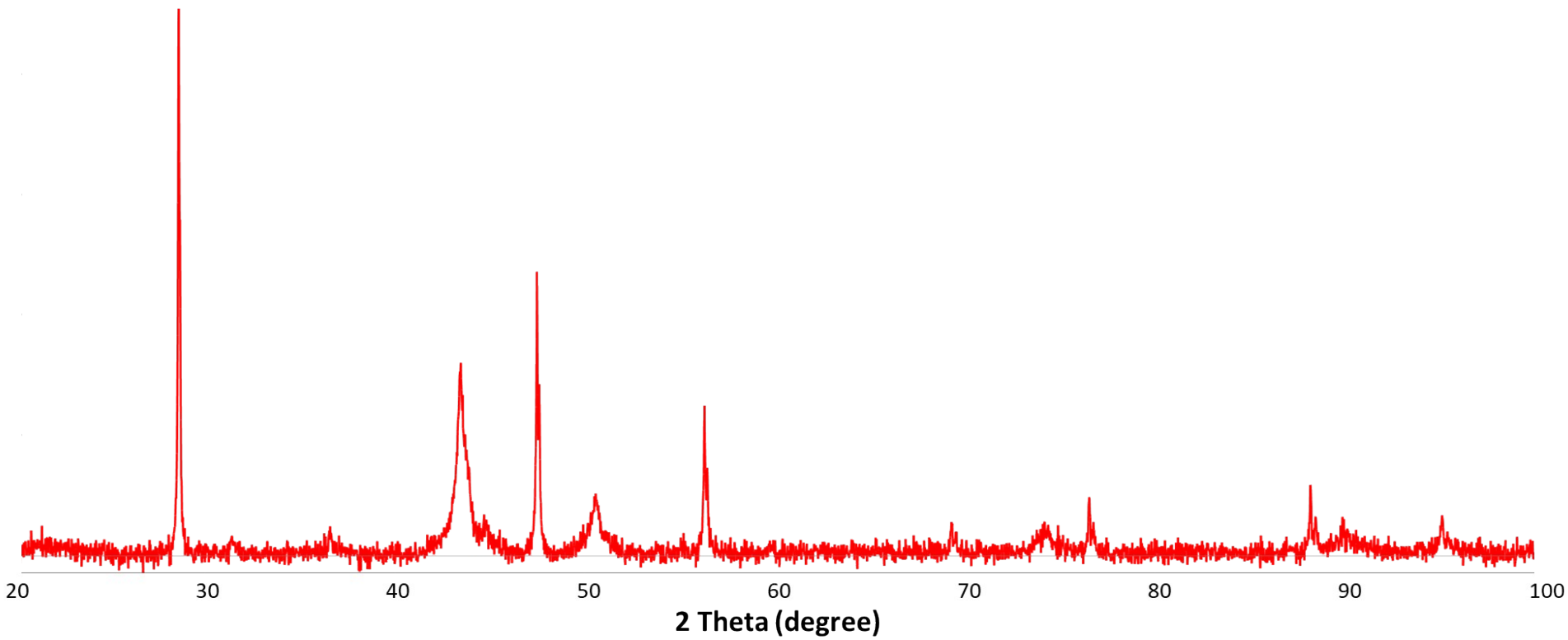

Figure S25. PXRD of contact mass Sn-240.

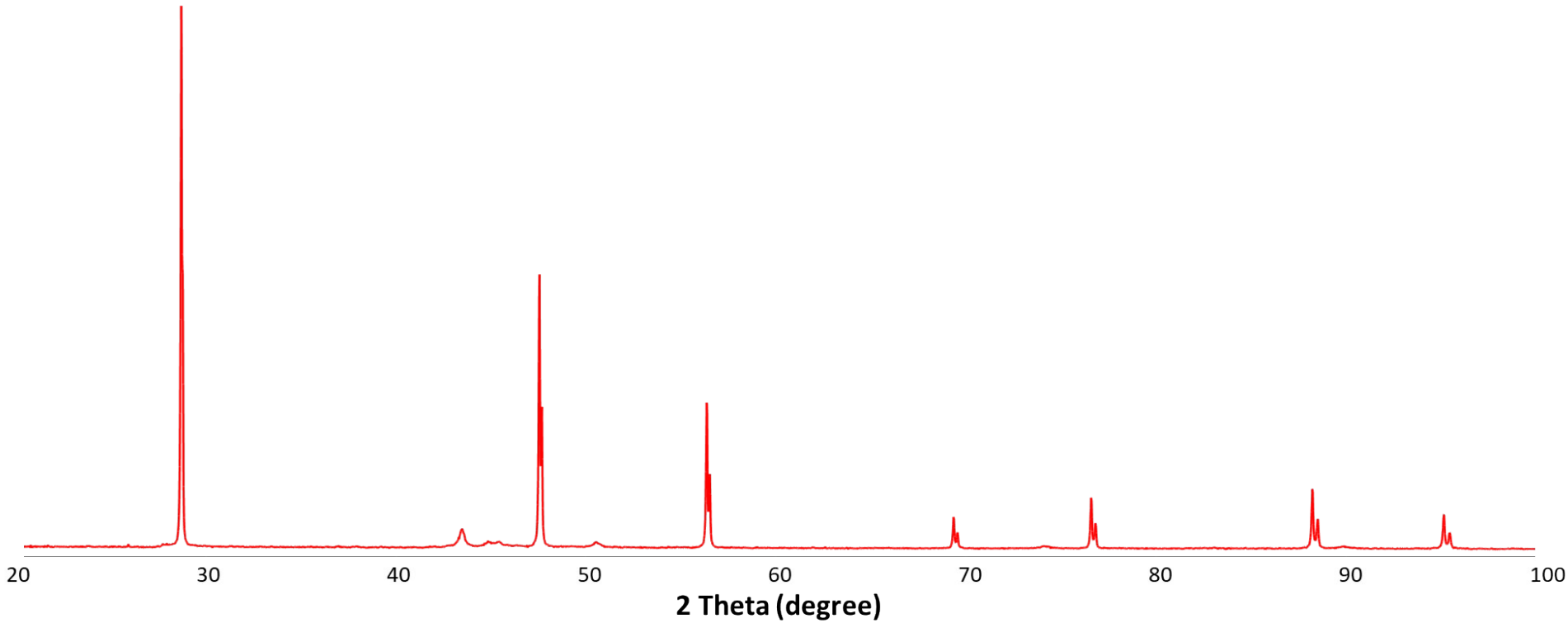

Figure S26. PXRD of contact mass $SnCl_2$-30.

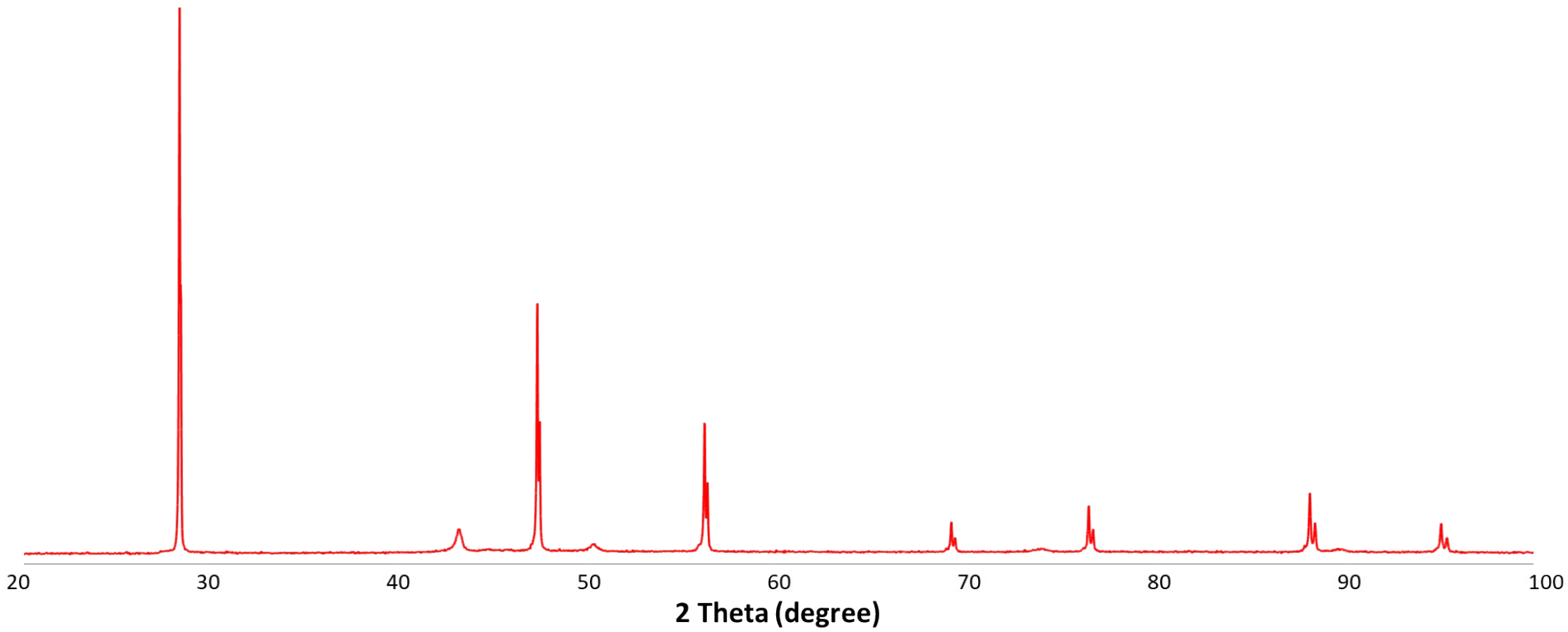

Figure S27. PXRD of contact mass $SnCl_2$-60.

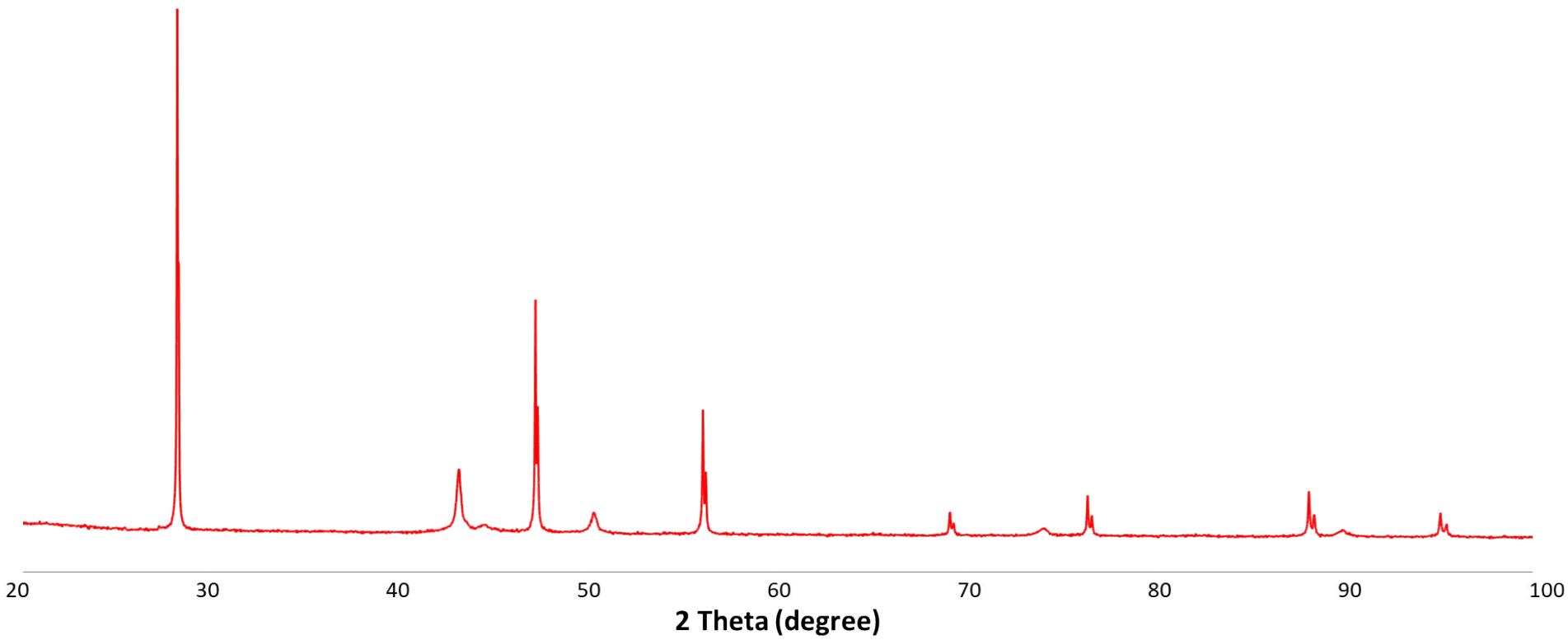

Figure S28. PXRD of contact mass $SnCl_2$-120.

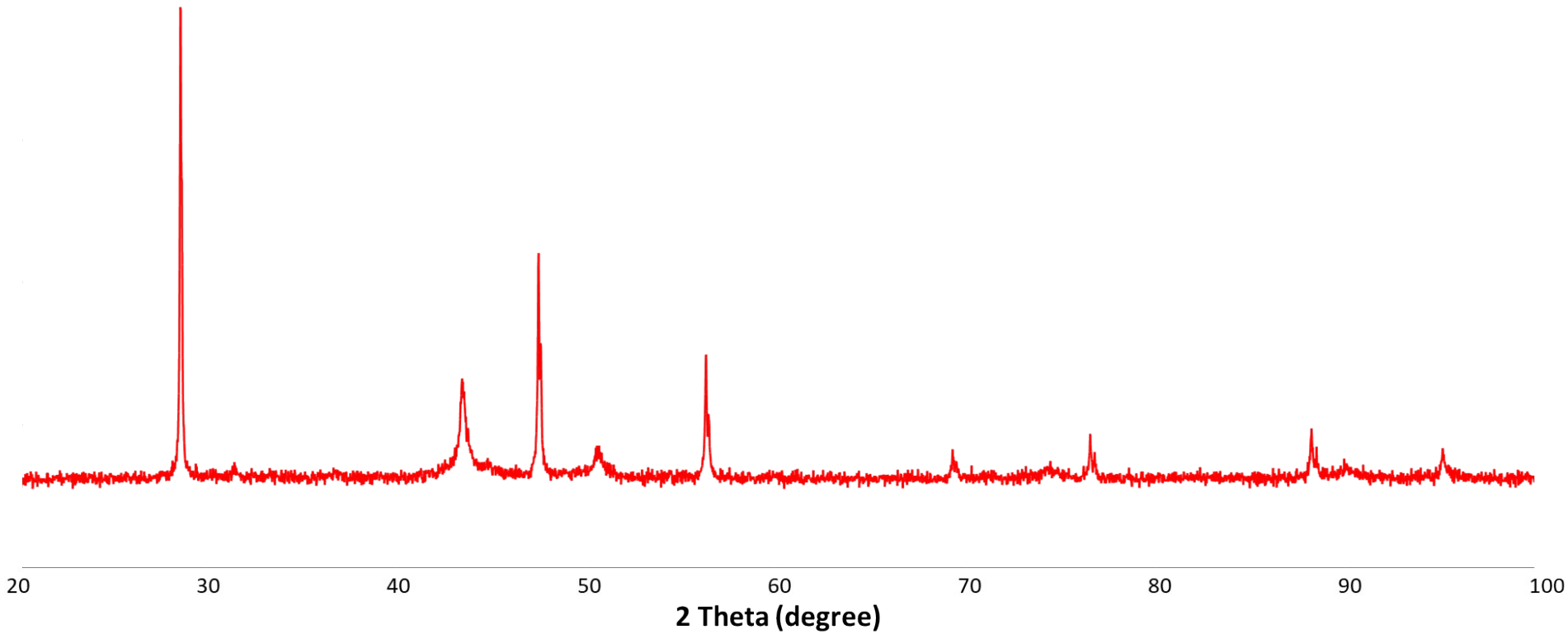

Figure S29. PXRD of contact mass $SnCl_2$-240.

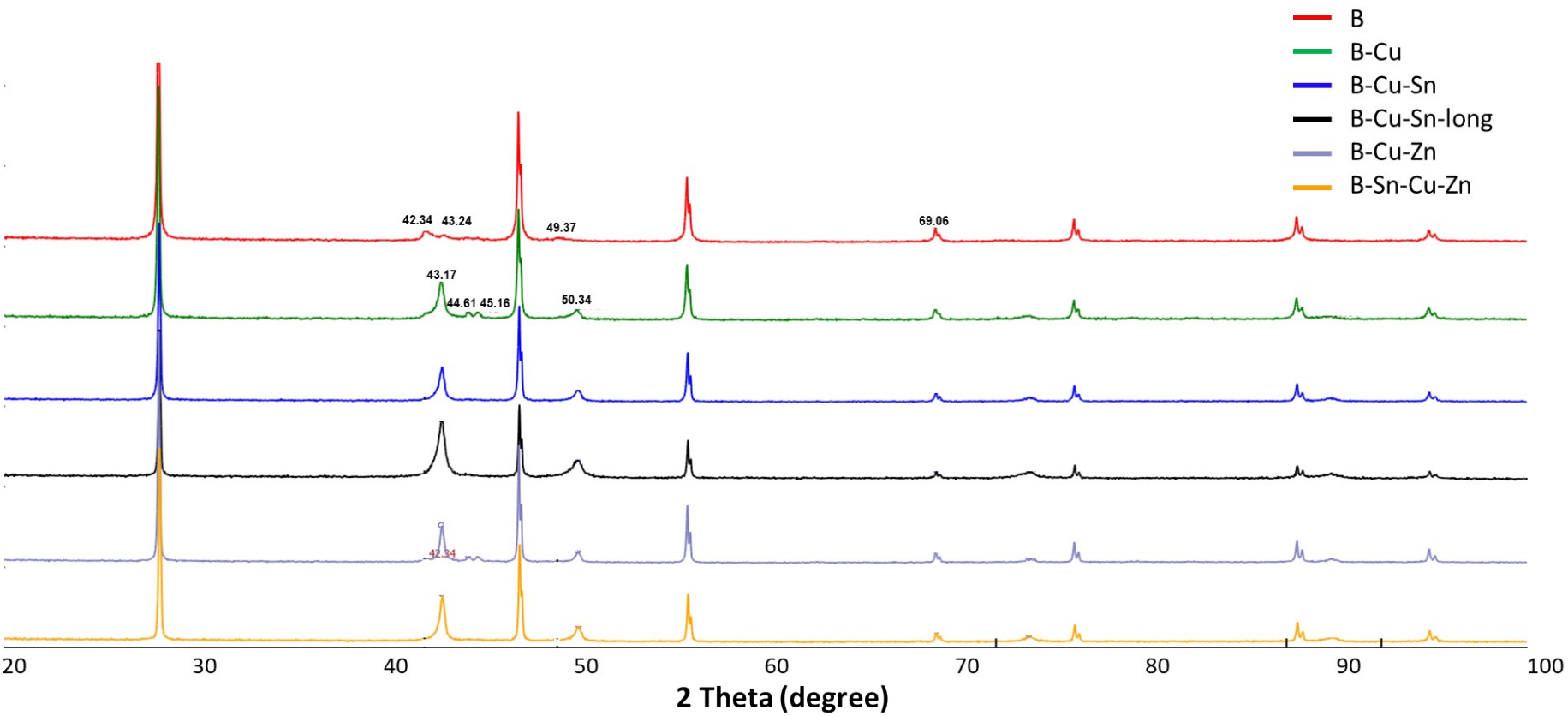

Figure S30. PXRD patterns of the direct synthesis contact masses obtained with brass milling bodies.

4.3. NMR

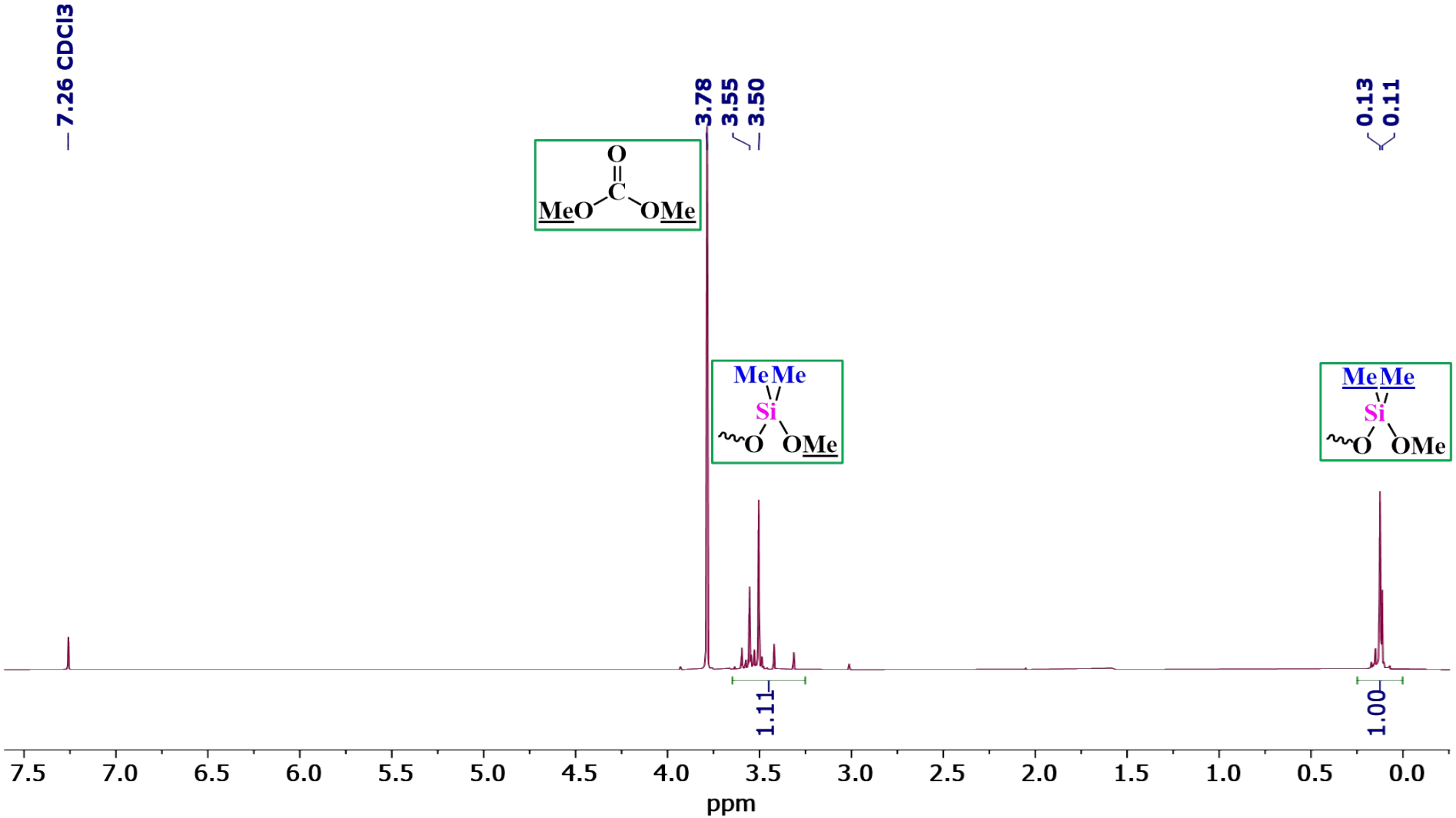

Figure S31. ^{1}H NMR spectrum for liquid products of direct methylmethoxysilanes synthesis.

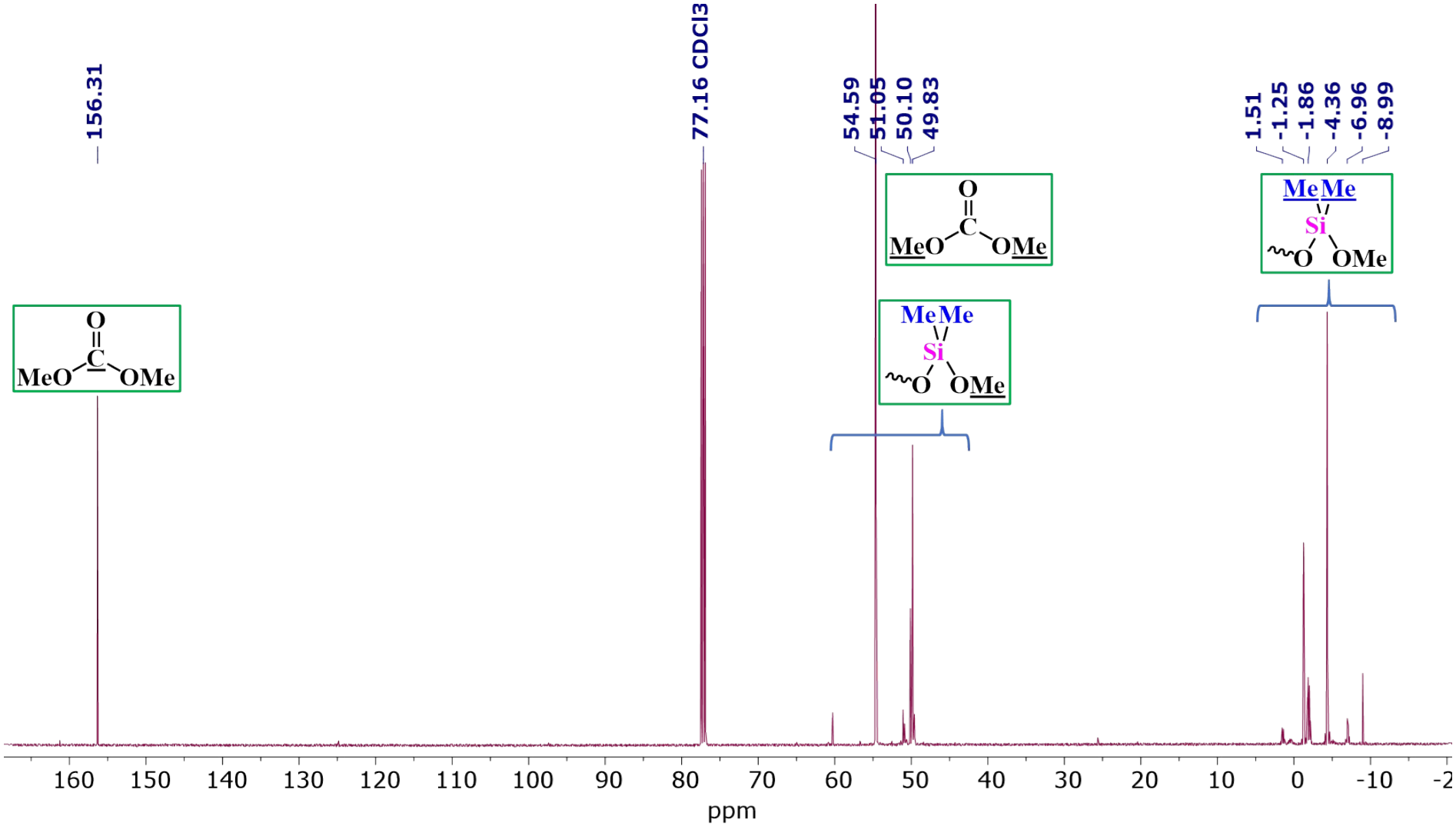

Figure S32. ^{13}C NMR spectrum for liquid products of direct methylmethoxysilanes synthesis.

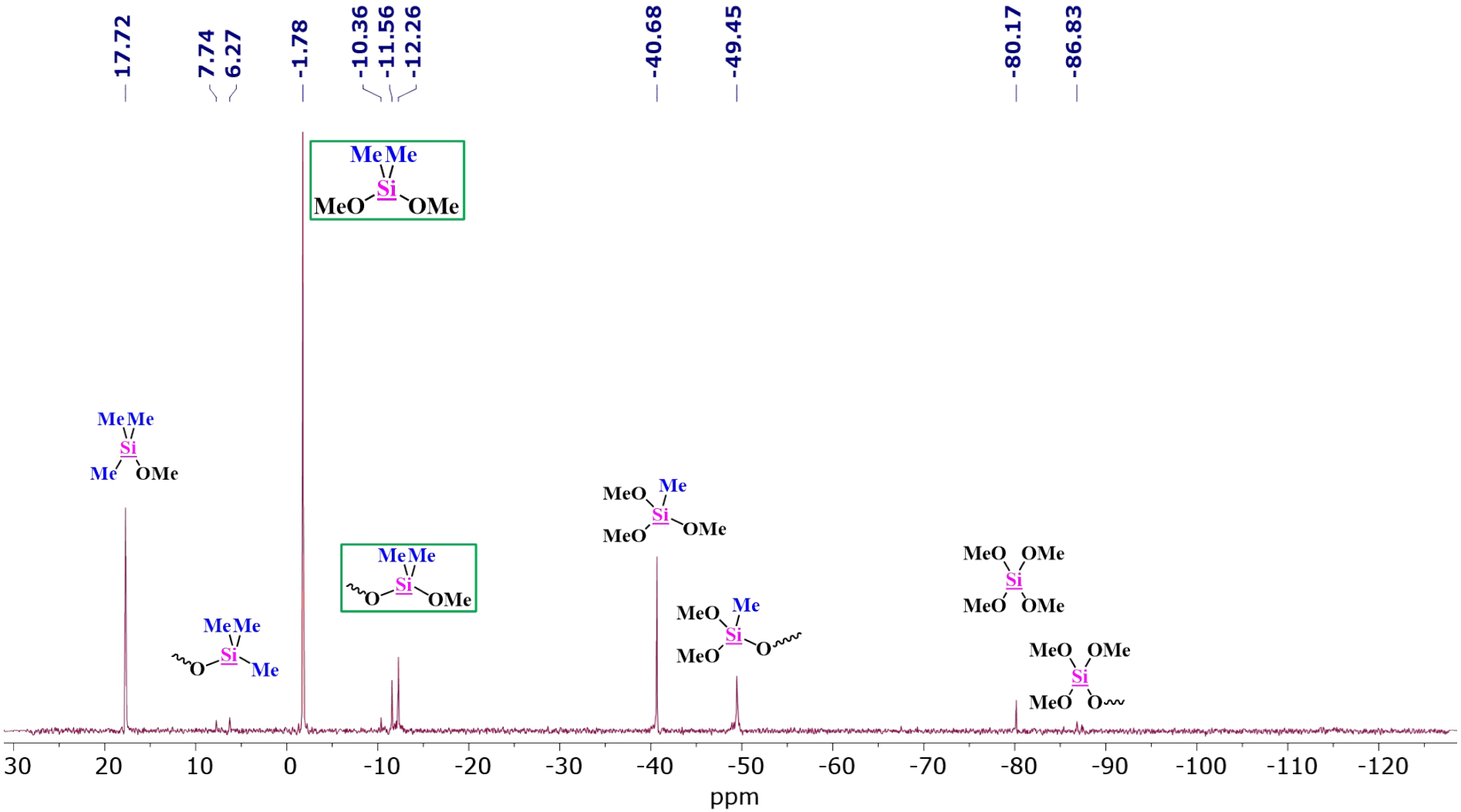

Figure S33. ^{29}Si NMR spectrum for liquid products of direct methylmethoxysilanes synthesis.

4.4. GC

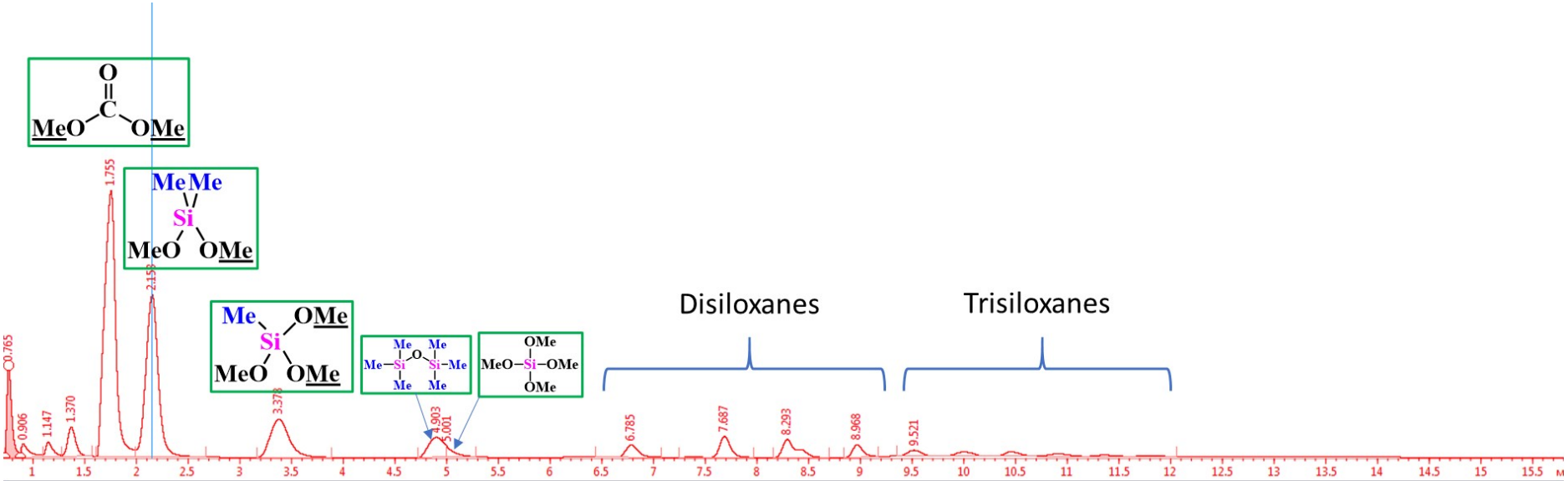

Time, min		Concentration, %
0.765	5.000	5.685
0.906	5.000	1.385
1.147	5.000	1.360
1.370	5.000	3.004
1.755	5.000	36.868
2.153	5.000	24.856
3.378	5.000	8.911
4.903	5.000	3.757
5.001	5.000	0.952
6.785	5.000	1.922
7.687	5.000	2.818
8.293	5.000	3.242
8.968	5.000	1.520
9.521	5.000	3.720

Figure S34. GC chromatogram for liquid products of direct methylmethoxysilanes synthesis.

4.5. GC-MS analysis

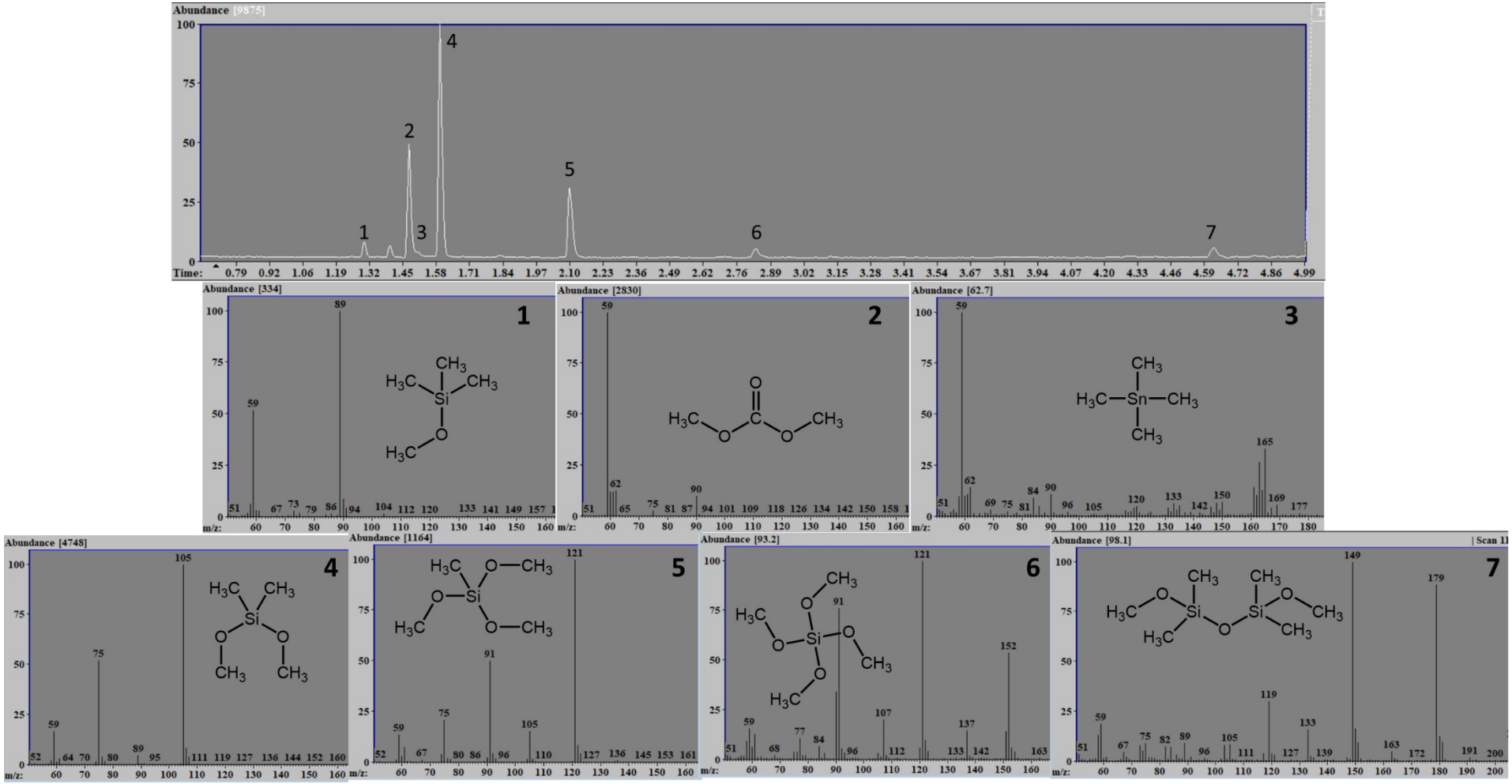

Figure S35. GC-MS analysis of products mixture after the synthesis with DMC in decane.

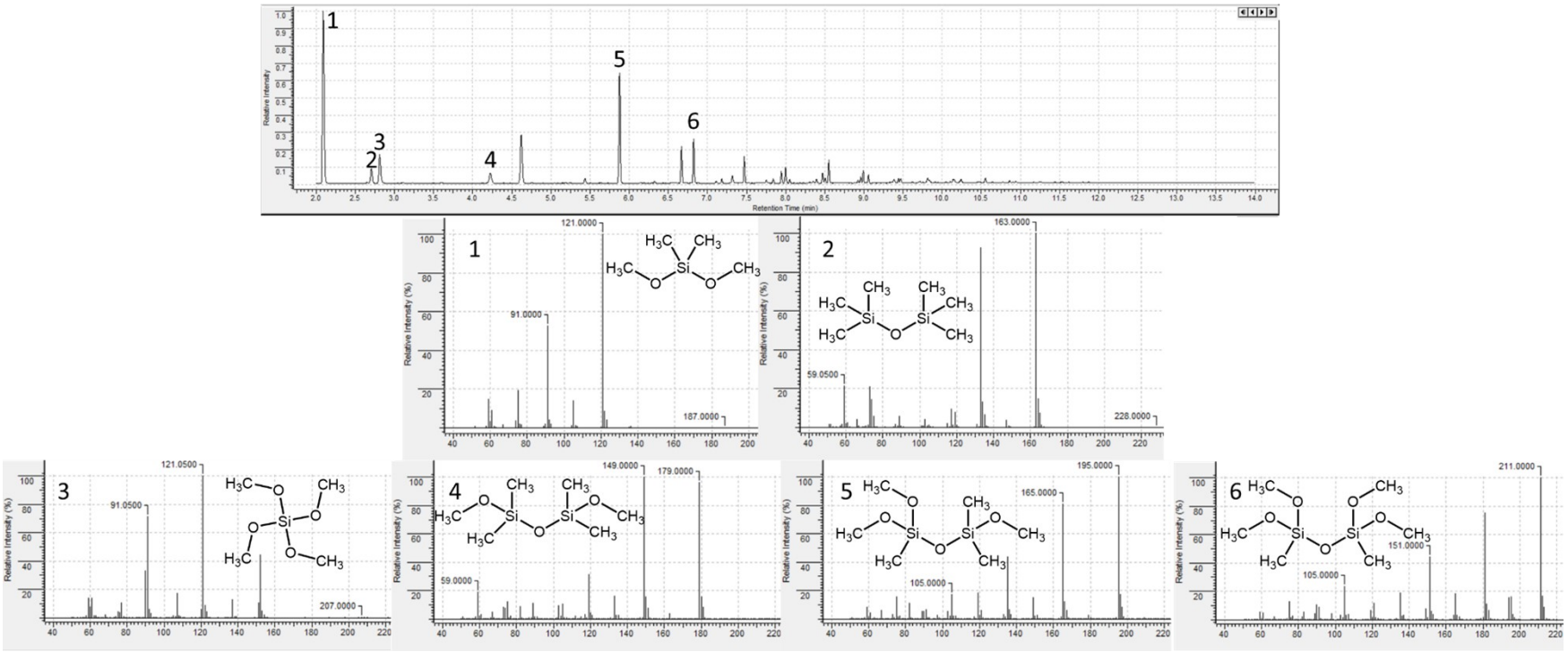

Figure S36. GC-MS analysis of products mixture after the synthesis with DMC in diethyl ether.

4.6. XPS – spectra, tables and description

Experiment

X-Ray photoelectron spectroscopy (XPS) was carried out on an Axis Ultra DLD spectrometer (Kratos) using monochromatic Al Kα radiation with an X-ray beam power of 150 W. Survey spectra and high-resolution spectra were recorded at pass energies of 160 and 40 eV, respectively. Survey spectra were recorded with a step of 1 eV, while high-resolution spectra were recorded with a step of 0.1 eV The dimensions of the explored area were 300 × 700 μm^2. Samples were mounted on a holder using a double-sided adhesive tape and studied at room temperature at the residual pressure in the spectrometer chamber no higher than 10−8 Torr. The energy scale of the spectrometer was calibrated according to the standard procedure based on the following binding energies (purified by ion sputtering of metal surfaces): Au $4f_{7/2}$ – 83.96 eV, Cu $2p_{3/2}$ – 932.62 eV, Ag $3d_{5/2}$ – 368.21 eV. To eliminate the effect of sample charging, the spectra were recorded using a neutralizer. Surface charging was taken into account based on the Si 2p3/2 peak of the Si(0) state with a binding energy of 99.34 eV.[1] The background due to electron inelastic energy losses was subtracted by the Shirley method. Quantification was performed using atomic sensitivity factors included in the software of the spectrometer.

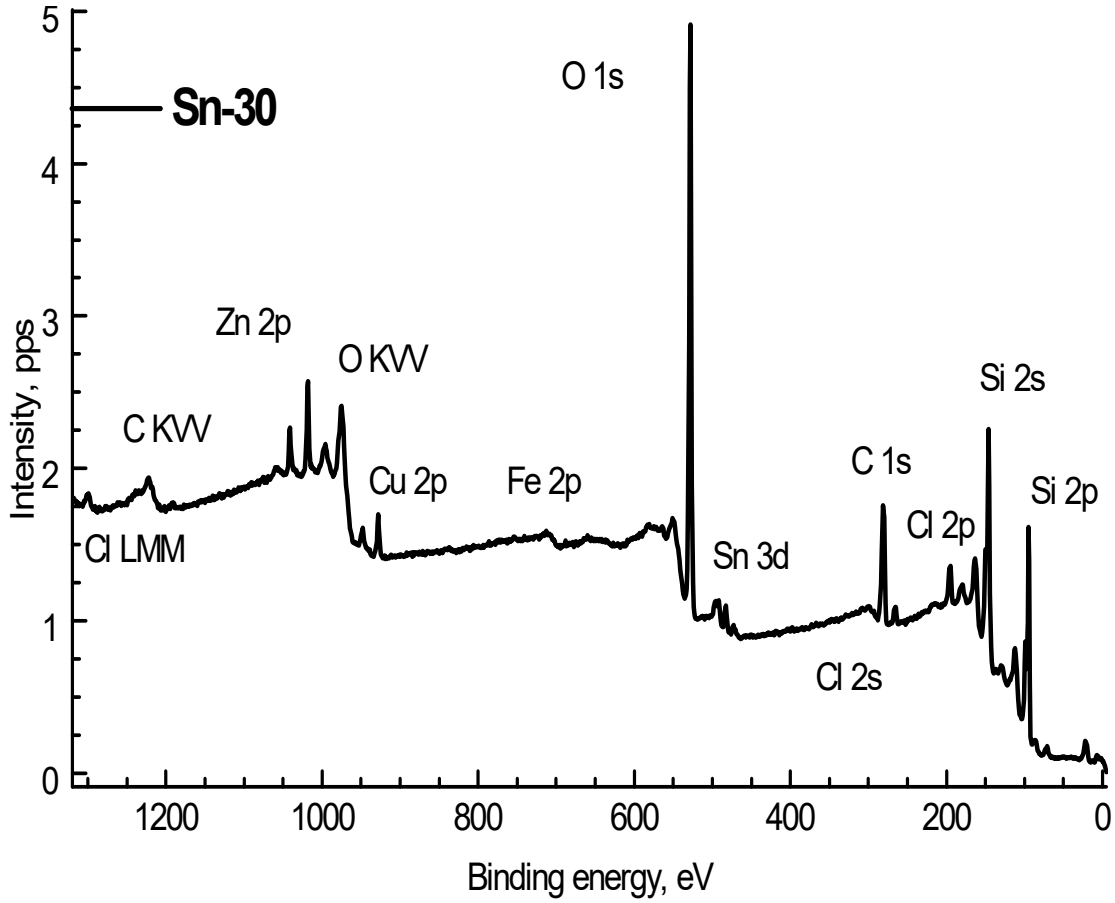

Figure S37. Survey spectrum of sample Sn-30.

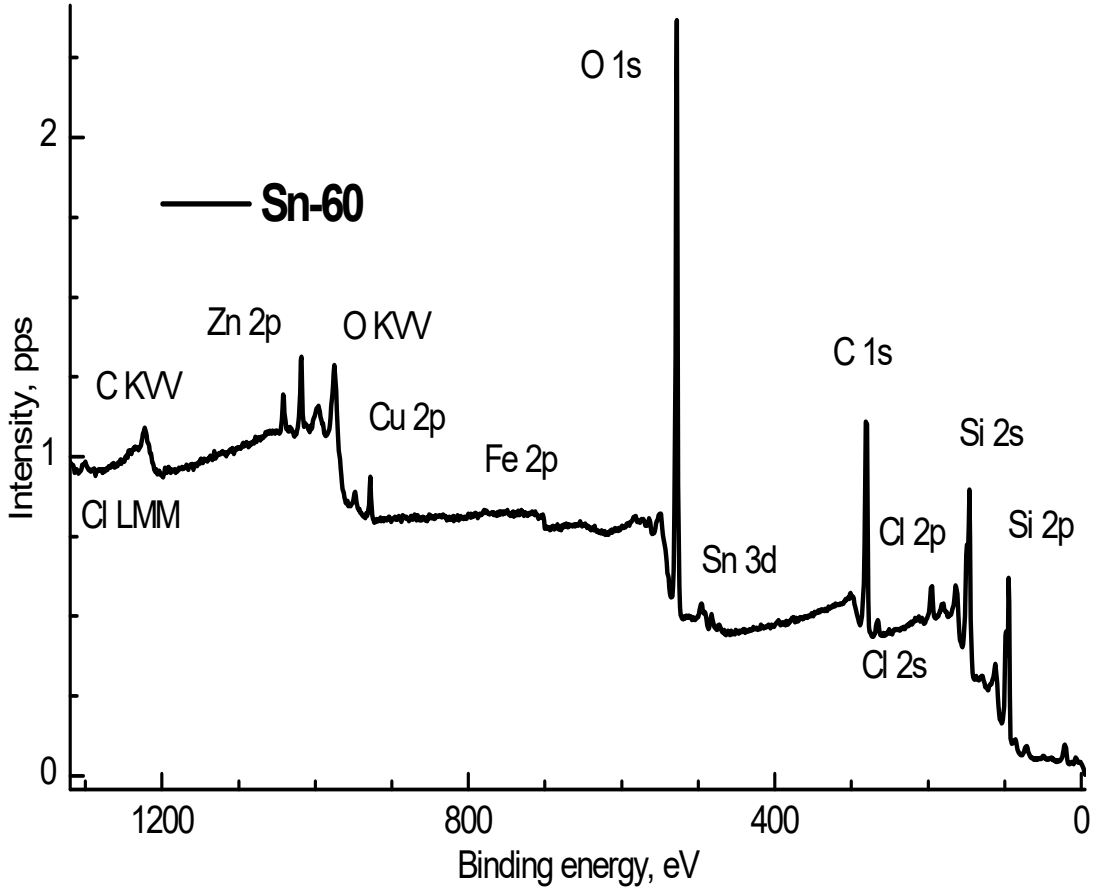

Figure S38. Survey spectrum of sample Sn-60.

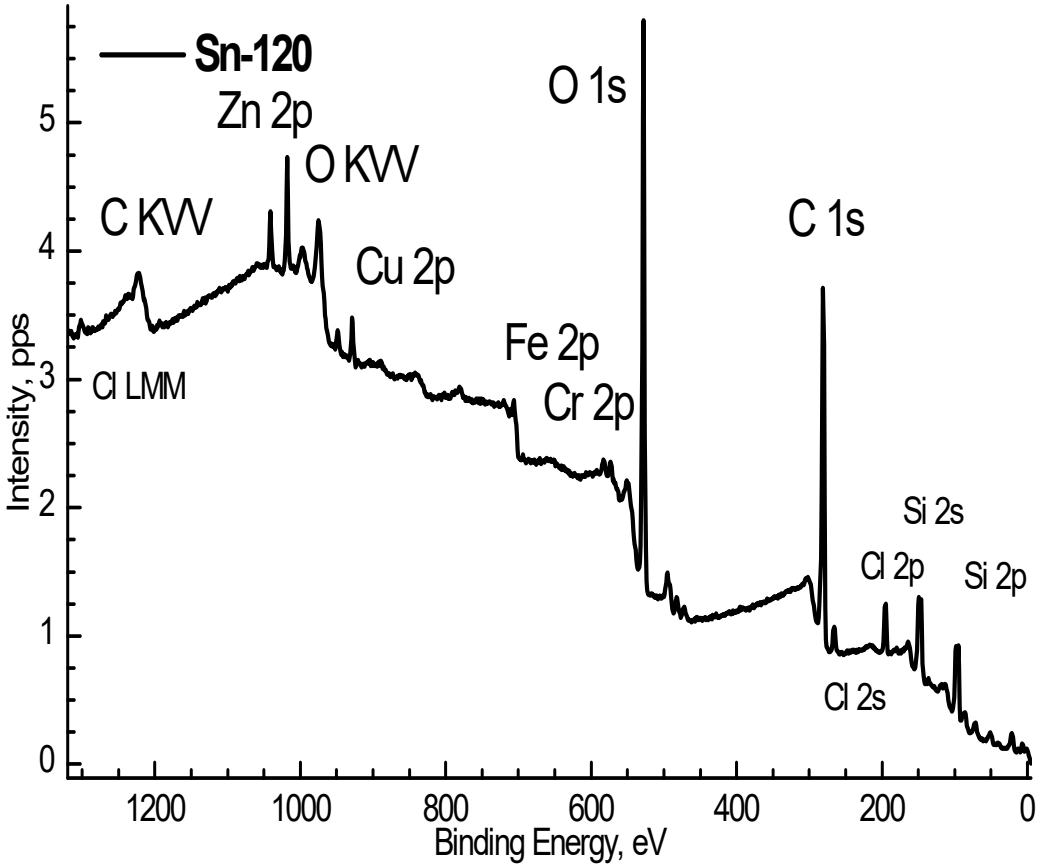

Figure S39. Survey spectrum of sample Sn-120.

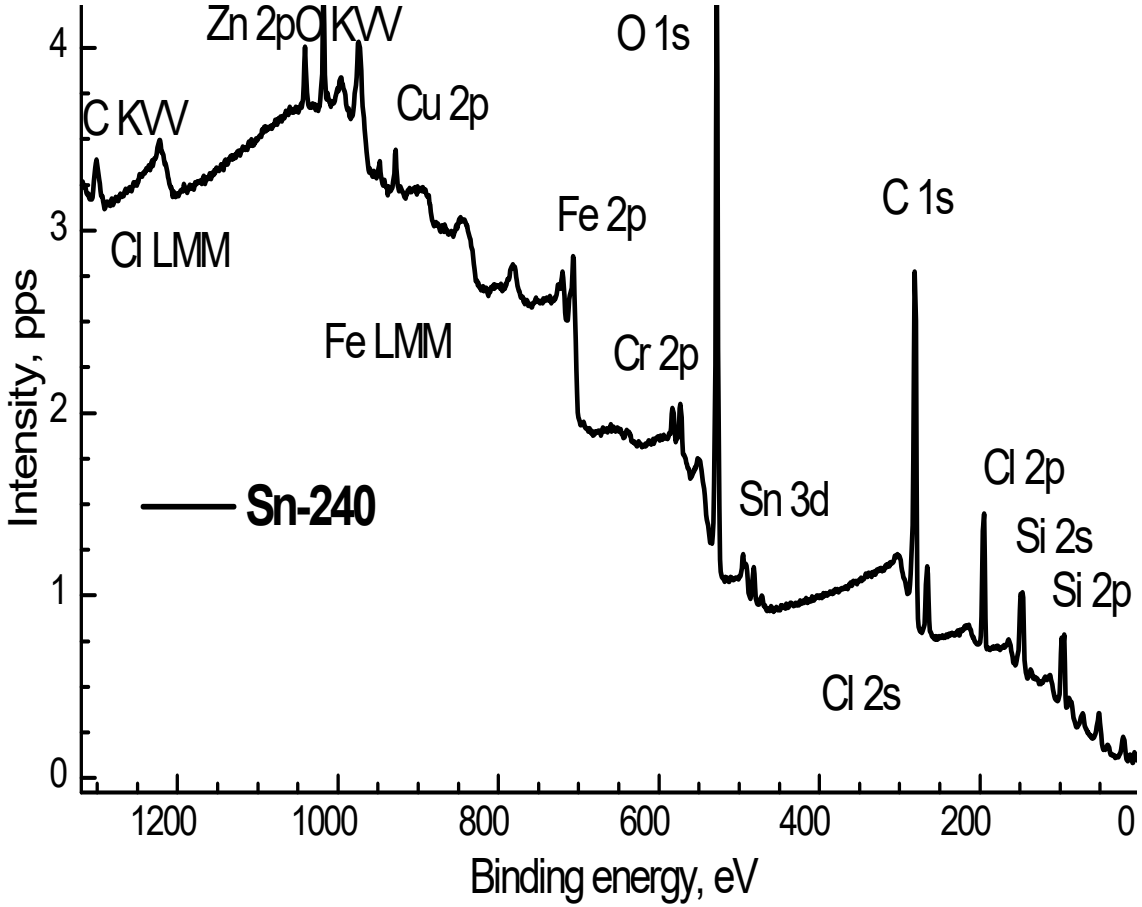

Figure S40. Survey spectrum of sample Sn-240.

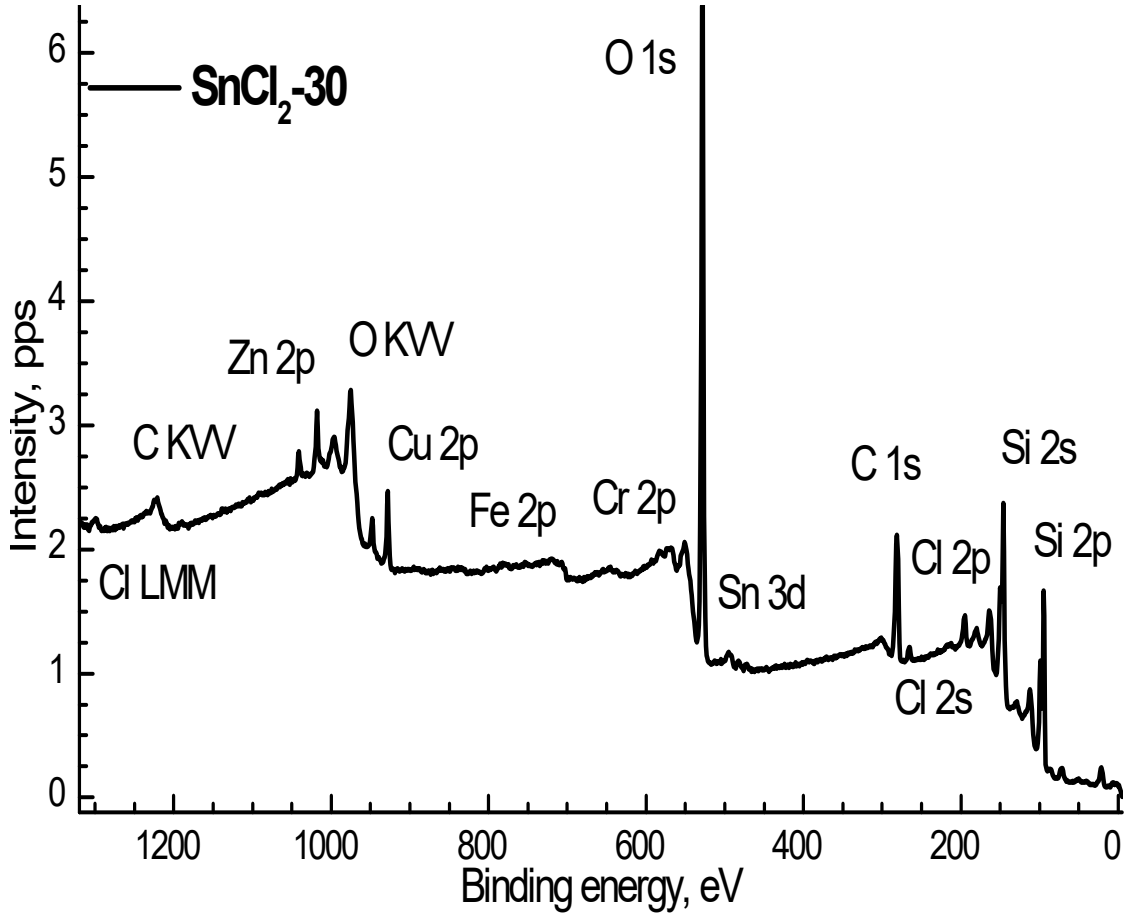

Figure S41. Survey spectrum of sample $SnCl_2$-30.

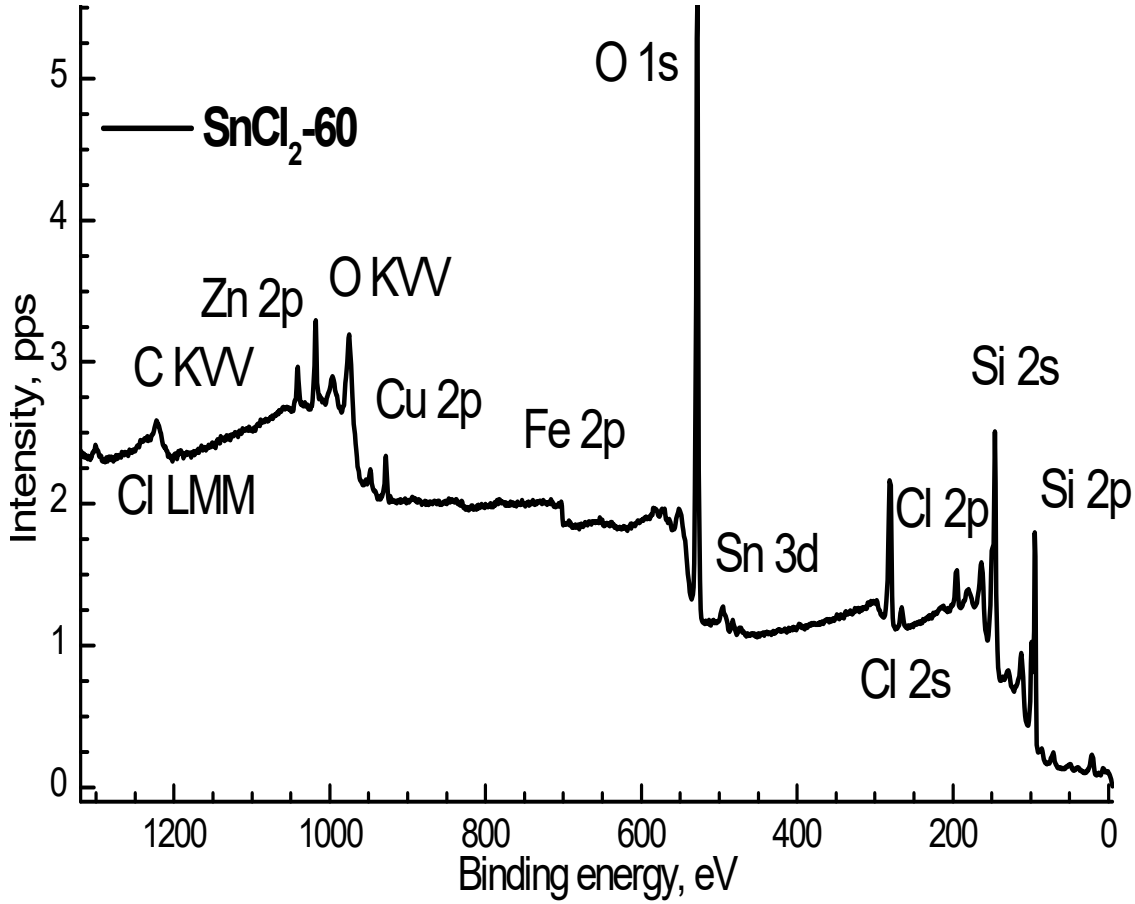

Figure S42. Survey spectrum of sample $SnCl_2$-60.

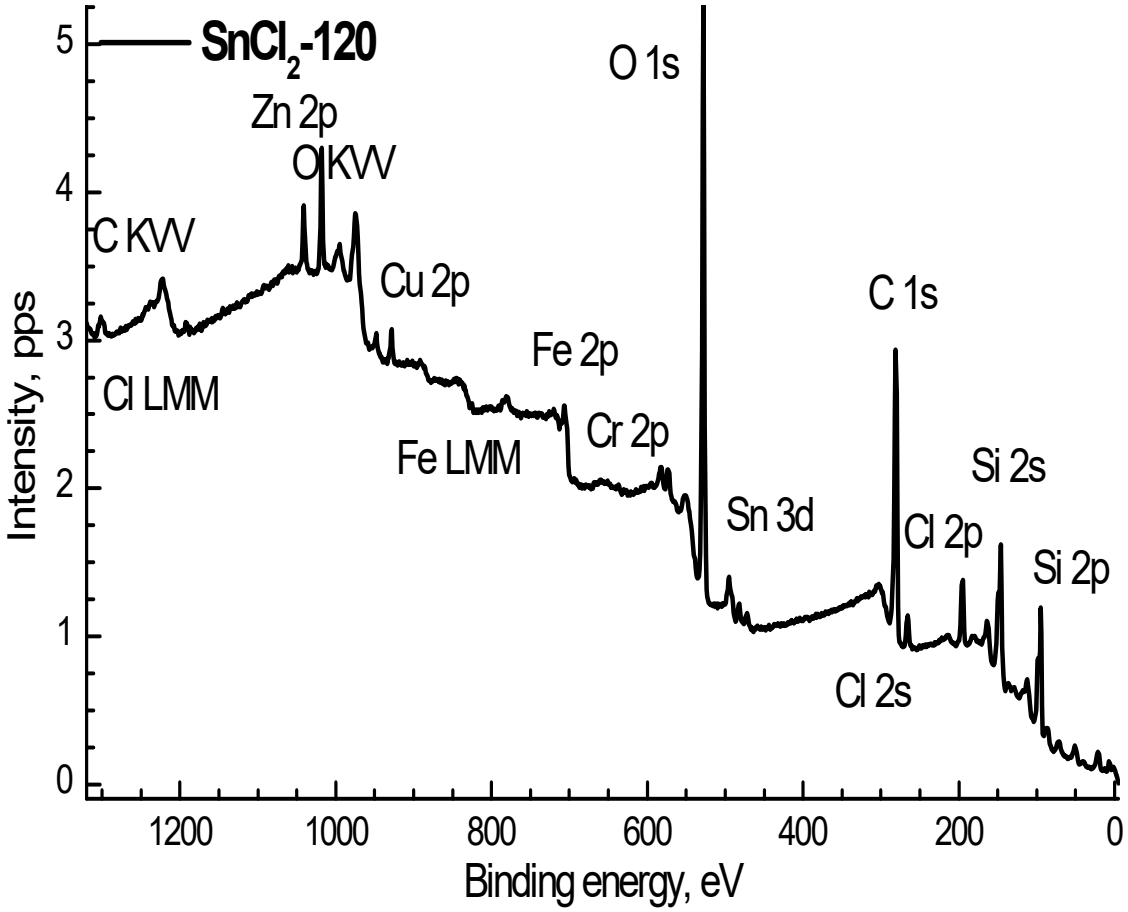

Figure S43. Survey spectrum of sample $SnCl_2$-120.

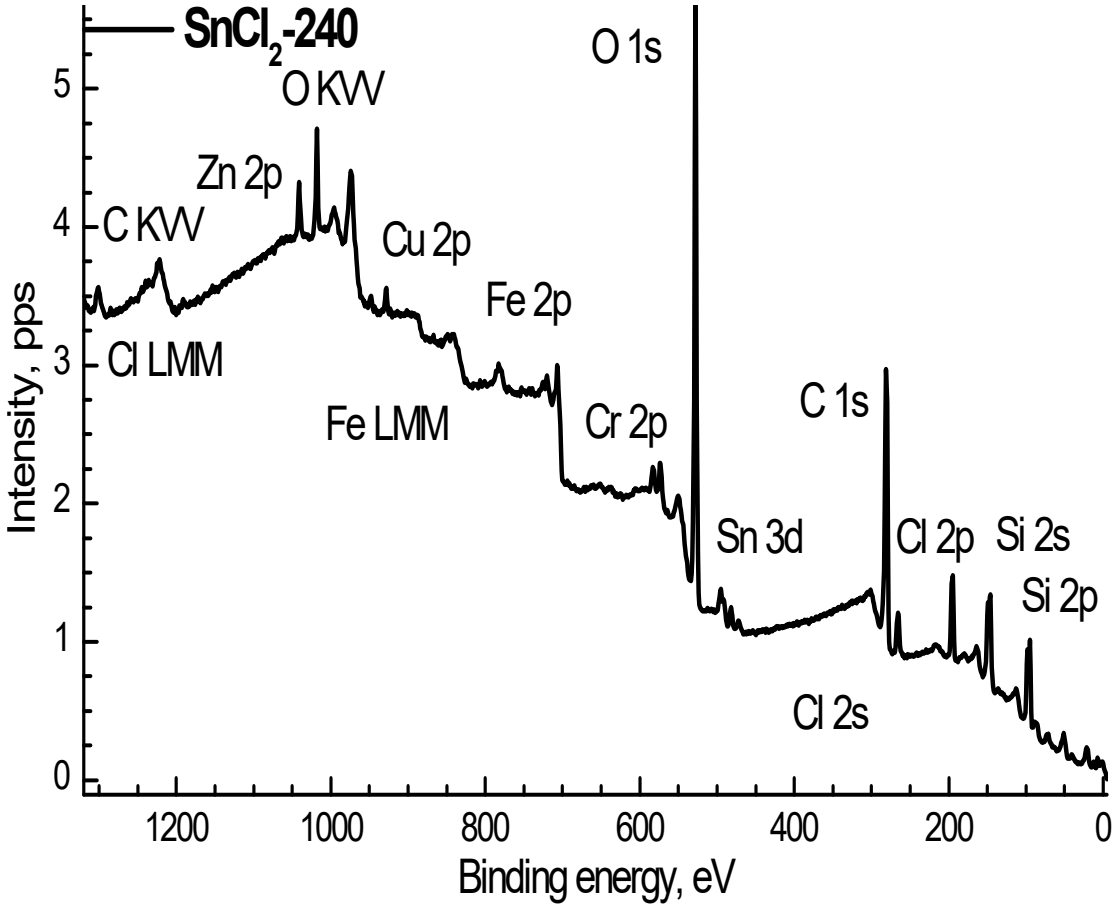

Figure S44. Survey spectrum of sample $SnCl_2$-240.

Considering the possibility of copper reduction under the influence of X-ray radiation, Cu 2p spectra were recorded at the beginning and end of the experiment (**Figure S45).** To minimize exposure, the recording of spectra commenced with the Cu 2p spectrum. The presented spectra show no changes in the shape of the spectral lines, indicating that copper was not reduced.

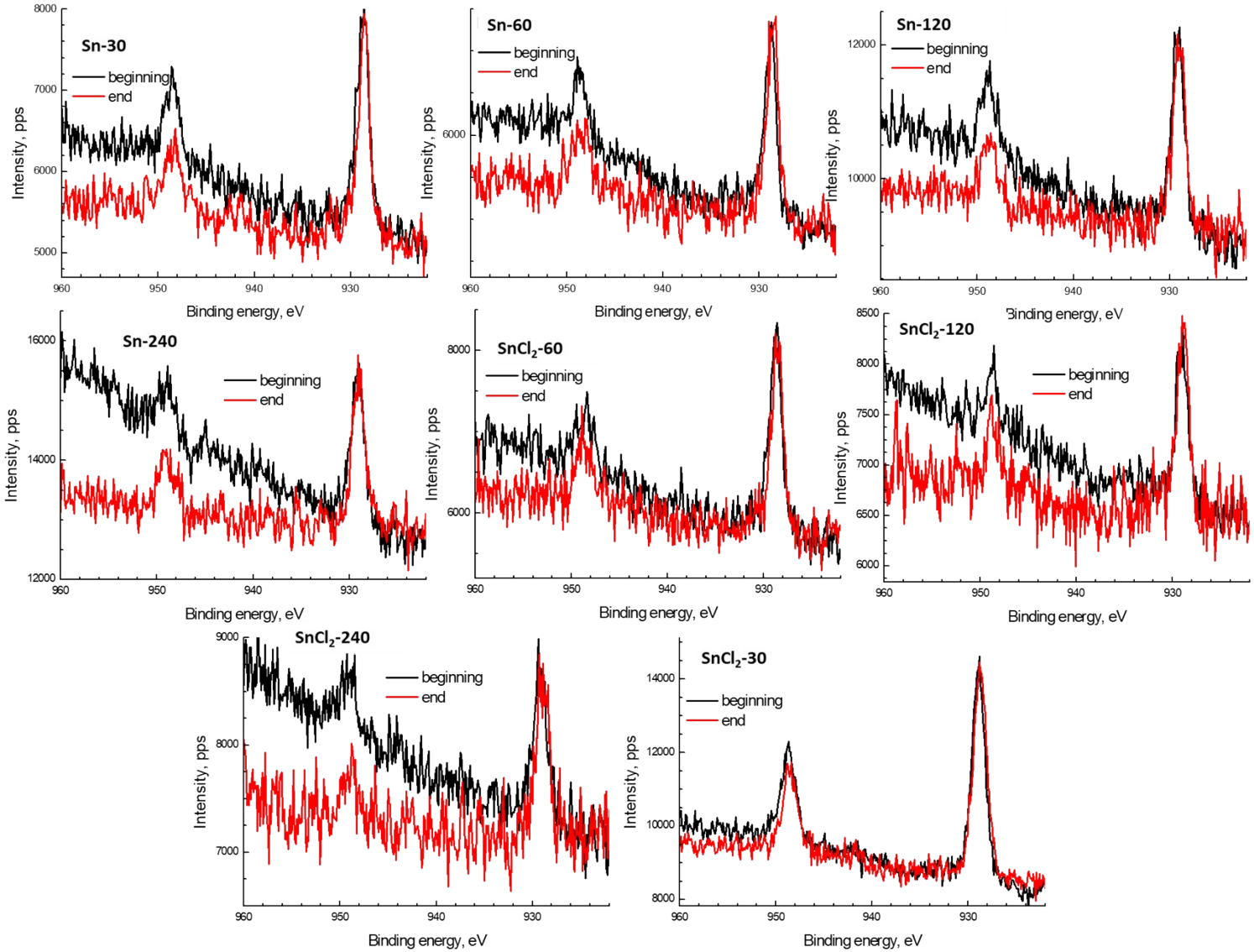

Figure S45. Photoelectron spectra of Cu 2p of the studied samples, measured at the beginning and end of the recording of the spectra.

Results and Discussion

Figure S46 displays the Si 2p photoelectron spectra of the examined samples, normalized by the intensity of the low-energy peak corresponding to the Si^0 state. These spectra qualitatively reflect the relative concentrations of Si^{4+} and Si^0 states, as well as being normalized by the Si concentration in the samples.

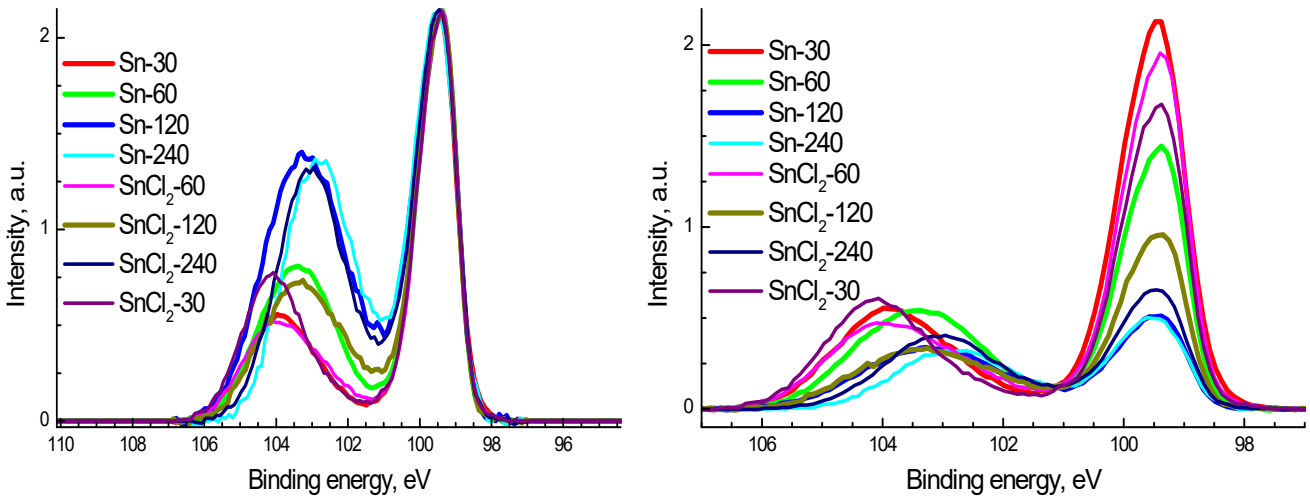

Figure S46. Si 2p photoelectron spectra of the examined samples, the spectra are normalized by intensity of the main peak (a) and Si concentration (b).

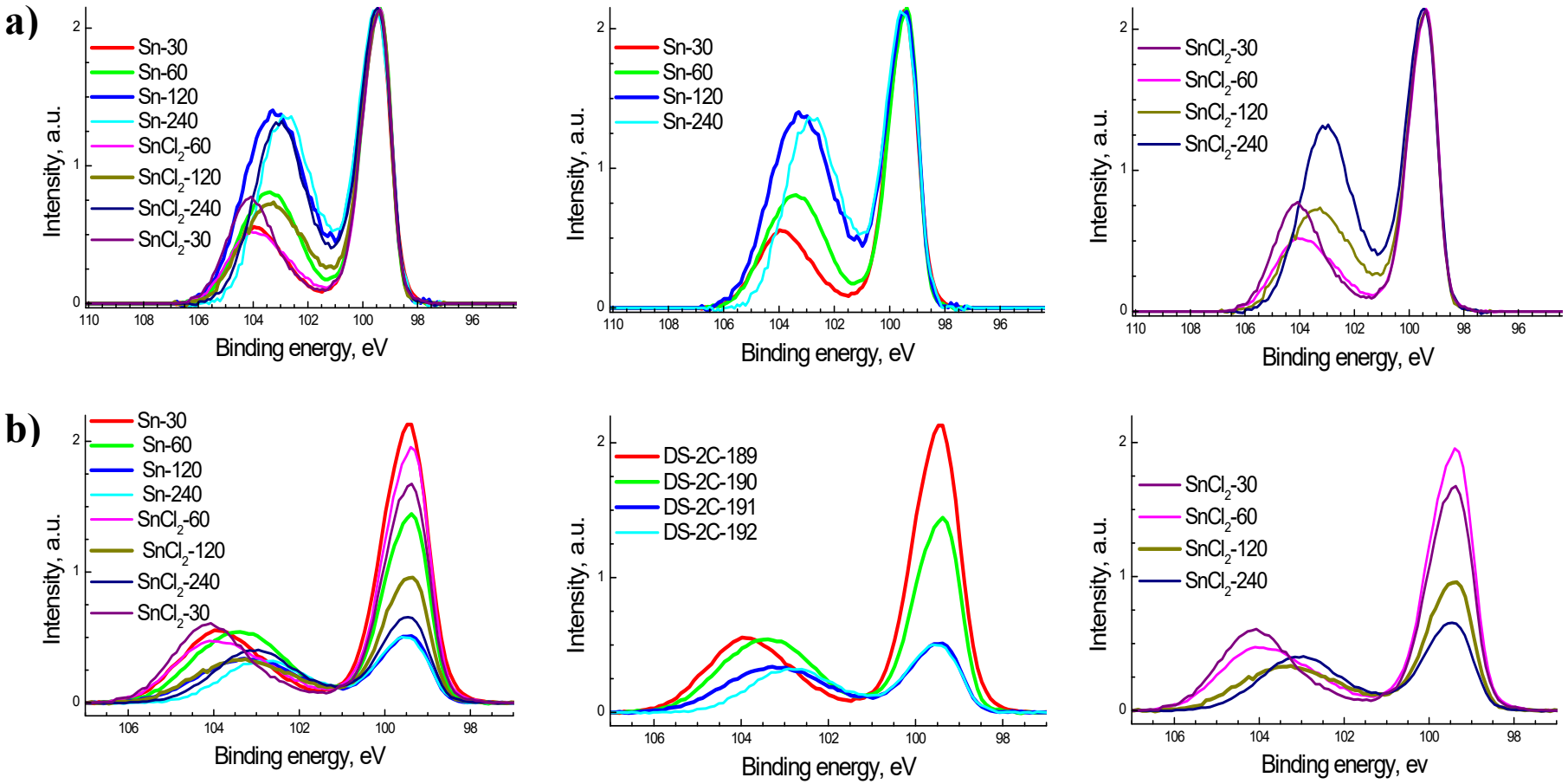

Figure S47. Si 2p photoelectron spectra of the studied samples, the spectra are normalized by intensity of the main peak (a) and Si concentration (b).

Figure S48 presents the photoelectron spectra of Si 2p, approximated by a set of Gaussian peaks consistent with the data on chemical shifts. The Si^0 state is represented by two peaks with a characteristic ratio of $2p_{1/2}/2p_{3/2}$ equal to 0.5 and a spin-orbital splitting of $2p_{1/2}$ - $2p_{3/2}$ equal to 0.605. Binding energies are assigned to the Si^+, Si^{2+}, Si^{3+} and Si^{4+} states 100.78 – 100.85, 101.77-101.9, 102.85-103.1 and 103.87 – 104.16 eV, respectively. **Figure S48**

illustrates the binding energies, Gaussian widths, and relative intensities of the photoelectron peaks, while **Table S7** lists these values along with the chemical shifts.

From **Figure S48**, it is evident that the predominant state in the Si 2p spectra is the Si^0 state, and the primary variations among the spectra pertain to the proportion of the Si^{4+} state.

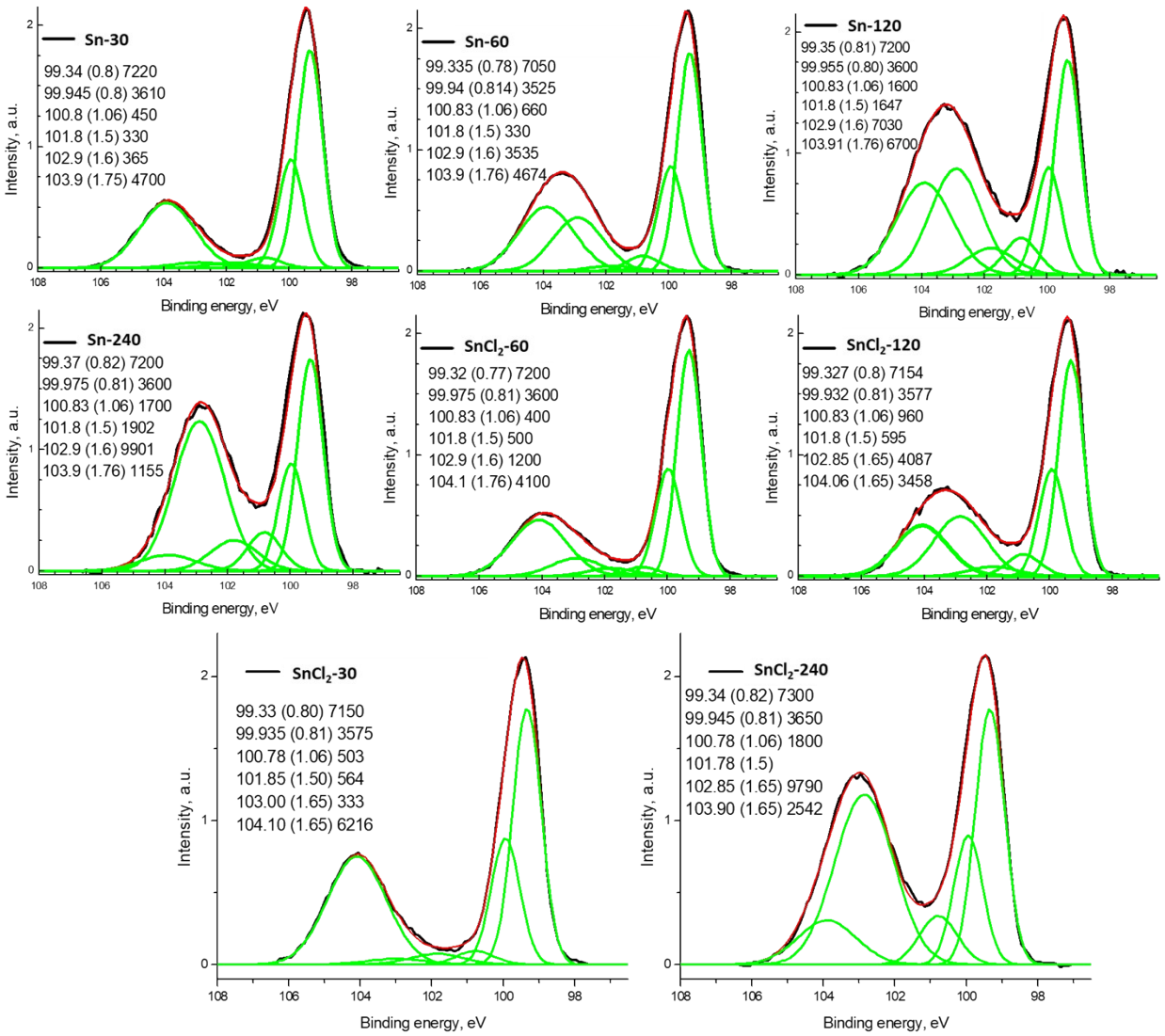

Figure S48. Photoelectron spectra of Si 2p the studied samples, decomposition into components.

Table S7. Characteristics of photoelectron spectra: binding energies (E_b), Gaussian widths (W) and relative intensities (I_{rel}) of photoelectron peaks related to different charge states in the Si 2p spectra.

		Si^0 $2p_{3/2}$	Si^0 $2p_{1/2}$	Si^+	Si^{2+}	Si^{3+}	Si^{4+}
		I	II	III	IV	V	VI
Sn-30	E_b, eV	99.34	99.945	100.8	101.8	102.9	103.9
	W, eV	0.8	0.8	1.06	1.5	1.6	1.75
	$I_{rel.}$	7220	3610	450	330	365	4700
	$I_{rel.}$	0.43	0.22	0.03	0.02	0.02	0.28
Sn-60	E_b, eV	99.34	99.945	100.84	101.81	102.91	103.91
	W, eV	0.78	0.814	1.06	1.5	1.6	1.76
	$I_{rel.}$	7050	3525	660	330	3535	4672
	$I_{rel.}$	0.36	0.18	0.03	0.02	0.18	0.24
Sn-120	E_b, eV	99.34	99.945	100.82	101.79	102.89	103.9
	W, eV	0.81	0.8	1.06	1.5	1.6	1.76
	$I_{rel.}$	7200	3600	1600	1647	7030	6700
	$I_{rel.}$	0.26	0.13	0.06	0.06	0.25	0.24
Sn-240	E_b, eV	99.34	99.945	100.80	101.77	102.88	103.87
	W, eV	0.82	0.81	1.06	1.5	1.6	1.76
	$I_{rel.}$	7200	3600	1700	1902	9901	1155
	$I_{rel.}$	0.28	0.14	0.07	0.07	0.39	0.05
$SnCl_2$-30	E_b, eV	99.34	99.945	100.79	101.86	103.01	104.11
	W, eV	0.8	0.81	1.06	1.5	1.65	1.65
	$I_{rel.}$	7150	3575	503	564	333	6216
	$I_{rel.}$	0.39	0.19	0.03	0.03	0.02	0.34
$SnCl_2$-60	E_b, eV	99.34	99.945	100.85	101.82	102.92	104.12
	W, eV	0.77	0.81	1.06	1.5	1.6	1.76
	$I_{rel.}$	7200	3600	400	500	1200	4100
	$I_{rel.}$	0.42	0.21	0.02	0.03	0.07	0.24
$SnCl_2$-120	E_b, eV	99.34	99.945	100.84	101.9	102.86	104.16
	W, eV	0.8	0.81	1.06	1.5	1.65	1.65
	$I_{rel.}$	7154	3577	960	595	4087	3458
	$I_{rel.}$	0.36	0.18	0.05	0.03	0.21	0.17
$SnCl_2$-240	E_b, eV	99.34	99.945	100.78		102.85	103.9
	W, eV	0.82	0.81	1.06		1.65	1.65
	$I_{rel.}$	7300	3650	1800	595	9740	2542
	$I_{rel.}$	0.28	0.14	0.07	0.02	0.38	0.10
		I	II	III	IV	V	VI

The corresponding photoelectron spectra of C 1s are displayed in **Figure S49** and **Figure S50**, and their characteristics are summarized in **Table S8**. These spectra are characterized by peaks with binding energies 283.58 – 283.91, 284.66, 285.11-285.77, 286.6, 287.6 and 288.93 – 289.56 eV, which can be ascribed to low-molecular-weight carbon fragments, graphitized carbon containing structural defects, groups C-C/C-H, C-OH/C-O-C, O-S-O/S=O and S(O)O. The relative intensities of the photoelectronic peaks reflect the relative concentrations of the isolated states.

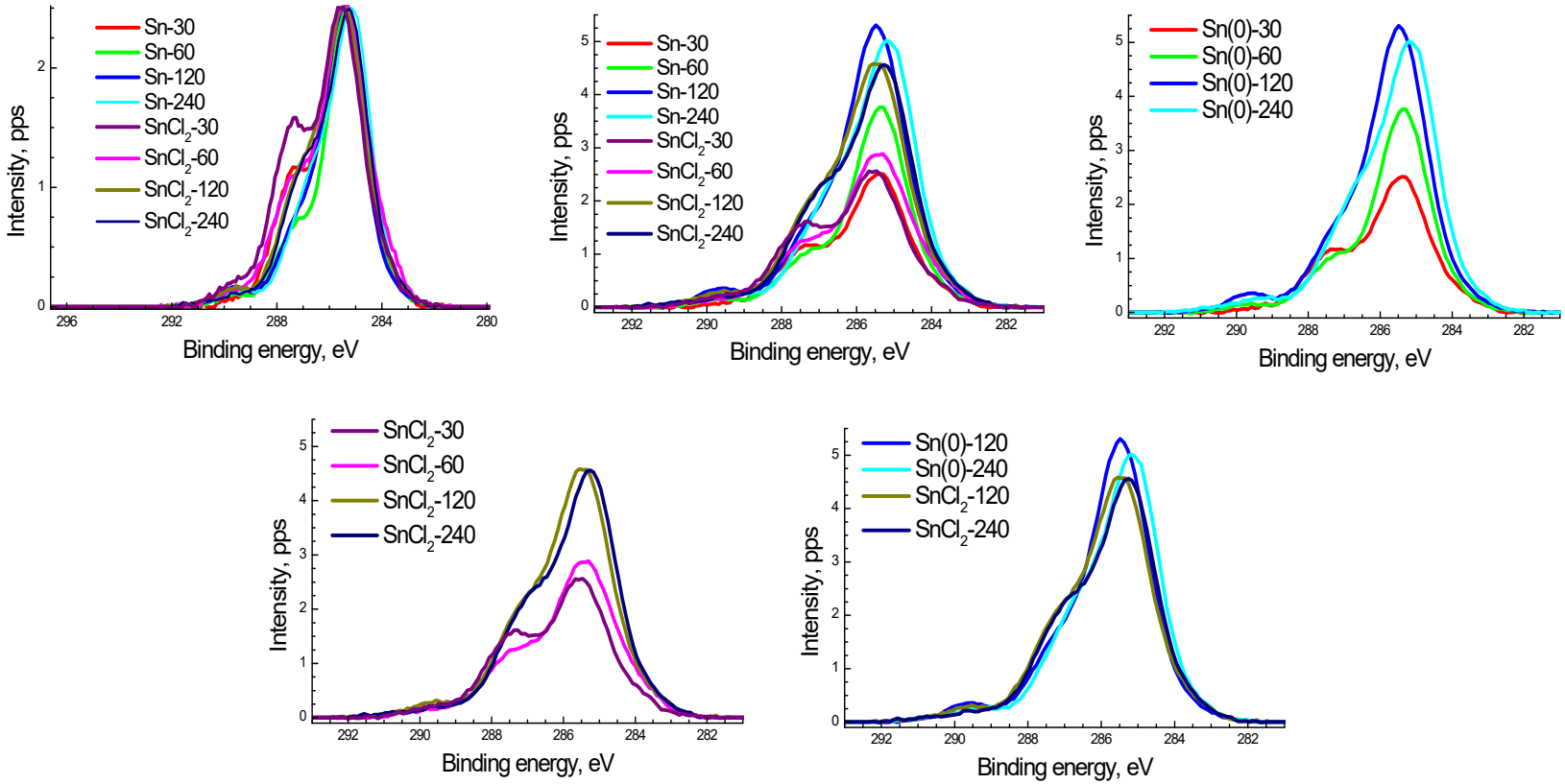

Figure S49. Photoelectron spectra of C 1s of the studied samples, the spectra are normalized by the intensity of the main peak and by the concentration of carbon.

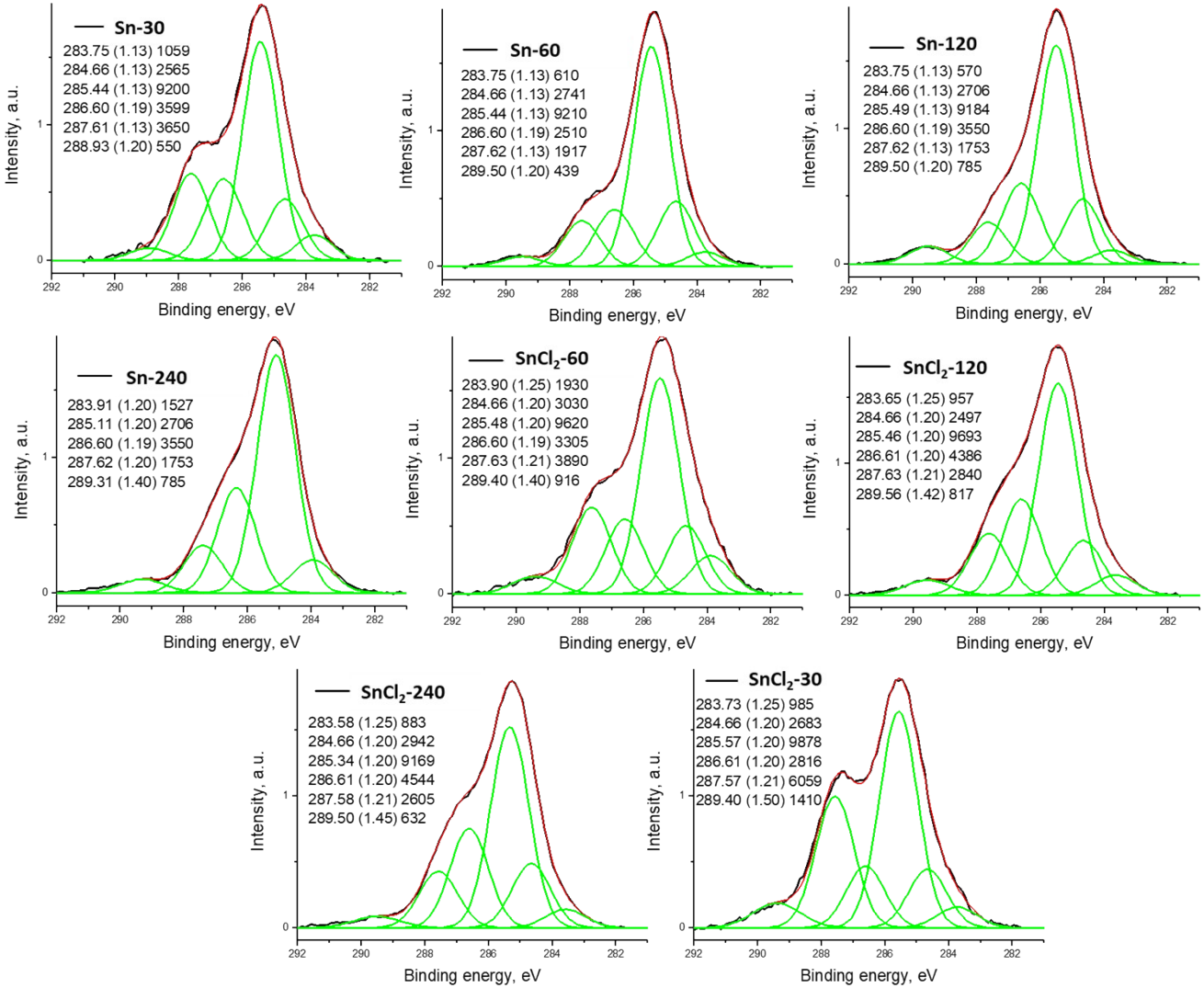

Figure S50. **Photoelectron spectra of C 1s of the studied samples, decomposition into components.**

Table S8. **Characteristics of photoelectron spectra: binding energies (E_b), Gaussian widths (W) and relative intensities (I_{rel}) of photoelectron peaks related to different chemical groups in the C 1s spectra.**

		C-C/C-H*	sp^2	C-C/C-H	C-OH/C-O-C	C=O/O-C-O	C(O)O
		I	II	III	IV	V	VI
Sn-30	E_b, eV	**283.75**	**284.66**	**285.44**	**286.60**	**287.61**	**288.93**
	W, eV	**1.13**	**1.13**	**1.13**	**1.19**	**1.13**	**1.2**
	$I_{rel.}$	**1059**	**2565**	**9200**	**3599**	**3650**	**550**
	$I_{rel.}$	**0.05**	**0.12**	**0.45**	**0.17**	**0.18**	**0.03**
Sn-60	E_b, eV	**283.75**	**284.66**	**285.44**	**286.60**	**287.62**	**289.5**
	W, eV	**1.13**	**1.13**	**1.13**	**1.19**	**1.13**	**1.2**
	$I_{rel.}$	**610**	**2741**	**9210**	**2510**	**1917**	**439**
	$I_{rel.}$	**0.04**	**0.16**	**0.53**	**0.14**	**0.11**	**0.03**
Sn-120	E_b, eV	**283.75**	**284.66**	**285.49**	**286.60**	**287.62**	**289.5**
	W, eV	**1.13**	**1.13**	**1.13**	**1.19**	**1.13**	**1.2**
	$I_{rel.}$	**570**	**2706**	**9184**	**3550**	**1753**	**785**
	$I_{rel.}$	**0.03**	**0.15**	**0.50**	**0.19**	**0.09**	**0.04**
Sn-240	E_b, eV	**283.91**		**285.11**	**286.60**	**287.62**	**289.31**
	W, eV	**1.2**		**1.2**	**1.19**	**1.2**	**1.4**
	$I_{rel.}$	**1527**		**2706**	**3550**	**1753**	**785**
	$I_{rel.}$	**0.15**		**0.26**	**0.34**	**0.17**	**0.08**
$SnCl_2$-60	E_b, eV	**283.90**	**284.66**	**285.48**	**286.60**	**287.63**	**289.4**
	W, eV	**1.25**	**1.2**	**1.2**	**1.19**	**1.21**	**1.5**
	$I_{rel.}$	**1930**	**3030**	**9620**	**3305**	**3890**	**916**
	$I_{rel.}$	**0.04**	**0.04**	**0.04**	**0.04**	**0.04**	**0.04**
$SnCl_2$-120	E_b, eV	**283.65**	**284.66**	**285.46**	**286.61**	**287.63**	**289.56**
	W, eV	**1.25**	**1.2**	**1.2**	**1.2**	**1.21**	**1.42**
	$I_{rel.}$	**957**	**2497**	**9693**	**4386**	**2840**	**817**
	$I_{rel.}$	**0.05**	**0.12**	**0.46**	**0.21**	**0.13**	**0.04**
$SnCl_2$-240	E_b, eV	**283.58**	**284.66**	**285.34**	**286.61**	**287.58**	**289.5**
	W, eV	**1.25**	**1.2**	**1.2**	**1.2**	**1.21**	**1.45**
	$I_{rel.}$	**883**	**2942**	**9169**	**4544**	**2605**	**632**
	$I_{rel.}$	**0.04**	**0.14**	**0.44**	**0.22**	**0.13**	**0.03**
$SnCl_2$-30	E_b, eV	**283.73**	**284.66**	**285.57**	**286.61**	**287.57**	**289.40**
	W, eV	**1.25**	**1.2**	**1.2**	**1.2**	**1.21**	**1.5**
	$I_{rel.}$	**985**	**2683**	**9878**	**2816**	**6059**	**1410**
	$I_{rel.}$	**0.04**	**0.11**	**0.41**	**0.12**	**0.25**	**0.06**
		I	II	III	IV	V	VI

Based on Figures **Figure S49** and **Figure S50** and **Table S8**, it is evident that although the same groups are present in the studied samples, they exhibit varying relative intensities due to the differing conditions of sample preparation.

Figure S51 depicts the Cu 2p photoelectron spectra of the studied samples, normalized by the intensity of the main peak and the concentration of copper. Notably, there are no satellite peaks with a binding energy of approximately 943 eV, indicating the absence of a Cu^{2+} state.

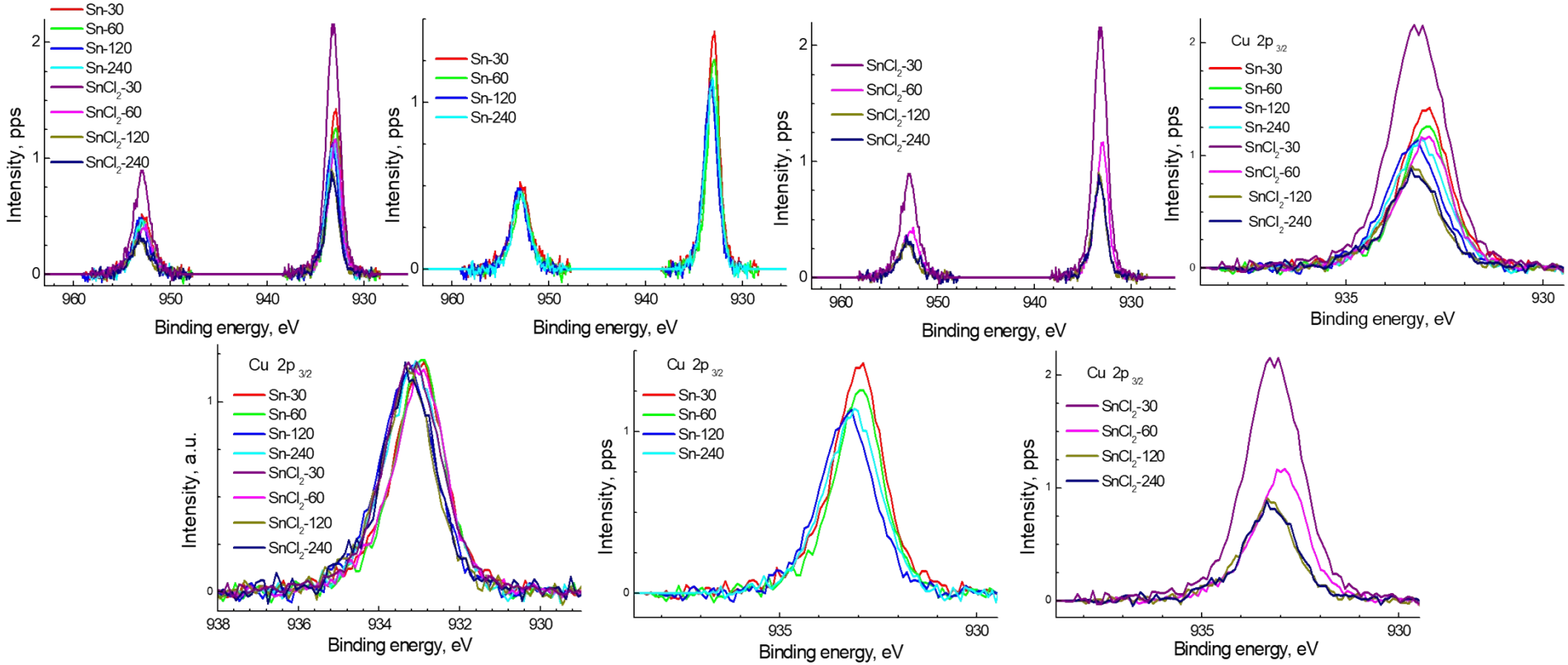

Figure S51. Photoelectron spectra of Cu 2p3/2 of the studied samples, the spectra are normalized by the concentration of copper on the surface of the CM.

Figure S52 displays the decomposition of the Cu $2p_{3/2}$ photoelectron spectra of the studied samples using three Gaussian profiles, and their characteristics are presented in Table 5. The binding energies of peaks I fall within the range 931.45 - 932.45 eV, corresponding to the Cu^{+} state.[3,4]

Regarding the positions of peaks II, two ranges can be identified: 932.94 – 932.98 eV and 933.15 – 933.33 eV. The former corresponds to the Cu^0 state for particles larger than several tens of nanometers, whereas the latter pertains to nanoparticles smaller than 10 nm, reflecting the size-dependent shift of the photoelectron peak, known as the so-called dimensional effect. However, based on electron microscopy data, the size of nanoparticles containing copper exceeds 1 μm. This observation suggests the presence of differential charging, implying that the copper-containing particles are enveloped by a substance with low electrical conductivity. The binding energies of peaks III surpass 934 eV and, according to available literature, should be assigned to the Cu^{2+} state.[4–6] Nonetheless, considering the absence of characteristic satellites and the inability to observe the dimensional effect, peaks III should also be attributed to the Cu^0 state. The binding energies of peaks III, as indicated in the **Table S9**, further highlight the occurrence of differential charging and suggest that copper-containing particles are encased in a thicker layer of a substance with low electrical conductivity or a layer of a substance with even lower electrical conductivity compared to the scenario involving peak II.

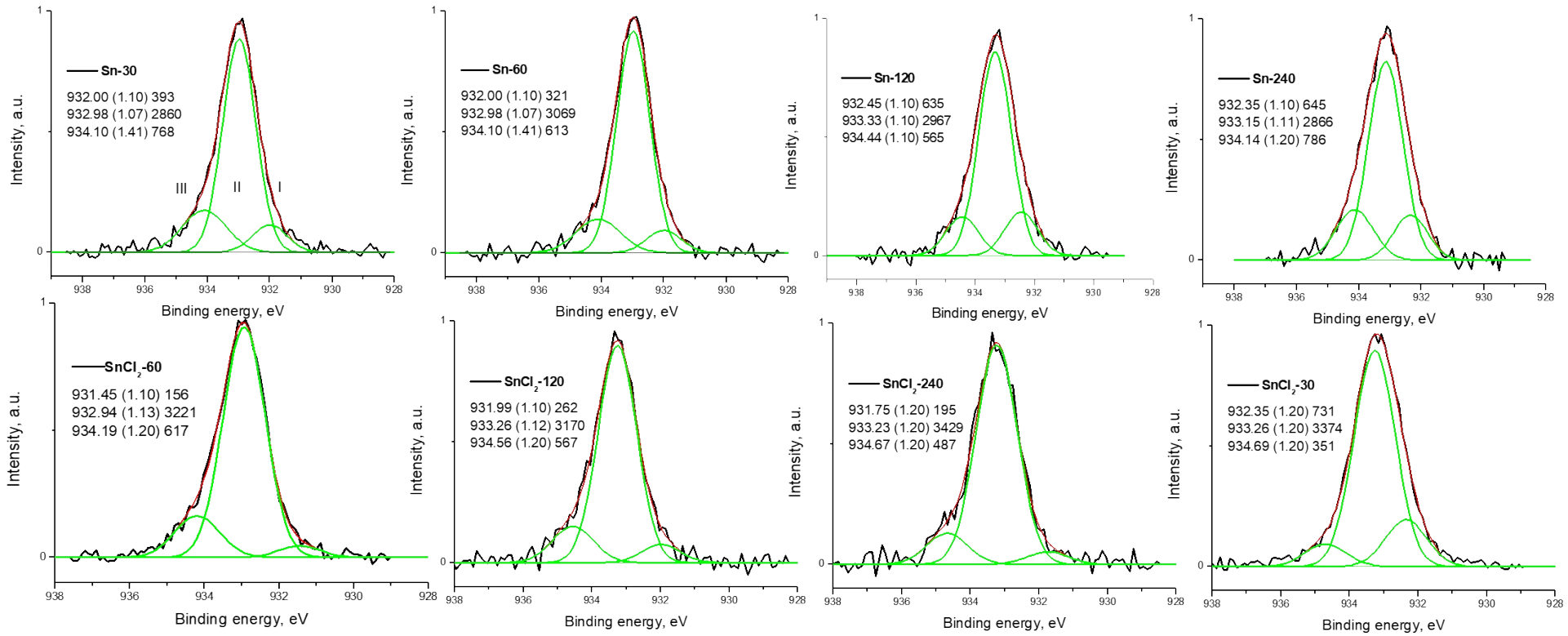

Figure S52. Photoelectron spectra of Cu $2p_{3/2}$ of the studied samples, decomposition into components.

Figure S53 displays the photoelectron spectra of Zn 2p of the examined samples, normalized by the intensity of the main peak and the Zn concentration.

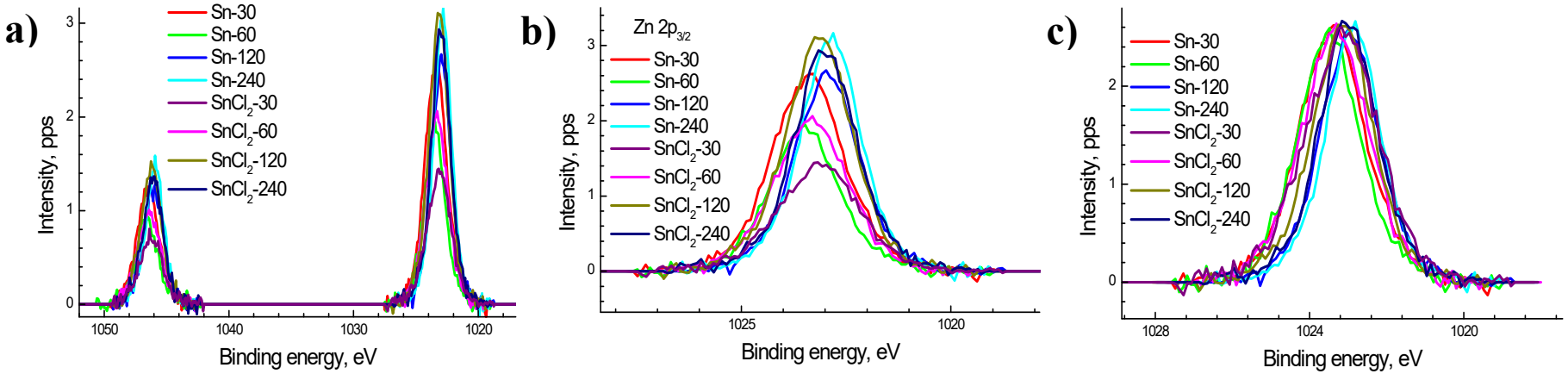

Figure S53. Photoelectron spectra of Zn $2p_{3/2}$ of the studied samples (a), the spectra are normalized by zinc concentration (b) and by the intensity of the main peak (c).

Figure S54 shows the decompositions of the Zn $2p_{3/2}$ photoelectron spectra of the studied samples using three Gaussian profiles, and their characteristics are presented in the Table. As in the case of Cu $2p_{3/2}$ spectra, the Zn $2p_{3/2}$ spectra are approximated by three Gaussian profiles.

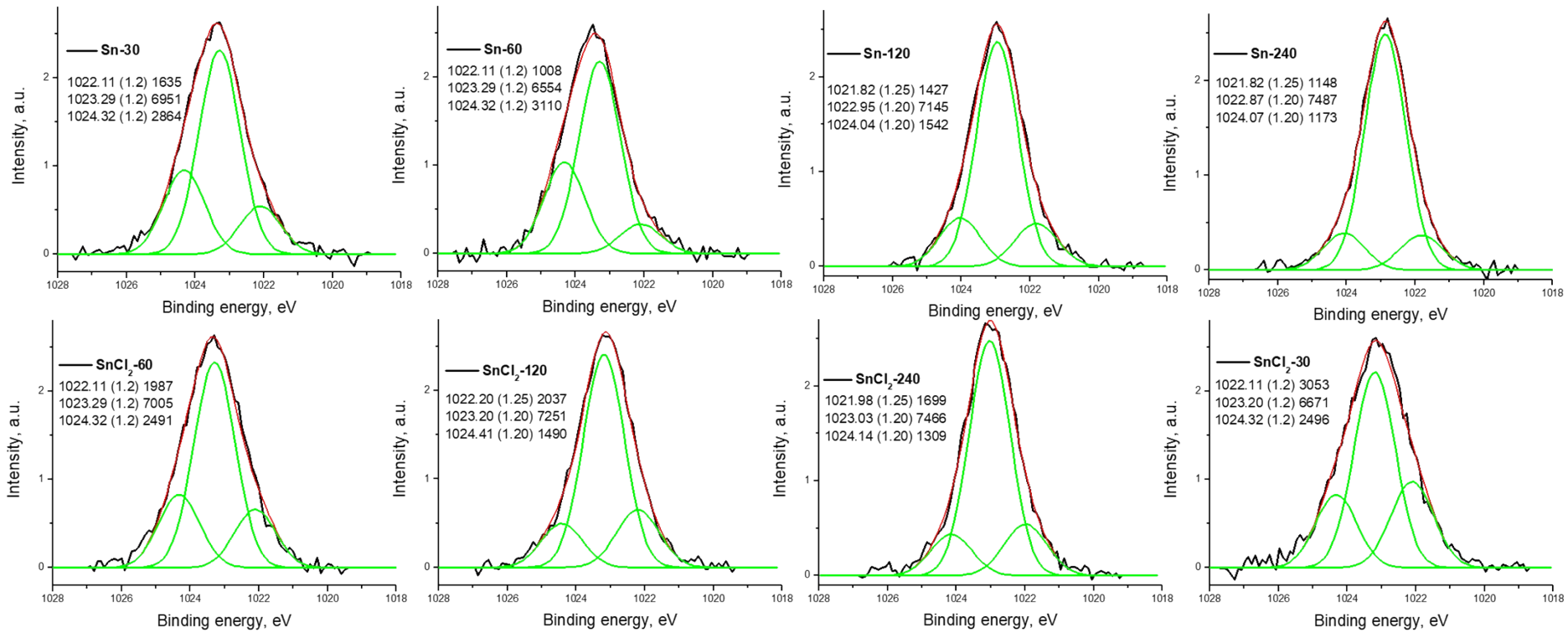

Figure S54. Photoelectron spectra of Zn $2p_{3/2}$ of the studied samples, decomposition into components.

The binding energies of the Zn $2p_{3/2}$ photoelectron peaks exhibit weak dependence on the chemical environment. One primary method to determine the charge state of Zn atoms involves utilizing the Auger parameter. However, at low concentrations, this approach necessitates prolonged registration times, potentially leading to metal reduction. The acquired binding energies of the Zn $2p_{3/2}$ peaks are approximately 1 eV higher than the reference values for ZnO, differing by 0.25 eV from those of pure Zn. Nevertheless, based on the interpretation of the Cu 2p spectra, the observed shift should also be ascribed to the dimensional effect (**Table S9**).

Table S9. Characteristics of photoelectron spectra: binding energies (E_b) and relative intensities (I_{rel}) of photoelectron peaks related to different charge states in the Cu $2p_{3/2}$ and Zn $2p_{3/2}$ spectra

		Cu $2p_{3/2}$			Zn $2p_{3/2}$			Substraction		
		I	II	III	I	II	III	I-I	II-II	III-III
Sn-30	E_b, eV	932.0	932.98	934.1	1022.11	1023.29	1024.32	**90.11**	**90.31**	**90.22**
	$I_{rel.}$	**0.10**	**0.71**	**0.19**	**0.14**	**0.61**	**0.25**			
Sn-60	E_b, eV	932.0	932.98	934.1	1022.11	1023.29	1024.32	**90.11**	**90.31**	**90.22**
	$I_{rel.}$	**0.10**	**0.72**	**0.19**	**0.09**	**0.61**	**0.29**			
Sn-120	E_b, eV	932.45	933.33	934.1	1021.82	1022.95	1024.04	**89.37**	**89.62**	**89.94**
	$I_{rel.}$	**0.15**	**0.71**	**0.14**	**0.14**	**0.71**	**0.15**			
Sn-240	E_b, eV	932.35	933.15	934.14	1021.82	1022.87	1024.07	**89.47**	**89.72**	**89.93**
	$I_{rel.}$	**0.15**	**0.67**	**0.18**	**0.12**	**0.76**	**0.12**			
$SnCl_2$-30	E_b, eV	931.45	932.94	934.19	1022.11	1023.29	1024.32	**90.66**	**90.35**	**90.13**
	$I_{rel.}$	**0.04**	**0.81**	**0.15**	**0.17**	**0.61**	**0.22**			
$SnCl_2$-60	E_b, eV	931.99	933.26	934.56	1022.2	1023.2	1024.41	**90.21**	**89.94**	**89.85**
	$I_{rel.}$	**0.07**	**0.79**	**0.14**	**0.19**	**0.67**	**0.14**			
$SnCl_2$-120	E_b, eV	931.75	933.23	934.67	1021.98	1023.03	1024.14	**90.23**	**89.8**	**89.47**
	$I_{rel.}$	**0.05**	**0.83**	**0.12**	**0.16**	**0.71**	**0.13**			
$SnCl_2$-240	E_b, eV	932.35	933.26	934.69	1022.11	1023.2	1024.32	**89.76**	**89.94**	**89.63**
	$I_{rel.}$	**0.16**	**0.76**	**0.08**	**0.25**	**0.55**	**0.20**			

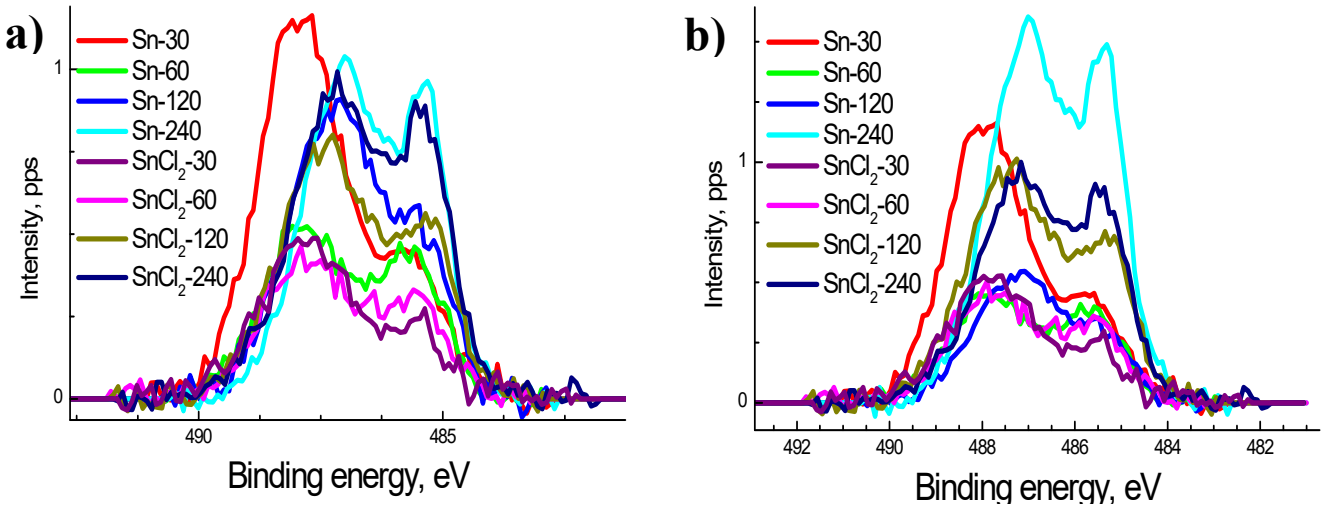

Figure S55. Photoelectron spectra of Sn $3d_{5/2}$ of the studied samples, the spectra are normalized by intensity of the main peak (a) and their concentration in contact mass (b).

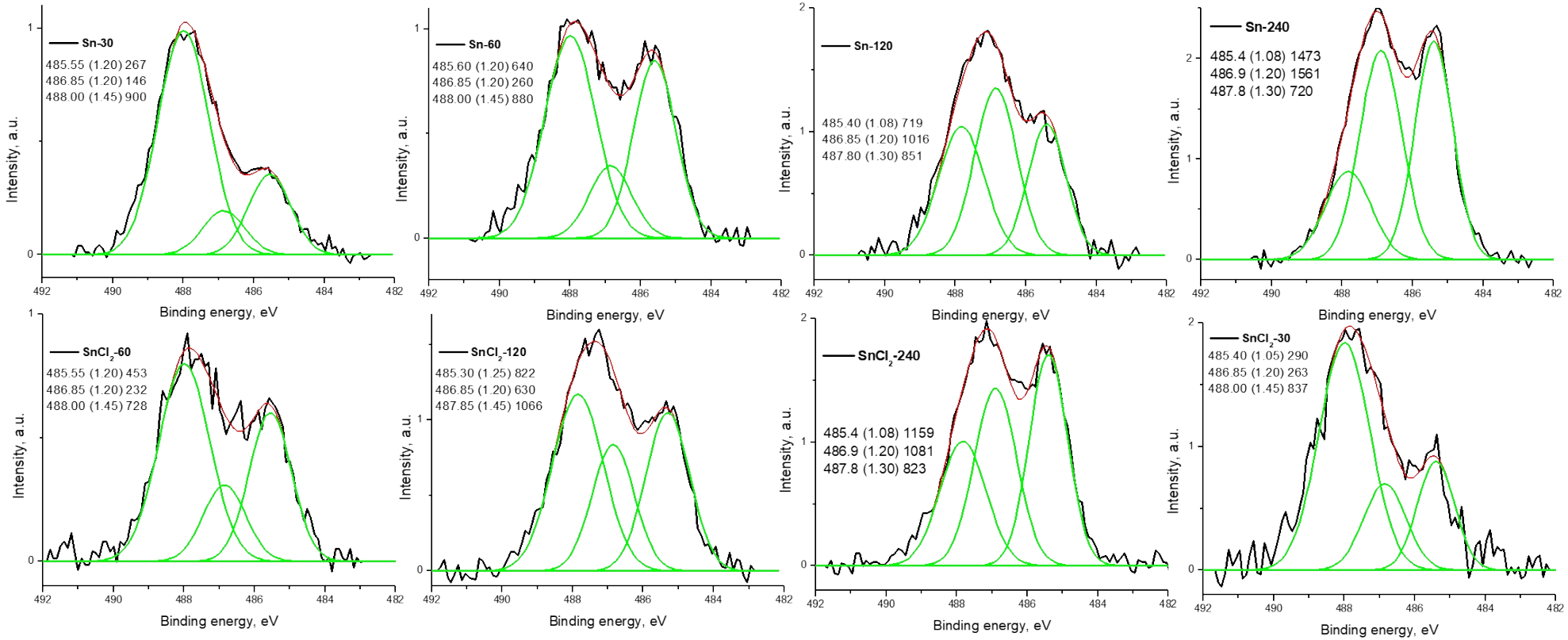

Figure S56. Photoelectron spectra of Sn $3d_{5/2}$ of the studied samples.

Table S10. Characteristics of the Sn $3d_{5/2}$ photoelectron spectra: binding energies (E_b, eV), Gaussian widths (W, eV), and relative intensities (I_{rel}) of photoelectron peaks.

		Sn(I)	Sn(II)	Sn(III)			Sn(I)	Sn(II)	Sn(III)
Sn-30	E_b, eV	485.55	486.85	488.0	$SnCl_2$-30	E_b, eV	485.40	486.85	488.0
	W, eV	1.2	1.2	1.45		W, eV	1.05	1.2	1.45
	I_{rel}	267	146	900		I_{rel}	290	263	837
	I_{rel}	0.20	0.11	0.69		I_{rel}	0.21	0.19	0.60
Sn-60	E_b, eV	485.6	486.85	488.0	$SnCl_2$-60	E_b, eV	485.55	486.85	488.0
	W, eV	1.2	1.2	1.45		W, eV	1.2	1.2	1.45
	I_{rel}	640	260	880		I_{rel}	453	232	728
	I_{rel}	0.36	0.15	0.49		I_{rel}	0.32	0.16	0.52
Sn-120	E_b, eV	485.40	486.85	487.8	$SnCl_2$-120	E_b, eV	485.3	486.85	487.85
	W, eV	1.08	1.2	1.35		W, eV	1.25	1.2	1.45
	I_{rel}	719	1016	851		I_{rel}	822	630	1066
	I_{rel}	0.28	0.39	0.33		I_{rel}	0.33	0.25	0.42
Sn-240	E_b, eV	485.40	486.9	487.8	$SnCl_2$-240	E_b, eV	485.40	486.9	487.8
	W, eV	1.08	1.2	1.30		W, eV	1.08	1.2	1.30
	I_{rel}	1473	1561	720		I_{rel}	1159	1081	823
	I_{rel}	0.39	0.42	0.19		I_{rel}	0.38	0.35	0.27

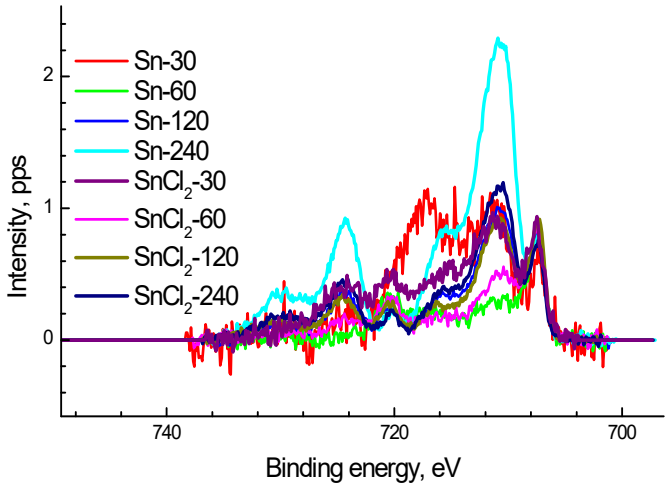

Figure S57. Photoelectron spectra of Fe $2p_{3/2}$ of the studied samples, the spectra are normalized by the intensity of the main peak.

5. References

(1) Powell, C. J. Elemental Binding Energies for X-Ray Photoelectron Spectroscopy. *Appl. Surf. Sci.* **1995**, *89* (2), 141–149. https://doi.org/10.1016/0169-4332(95)00027-5.

(2) Krizhanovskiy, I. N.; Temnikov, M. N.; Anisimov, A. A.; Ratnikov, A. K.; Levin, I. S.; Naumkin, A. V.; Chistovalov, S. M.; Muzafarov, A. M. Direct Synthesis of Tetraalkoxysilanes in a High-Pressure Mechanochemical Reactor. *React. Chem. Eng.* **2022**, *7* (3), 769–780. https://doi.org/10.1039/D1RE00522G.

(3) Vasquez, R. P. Cu2O by XPS. *Surf. Sci. Spectra* **1998**, *5* (4), 257–261. https://doi.org/10.1116/1.1247881.

(4) Barreca, D.; Gasparotto, A.; Tondello, E. CVD Cu2O and CuO Nanosystems Characterized by XPS. *Surf. Sci. Spectra* **2007**, *14* (1), 41–51. https://doi.org/10.1116/11.20080701.

(5) Vasquez, R. P. CuO by XPS. *Surf. Sci. Spectra* **1998**, *5* (4), 262–266. https://doi.org/10.1116/1.1247882.

(6) Vasquez, R. P. Cu(OH)2 by XPS. *Surf. Sci. Spectra* **1998**, *5* (4), 267–272. https://doi.org/10.1116/1.1247883.